

**TRANSCRIPTION FACTOR ZTF-17 REGULATES OXIDATIVE
STRESS RESPONSES IN *CAENORHABDITIS ELEGANS***

CINDY TRAN

A THESIS SUBMITTED TO THE FACULTY OF GRADUATE STUDIES
IN PARTIAL FULFILLMENT OF THE REQUIREMENTS FOR THE
DEGREE OF MASTER OF SCIENCE

GRADUATE PROGRAM IN BIOLOGY
YORK UNIVERSITY
TORONTO, ONTARIO

OCTOBER 2021

© CINDY TRAN, 2021

AUTHOR'S DECLARATION

I hereby declare that I am the sole author of this thesis which was written under the supervision of Dr. Terrance J. Kubiseski. This is a true copy of the thesis, including any required final revisions, as accepted by my examiners. I understand that my thesis may be made electronically available to the public.

ABSTRACT

Energy production is a biological process required for life by all living organisms. However, this process exerts a major effect on aging as energy metabolism at the mitochondria inevitably generates reactive oxygen species (ROS). ROS are by-products of cellular metabolism and have important physiological roles in cell signaling and homeostasis but can also harbor harmful effects. Because ROS readily react with other macromolecules, if ROS formation exceeds a physiological level and antioxidants are unable to balance out the damaging effects of ROS, a dangerous condition known as oxidative stress occurs. This accumulation of cellular damage severely compromises cell health and contributes to the onset of age-associated diseases. Many organisms have complex antioxidant systems to protect themselves and in *Caenorhabditis elegans*, SKN-1/Nrf2 and DAF-16/FOXO, promote the expression of stress resistance genes that aid in detoxifying ROS. Our lab has previously shown that transcription factors can influence the expression of phase II detoxifying genes, through SKN-1 activation, while phase I genes can be activated through DAF-16 which confer stress resistance. An RNAi screen against transcription factor ZTF-17 revealed that SKN-1 target, *gst-4p::gfp* expression, was enhanced. This suggested that ZTF-17 possessed repressor like functions during oxidative stress responses. I confirmed that ZTF-17 significantly reduced the activity of SKN-1 and DAF-16 on the *skn-1cp* and *sod-3p* target promoters indicating that ZTF-17 may interact directly and/or indirectly with DNA to modulate transcription through repression. Analysis through various experiments using *ztf-17(tm963)* deletion mutants showed that genes related to oxidative stress, lifespan and longevity were enhanced to promote short-term oxidative stress resistance, but interestingly, mutants also had compromised heat shock survival. The stress regulatory network is extremely complex, and although detoxification processes exist, the molecular players involved in maintaining proper function under oxidative stress remains unclear. Thus, my investigation of ZTF-17's function along with characterizing its role as a potential negative regulator will help elucidate the mechanism to achieve stress resistance and the implications this has on lifespan and longevity.

ACKNOWLEDGMENTS

The completion of this thesis is a huge milestone in my academic career. I attribute not only the success of this project but also many of the accomplishments made during my master's degree to the people in my life. I am incredibly grateful to everyone who made it all possible, without their guidance and motivation, I would not be where I am today.

First and foremost, I would like to thank my supervisor Dr. Terrance J. Kubiseski, my advisor Dr. Mark Bayfield and Dr. Andrew Donini and Dr. Georg Zoidl who were part of my defense committee. Dr. Bayfield, I thank you for your valuable insight, thoughtful feedback, and the refreshing perspective you brought to my project. To my supervisor, Dr. Kubiseski, I have nothing but the utmost respect and gratitude towards you for giving me the opportunity to conduct research in your lab. From day one, your mentorship and continuous support was influential in shaping my experimental approaches and creativity in finding solutions to the challenges I faced. I appreciated that you gave me full autonomy over the direction of my project and trusted in my abilities to conduct meaningful research. Of the many valuable lessons that you have taught me, the importance of keeping an open mind and being a freethinking scientist will always stay with me. Dr. Magdalena Jaklewicz, thank you for helping me capture the most beautiful images of my *C. elegans* and for my new profound appreciation of confocal microscopy.

A special recognition goes out to all the members of Dr. Chun Peng's lab, who shared their expertise in molecular biology with me. Vu Hong, Yanan, Esra and Joyce, thank you for never hesitating to help when I was in a pinch and for providing me with all those qPCR tubes. I cannot imagine what I would do if not for your generosity and good company. Ramsha who kept me sane throughout graduate school and for making sure that there was never a dull moment when we were together. Jake and Heyam, you are both extraordinary individuals who I consider to be my lab parents. In my eyes, you were the embodiment of who good scientists were. I am still in awe of the wealth of scientific knowledge you have, and I will always be thankful for the advice you gave me, both in the lab and in life. To my lab mates, Joon and Fozia, and all my cherished friends from the LSB: Nick, Christina, Naveed, Farnaz, Jennifer, Kyra, Vanessa, Marjan, Saptarshi, Vijaya, Esther, Wendy, Gaby, Vicki, David, Anna, Alex, and Daria. I will never forget our fun conversations and great times that we had in and out of academia. I will miss everyone dearly, but it was truly a privilege to meet you all and to have made such wonderful memories.

To my parents, Do Thi Kim Oanh and Tran Huu Toan, for their unconditional love and support which gave me the confidence to choose my own paths in life. Thanks mom and dad, I will be forever grateful for all the sacrifices and hard work you put into raising me and for believing in me every step of the way. My cousin and best friend Mimi Tran, for always picking up my late-night phone calls and allowing me to confide in her when my morale was low. Lastly, I would like to thank my love, Terry Bing Lam, for being the best boyfriend anyone could ever ask for. Thank you for staying by my side and taking care of me all these years, especially for the many cups of coffee you brewed in the last few months leading up to the completion of my thesis. Your emotional support and never-ending encouragement meant more to me than you could possibly ever imagine. Thank you for always making me laugh and being a pillar that I could lean on. I am so lucky to have you and everyone around me in my life.

TABLE OF CONTENTS

AUTHOR'S DECLARATION.....	ii
ABSTRACT.....	iii
ACKNOWLEDGEMENTS.....	iv
TABLE OF CONTENTS.....	v
LIST OF FIGURES	viii
LIST OF TABLES	xi
LIST OF <i>C. ELEGANS</i> GENES, FUNCTION AND MAMMALIAN HOMOLOGS.....	xii
LIST OF ABBREVIATIONS.....	xvi
CHAPTER 1: INTRODUCTION AND LITERATURE REVIEW.....	1
1.1 General Introduction.....	2
1.1.1 <i>C. elegans</i> : A powerful model organism ideal for genetic studies.....	2
1.2 Oxidative Stress.....	4
1.2.1 The duality of Reactive Oxygen Species	5
1.2.2 Detoxification of ROS in <i>C. elegans</i>	6
1.2.3 Aging, lifespan and longevity in <i>C. elegans</i>	9
1.3 Transcriptional regulation and stress response pathways in <i>C. elegans</i>.....	10
1.3.1 The Insulin/Insulin-like signaling (IIS) pathway.....	10
1.3.2 The mTOR pathway.....	13
1.3.3 The MAPK pathways.....	17
1.3.4 miRNA gene silencing pathway.....	21
1.4 SKN-1/Nrf2 and its involvement in the oxidative stress response.....	23
1.4.1 The Mechanism of SKN-1 function and activation.....	25
1.5 DAF-16/FOXO and its role in the oxidative stress response.....	29
1.5.1 The mechanism of DAF-16 function and activation.....	31
1.6 The evolution of the pluripotency marker mammalian ZFP42/REX1.....	31

1.7 Current understanding of Transcription Factor ZTF-17: The <i>C. elegans</i> Zinc Finger Putative Transcription Factor family.....	33
1.7.1 ZTF-17 positively regulates <i>lin-39</i>	36
1.7.2 <i>mir-77</i> is a candidate target gene of ZTF-17.....	37
1.8 Rationale, hypotheses and objectives of this thesis.....	37
1.9 References.....	39

CHAPTER 2: INVESTIGATION OF THE *CAENORHABDITIS ELEGANS* TRANSCRIPTION FACTOR ZTF-17 AND ITS ROLE IN THE OXIDATIVE STRESS PATHWAYS..... 48

2.1 Introduction.....	49
2.2 Materials and Methods	50
2.2.1 Maintenance of <i>C. elegans</i> Worm Strains	50
2.2.2 Generation of <i>ztf-17(tm963)</i> Transgenic Worms	51
2.2.3 Single Worm-Polymerase Chain Reaction	52
2.2.4 Confocal Microscopy and GFP Fluorescence Analysis	53
2.2.5 Worm Synchronization	53
2.2.6 RNAi (RNA interference)	54
2.2.7 RNA Extraction and Quantitative Real Time PCR.....	54
2.2.8 Oxidative Stress Assays.....	55
2.2.9 Thermotolerance Assay and Heat Stress Treatment.....	56
2.2.10 DAF-16 Nuclear Localization Assay	57
2.2.11 Primer Design and Subcloning	57
2.2.12 Cell Culture and Transfection	58
2.2.13 Luciferase Assay	58
2.2.14 Dual Luminescence-Based Co-Immunoprecipitation (DULIP) Assay	59
2.2.15 <i>ztf-17(+)</i> Overexpression Construct and Transgenic Worm Strains	59
2.2.16 SapTrap Assembly	60
2.2.17 Statistical Analysis	60
2.3 Results.....	61
2.3.1 Animals homozygous for the <i>ztf-17</i> gene deletion displayed increased expression of antioxidant genes found in phase I and II detoxification pathways.....	61

2.3.2	Loss of <i>ztf-17</i> via RNAi-mediated knockdown resulted in an upregulation of <i>gst-4</i> and <i>sod-3</i>	69
2.3.3	Transcription factor ZTF-17 is a repressor of the <i>skn-1c</i> and <i>sod-3</i> promoters and negatively regulates SKN-1 and DAF-16 target genes.....	81
2.3.4	<i>ztf-17(tm963)</i> mutants appear to have better resistance during the initial exposure to oxidative stress inducing compounds but no enhanced survivability.....	93
2.3.5	<i>ztf-17(tm963)</i> mutants are more susceptible to heat stress and genes related to thermotolerance are downregulated upon exposure to elevated temperatures.....	97
2.4	Discussion.....	105
2.5	References.....	114
 CHAPTER 3: GENERAL DISCUSSION.....		117
3.1	Identification of ZTF-17 as a transcription factor that negatively regulates basal expression levels of detoxification genes and target genes of the IIS pathway.....	118
3.2	Potential regulation of SKN-1 and DAF-16 target genes highlights new roles for ZTF-17 in <i>C. elegans</i>.....	121
3.3	Future directions and studies of ZTF-17 in <i>C. elegans</i>.....	125
3.3.1	ZTF-17 localization can be achieved using the SapTrap Assembly approach to generate <i>ztf-17::mNeonGreen</i> expressing transgenic worms.....	125
3.3.2	Future work to further elucidate the significance of ZTF-17 and the stress genes network.....	127
3.4	Conclusion.....	129
3.5	References	130
 APPENDIX.....		131

LIST OF FIGURES

Figure 1.1 The generation of Reactive Oxygen Species and the detoxification by antioxidant enzymes.....	8
Figure 1.2 Schematic showing the conserved insulin and IGF-1-like signalling pathways in nematodes, flies, and mice.....	12
Figure 1.3 Pathways affecting mechanistic TOR1 and TOR2 complexes and their downstream targets and biological processes.....	16
Figure 1.4 Schematic representation of JNK, ERK and p38 MAP Kinase pathway that regulate SKN-1 and DAF-16 in the <i>C. elegans</i> oxidative stress response.....	20
Figure 1.5 MicroRNA processing and function in <i>C. elegans</i>	22
Figure 1.6 SKN-1 is the <i>C. elegans</i> ortholog of the highly conserved mammalian Nrf/CNC proteins.....	24
Figure 1.7 Comparison of the Ras-MAPK signalling and the proteasomal degradation pathway that regulates Nrf2/SKN-1 in mammals and <i>C. elegans</i>	28
Figure 1.8 Schematic comparing the <i>C. elegans</i> DAF-16 and human FOXO.....	30
Figure 1.9 Exon structures of PHO and PHOL in <i>D. melanogaster</i> , YY1, YY2 and REX1 in humans and ZTF-17 in <i>C. elegans</i>	35
Figure 2.1 <i>ztf-17(tm963)</i> mutants display increased <i>gst-4p::GFP</i> and <i>sod-3p::GFP</i> expression compared to N2 wildtype worms.....	64
Figure 2.2 <i>ztf-17(tm963)</i> mutants showed enhanced expression of <i>gst-4</i> and <i>sod-3</i> mRNA levels under non-oxidative stress inducing conditions.....	66
Figure 2.3 Phase II detoxification genes, <i>gst-4</i> and <i>gcs-1</i> had higher mRNA expression levels in <i>ztf-17(tm963)</i> mutants under normal conditions.....	67
Figure 2.4 DAF-16 target genes, <i>sod-3</i> , <i>ctl-1</i> and <i>ins-7</i> , mRNA expression levels were higher in <i>ztf-17(tm963)</i> mutants under normal conditions.....	68

Figure 2.5 mRNA expression levels of <i>gst-4</i> during RNAi-mediated knockdown of <i>ztf-17</i> showed no significant differences but there was enhanced <i>sod-3</i> expression.....	73
Figure 2.6 <i>ztf-17</i> RNAi increases the basal expression levels of <i>sod-3p::GFP</i> under non-oxidative stress-inducing conditions.....	74
Figure 2.7 <i>ztf-17</i> RNAi and <i>ztf-22</i> RNAi increases the basal expression levels of <i>gst-4p::GFP</i> under non-oxidative stress-inducing conditions.....	76
Figure 2.8 Loss of both <i>ztf-17</i> and <i>ztf-22</i> resulted in a further increase of <i>gst-4p::GFP</i> when deletion mutants were treated with RNAi.....	77
Figure 2.9 The NIR for ZTF-22 and ZTF-17 suggest no detectable interaction between the two proteins.....	79
Figure 2.10 The activity of the <i>skn-1c</i> promoter was robustly enhanced in the presence of SKN-1 and DAF-16A suggesting that there is a synergistic activating effect.....	86
Figure 2.11 DAF-16A alone enhanced the <i>sod-3</i> promoter activity but activity was attenuated by the presence of SKN-1.....	87
Figure 2.12 ZTF-17 significantly reduced the promoter activity of both <i>skn-1cp</i> and <i>sod-3p</i> that was enhanced by DAF-16A and SKN-1.....	88
Figure 2.13 Overexpression of <i>ztf-17</i> in transgenic worms resulted in a significant reduction in the mRNA expression levels <i>gst-4</i> but no significant changes to DAF-16 target genes.	89
Figure 2.14 <i>ztf-17(tm963)</i> mutants displayed an increase in DAF-16::GFP nuclear localization under normal, non-stress inducing conditions.....	91
Figure 2.15 DAF-16A and ZTF-17 NIRs suggest that the interaction between both proteins is unlikely.....	92
Figure 2.16 <i>ztf-17(tm963)</i> mutants showed no significant differences in oxidative stress resistance when treated with As but are more resistant when exposed to tBHP.....	95
Figure 2.17 <i>ztf-17(tm963)</i> mutants had increased mRNA expression for genes related to the DAF-2/insulin signalling pathway but had a reduction in <i>hsp-16.2</i> and <i>cey-1</i>	96

Figure 2.18 Exposure to 35°C heat stress resulted in a reduction of <i>sod-3p::GFP</i> expression in <i>ztf-17(tm963)</i> mutants when compared to worms under non-stress inducing conditions.....	100
Figure 2.19 mRNA expression levels of DAF-16 target genes that were significantly enhanced in <i>ztf-17(tm963)</i> mutants were downregulated under heat stress.....	102
Figure 2.20 <i>ztf-17(tm963)</i> animals were significantly more sensitive to heat stress at 35°C with an increased mortality rate compared to wildtype animals.....	103
Figure 2.21 mRNA expression levels of <i>skn-1</i> isoforms, <i>daf-16</i> and upstream regulators were relatively unchanged in <i>ztf-17(tm963)</i> mutants but <i>skn-1a</i> and <i>sgk-1</i> was enhanced	104
Figure 2.22 mTOR and insulin signaling in <i>C. elegans</i> collaborate to modulate vitellogenin expression.....	113
Figure 3.1 The proposed model for the mechanism of ZTF-17 function in the regulation of phase I and phase II detoxification pathways.....	124
Figure 3.2 CRISPR/Cas-9 mediated <i>ztf-17::mNG</i> knock-in using the SapTrap assembly for ZTF-17 localization.....	126
Supplementary Data Figure S1. Schematic of the backcross of <i>ztf-17(tm963)</i>	140
Supplementary Data Figure S2. Schematic of the approach done to generate the <i>ztf-17(tm963); dvIs(gst-4p::gfp)</i> worms and similar transgenic worm strains	141
Supplementary Data Figure S3. Schematic of the cross done to generate the <i>ztf-17(tm963); daf-2(e1370)</i> double mutant worm strain.....	142

LIST OF TABLES

Table 1. List of Mammalian homologs of <i>C. elegans</i> genes and function.....	xii
Table 2. List of Abbreviations.....	xvi
Table 3. Statistics for the As oxidative stress assay.....	132
Table 4. Statistics for the tBHP oxidative stress assay.....	133
Table 5. Statistics for the thermotolerance assay.....	134
Table 6. List of Worm Strains.....	135
Table 7. List of primers used for genotyping <i>ztf-17</i> with SW-PCR and in the SapTrap Assembly...	136
Table 8. List of forward and reverse primers for qRT-PCR.....	137
Table 9. List of plasmids used for subcloning constructs.....	139

Table 1. List of Mammalian homologs of *C. elegans* genes and function. Information of the genes were obtained from WormBase and/or cited within this project.

<i>C. elegans</i> gene	Mammalian Homolog	Description of function in <i>C. elegans</i>
<i>aak-2</i> (AMP-activated kinase)	Protein kinase AMP-activated catalytic subunit α 1 and 2 (PRKAA1 and PRKAA2)	<ul style="list-style-type: none"> - Enables AMP-activated protein kinase activity. - Involved in determination of adult lifespan, positive regulation of dauer larval development and protein secretion.
<i>act-1</i> (ACTin)	Actin Beta (ACTB) and Actin γ 1 (ACTG1)	<ul style="list-style-type: none"> - Structural constituent of cytoskeleton. - Involved in cortical actin cytoskeleton organization, mitotic cytokinesis, and muscle organ development.
<i>age-1</i> (AGEing alteration)	Phosphatidylinositol-4,5-bisphosphate 3-kinase catalytic subunit α and δ (PIK3CA and PIK3CD)	<ul style="list-style-type: none"> - Enables 1-phosphatidylinositol-3-kinase activity. - Involved in multicellular organism development, regulation of synaptic growth at neuromuscular junction, and response to cadmium ion.
<i>akt-1/2</i> (AKT kinase family)	AKT serine/threonine kinase 1 and 2 (AKT1 and AKT2)	<ul style="list-style-type: none"> - Enables calmodulin binding activity, phosphatidylinositol-3,4,5-trisphosphate binding activity, and protein serine/threonine kinase activity. - Involved in cellular protein modification process, determination of adult lifespan, and insulin receptor signaling pathway.
<i>brap-2</i> (BRCA1 associated protein)	BRCA1 associated protein 2 (BRAP2)	<ul style="list-style-type: none"> - Enables zinc ion binding activity. - Involved in DNA damage induced germline apoptosis, and insulin signaling pathway.
<i>cdc-42</i> (Cell Division Cycle related)	Cell division cycle 42 (CDC42)	<ul style="list-style-type: none"> - Enables GTP binding activity and GTPase activity. - Involved in establishment of mitotic spindle orientation, cellular organization, and positive regulation of nematode male tail tip morphogenesis.
<i>cey-1</i> (C. Elegans Y-box)	Y-Box binding protein 3 (YBX3)	<ul style="list-style-type: none"> - Enables nucleic acid binding activity. - Involved in gametogenesis, polysome formation, and polysome-mediated transcript stabilization.
<i>ctl-1/2</i> (CaTaLase)	Catalase (CAT)	<ul style="list-style-type: none"> - Enables catalase activity. - Involved in determination of adult lifespan, and peroxisome organization.

<i>gcs-1</i> (γ Glutamyl Cysteine Synthetase)	Glutamate-cysteine ligase catalytic subunit (GCLC)	<ul style="list-style-type: none"> - Enables ATP binding activity and glutamate-cysteine ligase activity. - Involved in glutathione biosyntheses and responses to arsenic-containing substances and superoxide.
<i>gst-4</i> (Glutathione S-Transferase)	Hematopoietic prostaglandin D synthase (HPGDS)	<ul style="list-style-type: none"> - Enables glutathione transferase activity and family of phase II detoxification enzymes. - Involved in conjugation of reduced glutathione and protect from attack by reactive electrophiles.
<i>daf-2</i> (abnormal DAuer Formation)	Insulin like growth factor 1 receptor (IGF1R)	<ul style="list-style-type: none"> - Enables PTB domain, SH2 domain binding activity and protein kinase binding activity. - Involved in dauer regulation, developmental and metabolic process. Acts upstream, with negative effect on protein import into nucleus.
<i>daf-16</i> (abnormal DAuer Formation)	Forkhead box O (FOXO1, FOXO3, and FOXO4)	<ul style="list-style-type: none"> - Enables 14-3-3 protein binding, DNA-binding transcription factor and enzyme binding activity. - Involved in defense responses, regulation of dauer larval development and primary metabolic process.
<i>dod-3</i> (Downstream of DAF-16)	N/A	<ul style="list-style-type: none"> - Regulated by DAF-16, unknown function - Enriched at coelomocyte, head mesodermal cell, pharyngeal muscle cell, sensory neurons and ventral nerve cord; affected by <i>daf-16</i>, <i>daf-2</i> and <i>glp-1</i> genes.
<i>dod-17</i> (Downstream of DAF-16)	N/A	<ul style="list-style-type: none"> - Regulated by DAF-16, contains a DFU141 domain with unknown function. - Is involved in innate immune response.
<i>hsp-16.2</i> (Heat Shock Protein)	Crystallin α B (CRYAB)	<ul style="list-style-type: none"> - Enables unfolded protein binding activity. - Involved in response to heat stress/heat shock.
<i>ins-7</i> (INSulin related)	Class of Insulin-like peptides (ILPs)	<ul style="list-style-type: none"> - Enables hormone activity, insulin-like type β subfamily. - Involved in insulin signalling and olfactory learning.
<i>lin-39</i> (abnormal cell LINEage)	Homeobox A5 (HOXA5)	<ul style="list-style-type: none"> - Enables <i>cis</i>-regulatory region sequence-specific DNA binding activity. - Involved in regulation of developmental processes, positive regulation of transcription and cell division.

<i>mek-2</i> (MAP kinase kinase or Erk Kinase)	mitogen-activated protein kinase kinase 1 and 2 (MAP2K1/MAP2K2)	<ul style="list-style-type: none"> - Enables MAP kinase kinase activity and scaffold protein binding activity. - Involved in defense response to bacterium, signal transduction and vulval development.
<i>mpk-1</i> (MAP Kinase)	Mitogen activated protein kinase 1 (MAPK1)	<ul style="list-style-type: none"> - Enables MAP kinase activity. - Involved in oocyte maturation, regulation of macro-molecule metabolic process and signal transduction.
<i>mtl-1/2</i> (MeTaLlothionein)	N/A	<ul style="list-style-type: none"> - Enables cadmium ion and zinc ion binding. - Involved in responses to heat and metal ions.
<i>pdk-1</i> (PDK-class protein kinase)	3-phosphoinositide dependent protein kinase 1 (PDPK1)	<ul style="list-style-type: none"> - Enables protein kinase activity. - Involved in dauer larval development, learning, memory and regulation of synaptic growth at neuromuscular junction.
<i>pmk-1</i> (p38 MAPK family)	Mitogen-activated protein kinase 11/14 (MAPK11 and MAPK14)	<ul style="list-style-type: none"> - Enables MAP kinase activity, transcription factor binding and regulator activator activity. - Involved in behavioral response to nicotine and defense responses via p38 MAPK cascade.
<i>pmp-3</i> (Peroxisomal Membrane Protein related)	ATP binding cassette subfamily D member 4 (ABCD4)	<ul style="list-style-type: none"> - Enables ATP binding and ATPase-coupled transmembrane transporter activity
<i>pqm-1</i> (ParaQuat Methylviologen responsive 1)	N/A	<ul style="list-style-type: none"> - Involved in defense response to Gram-negative bacterium, determination of adult lifespan and innate immune response. - Cytoplasmic but translocation into nucleus upon activation to regulate transcription
<i>sdz-8</i> (SKN-1 Dependent Zygotic transcript)	Carbonyl reductase 3 (CBR3)	<ul style="list-style-type: none"> - Encodes a protein with short chain dehydrogenase/reductase SDR and NAD(P)-binding domains. - Affected by <i>daf-16</i>, <i>daf-2</i>, and <i>skn-1</i> genes, enriched in body wall muscle cell.
<i>sem-4</i> (SEx Muscle abnormal)	Spalt like transcription factor 1 and 3 (SALL1 and SALL3)	<ul style="list-style-type: none"> - Enables RNA polymerase II transcription region sequence-specific DNA binding - Involved in cell differentiation and negative regulation of RNA polymerase II.
<i>sgk-1</i> (Serum- and Glucocorticoid- inducible Kinase)	Serum/glucocorticoid regulated kinase 2 (SGK2)	<ul style="list-style-type: none"> - Enables phosphatidylinositol-3,4,5-trisphosphate binding and protein serine/threonine kinase activity. - Involved in mesendoderm development, peptidyl-serine phosphorylation, and regulation of protein localization to basolateral plasma membrane.

<i>skn-1</i> (SKiNhead)	Nuclear factor erythroid 2-related factor 2 (Nrf2)	<ul style="list-style-type: none"> - Enables Hsp70 protein binding and RNA polymerase II transcription region sequence-specific DNA binding activity. - Involved in endoderm development, endoplasmic reticulum unfolded protein response, regulation of defense responses and organism development.
<i>skr-1/2</i> (SKp1 Related)	S-phase kinase associated protein 1 (SKP1)	<ul style="list-style-type: none"> - Ubiquitin ligase complex component. - Involved in negative regulation of centrosome duplication, responses to DNA damage stimulus and protein stability.
<i>sod-3</i> (SuperOxide Dismutase)	Superoxide dismutase 2 (SOD2)	<ul style="list-style-type: none"> - Enables protein homodimerization and manganese superoxide dismutase activity. - Involved in removal of superoxide radicals.
<i>tba-1</i> (TuBulin, α)	Tubulin α 4a and 8 (TUBA4A and TUBA8)	<ul style="list-style-type: none"> - Enable GTP binding and GTPase activity. - Structural constituent of cytoskeleton. - Involved in embryo development, establishment of mitotic spindle orientation and regulation of cytokinesis.
<i>tra-1</i> (TRAnformer: XX animals into males)	GLI family zinc finger (GLI1, GLI2, GL3)	<ul style="list-style-type: none"> - Enables RNA polymerase II intronic transcription region sequence-specific DNA binding activity. - Involved in development and reproduction, negative regulator RNA polymerase II, and positive regulator of neuron apoptosis.
<i>vit-2</i> and <i>vit-5</i> (VITellogenin structural genes)	N/A	<ul style="list-style-type: none"> - Yolk protein genes - Enables lipid transporter and nutrient reservoir activity.
<i>wdr-23</i> (WD Repeat protein)	DDB1 and CUL4 associated factor 11 (DCAF11)	<ul style="list-style-type: none"> - Enables transcription factor binding activity. - Involved in determination of adult lifespan, negative regulation of cellular response to manganese ion and proteasomal ubiquitin-dependent protein degradation.
<i>ztf-17</i> and <i>ztf-22</i> (Zinc finger putative Transcription Factor family)	ZFP42 zinc finger protein (ZFP42/REX1)	<ul style="list-style-type: none"> - Enables RNA polymerase II transcription regulatory region sequence-specific DNA binding activity. - Encodes a protein with a Zinc finger C2H2-type domain. - Predicted to be involved in regulating larval developmental processes and negative regulator of gene transcription.

Table 2. List of Abbreviations.

¹O₂	Oxygen singlets
3'UTR	3' Untranslated Region
ALR-1	<u>A</u> rgonaute- <u>L</u> ike <u>G</u> ene
AMP	Adenosine monophosphate
AMPK	AMP-activated protein kinase
As	Sodium Arsenite
ATP	Adenosine triphosphate
BED-3	<u>B</u> ED-type zinc finger putative transcription factor <u>3</u>
BLI-3/NADPH	<u>B</u> L <u>I</u> stered cuticle <u>1</u> / Nicotinamide adenine dinucleotide
BR	Basic Region
BRCA	<u>B</u> reast <u>C</u> ancer
bZIP	<u>B</u> asic Leucine <u>Z</u> ipper
cDNA	<u>C</u> omplementary <u>D</u> N <u>A</u>
<i>C. elegans</i>	<u>C</u> aenorhabditis <u>e</u> legans
ChIP	<u>C</u> hromatin <u>I</u> mmunoprecipitation
CNC	Cap'n'Collar
CUL-4	Cullin 4
dsRNA	<u>D</u> ouble-stranded <u>R</u> N <u>A</u>
DAE	<u>D</u> AF-16 <u>A</u> ssociate <u>E</u> lement
DAF-15/Rapter	abnormal <u>D</u> A <u>e</u> r <u>F</u> ormation <u>15</u> / Regulatory Associated Protein of mTOR
DBE	<u>D</u> AF-16 <u>B</u> inding <u>E</u> lement
DDB-1	<u>U</u> V- <u>D</u> amaged <u>D</u> N <u>A</u> <u>B</u> inding protein <u>1</u>
<i>D. melanogaster</i>	<u>D</u> rosophila <u>m</u> elanogaster
DNA	<u>D</u> eoxyribonucleic <u>A</u> cid
<i>E. coli</i>	<u>E</u> scherichia <u>c</u> oli
ELT	Erythroid/Erythrocyte-like Transcription Factor
ER	Endoplasmic Reticulum
ERK	Extracellular signal-regulated protein kinases
ETC	<u>E</u> lectron <u>T</u> ransport <u>C</u> hain
eY1H	Enhanced yeast one-hybrid
FOXO	Forkhead Box
GATA	<u>G</u> A <u>T</u> A Family Transcription Factors
GDP	<u>G</u> uanine <u>D</u> iphosphate
GEF	<u>G</u> uanine Nucleotide <u>E</u> xchange <u>F</u> actor
GFP	<u>G</u> reen <u>F</u> luorescent <u>P</u> rotein
Grb2	Growth factor receptor-bound protein 2
GPx	<u>G</u> lutathione <u>P</u> ero <u>X</u> idase
GSK-3	<u>G</u> lycogen <u>S</u> ynthase <u>K</u> inase <u>3</u>
GTP	<u>G</u> uanine <u>T</u> riphosphate
HEK293T	Human embryonic kidney 293 T cells
H₂O₂	Hydrogen peroxide
IGF-1	Insulin-like growth factor 1
IIS	<u>I</u> nsulin/ <u>I</u> nsulin-like <u>S</u> ignaling
IRE-1	<u>I</u> nositol- <u>R</u> equiring <u>E</u> nzyme <u>1</u>

IRS-1	Insulin receptor substrate 1
JNK	c-Jun <u>N</u> -terminal <u>k</u> inase
Keap1	<u>K</u> elch-like <u>E</u> CH- <u>A</u> ssocaited <u>P</u> rotein <u>1</u>
LET	<u>L</u> ethal
LCR	<u>L</u> ow <u>C</u> omplexity <u>R</u> egion
Maf	Musculoaponeurotic fibrosarcoma
MAPK	<u>M</u> itogen- <u>A</u> ctivated <u>P</u> rotein <u>k</u> inase
MAPKK	<u>M</u> itogen- <u>A</u> ctivated <u>P</u> rotein <u>k</u> inase <u>k</u> inase
MAPKKK	<u>M</u> itogen- <u>A</u> ctivated <u>P</u> rotein <u>k</u> inase <u>k</u> inase <u>k</u> inase
miRNA	<u>m</u> icro <u>R</u> NA
miRISC	<u>m</u> iRNA <u>I</u> nduced <u>S</u> ilencing <u>C</u> omplex
mNG	<u>m</u> NEON <u>G</u> reen fluorescent protein
mRNA	<u>m</u> essenger <u>R</u> NA
mTOR	<u>M</u> echanistic <u>T</u> arget <u>O</u> f <u>R</u> apamycin
NGM	<u>N</u> ematode <u>G</u> rowth <u>M</u> edium
NHR-43	<u>N</u> uclear <u>H</u> ormone <u>R</u> eceptor <u>43</u>
·NO	Nitric oxide
NSY-1	<u>N</u> euronal <u>S</u> ymmetry <u>1</u>
PI and PII	<u>P</u> hase <u>I</u> and <u>P</u> hase <u>II</u>
p38	<u>P</u> rotein <u>38</u> MAPK
PHO	Pleiohomeotic
PHOL	Pleiohomeotic-like
PPI	Protein-protein interaction
O₂^{·-}	Superoxide anion
OH·	Hydroxyl radicals
OCT3/4	Octamer-binding transcription factor
OASIS	<u>O</u> nline <u>A</u> pplication for the <u>S</u> urvival <u>A</u> nalysis
qRT-PCR	<u>Q</u> uantitative <u>R</u> eal <u>T</u> ime <u>P</u> olymerase <u>C</u> hain <u>R</u> eaction
Raf	Rapidly accelerated fibrosarcoma
Ras	Rat sarcoma oncogene
REX1	Reduced Expression Protein 1
RICT-1/Rictor	<u>R</u> apamycin- <u>I</u> nsensitive <u>C</u> ompanion of <u>T</u> OR
RNA	<u>R</u> ibonucleic <u>A</u> cid
RNAi	<u>R</u> NA <u>i</u> nterference
ROS	Reactive Oxygen Species
RTK	Tyrosine kinase receptor
SEK-1	<u>S</u> APK/ <u>E</u> RK <u>k</u> inase <u>1</u>
SKP1	S-phase kinase-associated protein 1
SW-PCR	<u>S</u> ingle <u>W</u> orm <u>P</u> olymerase <u>C</u> hain <u>R</u> eaction
tBHP	<i>tert</i> -Butyl hydroperoxide
TBX-9	<u>T</u> <u>B</u> o <u>X</u> family <u>9</u>
VPC	Vulval precursor cell
WD40	Beta transducing repeat
YF	Kubiseski Lab strains
YY1 and YY2	Ying Yang 1/ Ying Yang 2

**CHAPTER 1: INTRODUCTION AND
LITERATURE REVIEW**

1.1 General Introduction

Reactive oxygen species (ROS) are products of endogenous cellular metabolism and are generated through natural biological processes occurring in the bodies of all living organisms. ROS are chemically reactive oxygen containing molecules that causes oxidative damage when there is an excess of free radicals to antioxidants [1]. Various environmental factors and stresses can induce the excess production of ROS and this is thought to be a major contributor to the onset of age-associated diseases [2,3]. As ROS readily react with other macromolecules within the cell, if there is progressive damage, a condition known as oxidative stress can occur [4,5]. The accumulation of ROS targets RNA, DNA, proteins, and lipids causing extensive damage to tissues that may eventually lead cell death [2,5]. Thus, levels of ROS generation and the signalling that results from the presence of ROS are important factors that determine how an organism responds to oxidative stress. Many organisms have devised elaborate defense mechanisms that protect against ROS by eliminating excess free radicals and/or promoting the expression of stress resistance genes [6]. Although extensive research has been done to help elucidate the signalling pathways involved in oxidative stress resistance, it is vital that we determine what molecular components are crucial to combating oxidative stress as it is the first step to understanding this complex process and how preventing ROS damage can affect an organism's lifespan. Signalling pathways and their effects are often conserved across species allowing scientists to use simpler model organisms, such as *D. melanogaster* and *C. elegans*, to study complex processes that are difficult to understand in humans.

1.1.1. *C. elegans*: A powerful model organism ideal for genetic studies

Since the *C. elegans* Genome Sequencing Project that was completed over two decades ago, this transparent free-living nematode worm has proven to be a highly useful model for studying

anatomy, behaviour, genetics and development [7,8]. Many advantages come from using *C. elegans*. First, worms have two sexes, hermaphrodites are self-fertile and can produce thousands of progenies very quickly and with the presence of males, hermaphrodites can mate with the males allowing for genetic crosses to take place. Although the *C. elegans* is a relatively simple organism, it shares many molecular mechanisms, signalling pathways and exhibit behaviours that are also found in higher, more complex organisms. Numerous human related genes have orthologs in the worm that can be easily manipulated and mutant forms of *C. elegans*, where specific genes are altered, can be produced very easily to study human diseases [9]. Moreover, these animals equip scientists with the ability to conduct studies in the context of a whole, living, and intact organism which can be more insightful than if we were to perform the same experiments in isolated cells.

One feature that makes the *C. elegans* a superior model organism is the ease at which we can manipulate the system and perform genetics. The use of forward and reverse genetic screening, the construction of transgenic animals, mutation mapping, RNAi-mediated knock down and cell biology visualization with florescent probes *in vivo* are just some examples of the genomic tools available for research in *C. elegans*. With its rapid lifecycle, small size and ease of cultivation, the *C. elegans* is an attractive system for characterizing factors that regulate gene expression and biological studies conducted in the worm may be directly applicable to human development and diseases [10].

Historically, many key discoveries made in developmental biology are attributed to the *C. elegans* with Sydney Brenner being the first major figure to adopt the *C. elegans* for research use in the early 1960s [11]. Today, the *C. elegans* continue to be a multifaceted model organism and

the work presented in this thesis, highlights its role in elucidating the oxidative stress response pathways that is also implicated in aging, lifespan, and longevity.

1.2 Oxidative Stress

A fundamental element that is key to survival is the ability of an organism to perceive changes in the environment and respond appropriately to the stressors encountered. Responding to oxidative stress requires a system that is capable of accurately detecting stress-induced cues and to have mechanisms that combats subsequent damaging effects. Accordingly, animals have evolved to have multiple inducible pathways that allow for the upregulation of specific stress-response factors and protection against different types of stressors [12,13]. Originally proposed by Harman, the “free radical and oxidative stress” theory of aging suggests that spontaneous reactions between free radicals exerts damaging effects on cells and contributes to various degenerative diseases including Alzheimer’s disease, Parkinson’s disease and many cancers [11,14,15]. More recently, traditional views surrounding the correlation between excess ROS and oxidative stress have been challenged with new evidence supporting that moderate ROS levels could extend lifespan in *C. elegans* [16,17]. Other theories such as the “oxidative stress theory of life-history trade-offs” emphasises the immediate effects of ROS damage, but also sheds light on how oxidative stress management impacts the livelihood of organisms over longer timescales [18]. The need to expend energy to sustain life at the cost of mediating the toxicity that is produced by oxygen metabolism is a prime example of such life-history trade-offs. Higher oxidative stress levels have been shown to positively influence growth, are indicators for improved ability to combat disease, are involved in production of sexual signals during mating, can cause senescence to impact lifespan and influences diet and foraging behaviours – all of which are aspects related to genetic variations of fitness [18]. As more evidence supporting new

roles for ROS emerges, perhaps our simplistic view, lack of understanding, and the negative connotations associated with oxidative stress needs to be re-evaluated.

1.2.1 The duality of Reactive Oxygen Species

Despite such findings, the fact that ROS causes cellular damage remains unchanged. ROS are oxygen containing molecules and are categorized as free radicals or non-radical oxidants [18]. ROS can originate from exogenous sources, such as UV radiation, pollutants or environmental stressors, but the greatest threat appears to be from endogenously produced ROS [19]. Free radicals have unpaired electrons making them highly unstable and chemically reactive [1]. Majority of free radicals are generated in the form of superoxide anions ($O_2^{\cdot-}$), hydroxyl radicals (OH^{\cdot}) and nitric oxide ($\cdot NO$) which exist for only micro or nanoseconds before triggering reactions, while non-radicals, like hydrogen peroxide (H_2O_2) and oxygen singlets (1O_2), can remain for minutes [20,21]. Although ROS has always been thought to be a purely damaging agent, it is important to recognize that not all ROS molecules cause damage [22]. Recently, studies on the role of ROS outside of its damaging effects has revealed that superoxide can possess regulatory functions and participates in ROS-mediated signaling to increase longevity [23,24]. Approximately 10% of ROS are produced in a controlled manner by specific enzymes, such as NADPH oxidases and NO synthases, and have functions in cell signalling, cell transformation, cell regulation and immune defenses [18,25]. ROS can also oxidize specific DNA bases at promoters to affect mRNA expression at the transcription level or can act as a signalling molecule participating in post-translational modifications to target protein localization or stability [22,26]. Although recent literature has found new functions for ROS, given the number of potential ROS targets, the ability of ROS to be localized and how ROS signalling can modulate specific targets remain unclear. The remaining 90% of ROS molecules are the culprits

contributing to cellular damage. Located at the ATP generating machinery, ROS molecules surface as by-products of aerobic energy metabolism from the mitochondrial electron transport chains (ETC) during the oxidative phosphorylation step [27]. In lower eukaryotes, the ETC and mitochondrial components are very similar to those of mammals indicating that the bioenergetics and oxidative stress pathways are also highly conserved in nematodes [25]. Organisms employ various antioxidant defense mechanisms to neutralize the harmful effects of ROS as downstream reactions can create more damaging effects if ROS were left untreated [20].

1.2.2 Detoxification of ROS in *C. elegans*

Upon exposure to oxidative stress and subsequent damage from cellular ROS, defense mechanisms within nematodes are triggered and a delicate balancing act between ROS production and the antioxidant system is needed to maintain homeostasis. Transcriptional activation of detoxification genes and expression of antioxidant enzymes, such as superoxide dismutase (SOD), catalase (CAT), glutathione peroxidase (GPx) and glutathione S-transferase (GST), can help confer stress resistance [28–32]. SODs are the only enzymes capable of detoxifying superoxide and catalyzes the reaction from $O_2^{\cdot-}$ to H_2O_2 which can then be later converted into neutral oxygen molecules or water by CAT, GPx and similar enzymes [5,16]. *C. elegans* have six SOD isoforms. *sod-2* and *sod-3* encode for mitochondrial isoforms while *sod-1* and *sod-5* are for the cytosolic isoforms. *sod-4* produces two predicted extracellular variants [33]. *sod-1* and *sod-2* are expressed during normal development; however, *sod-3* and *sod-5* expression is elevated during dauer stage [34]. Dauer larvae is a stress-resistant, developmentally arrested stage formed in response to adverse environmental conditions and this stage is thought to be important for *C. elegans* increased lifespan [34,35]. Interestingly, loss of individual and/or

multiple *sod* genes does not appear to affect *C. elegans* lifespan, but SOD activity was required for worm survival to acute stressors [36].

CAT is an oxidoreductase heme-containing enzyme that eliminates toxic levels of H₂O₂ through the generation of water and oxygen [32]. *C. elegans* have three catalase genes *ctl-1*, *ctl-2* and *ctl-3*. *ctl-1* and *ctl-2* are known to affect lifespan as loss of *ctl-2* shortens lifespan and oxidative stress was also found to increase catalase activity [37]. Among the catalases, *ctl-3* is not well characterized. GSTs catalyze the conjugation of oxidized lipids and free radicals to the electron donor glutathione (GSH). These enzymes function as both antioxidants and detoxification cofactors through the process of neutralizing ROS [5,38,39]. GPxs utilize the cofactor GSH to reduce hydrogen peroxide resulting in the formation of oxidized glutathione (GSSG) and water molecules as a by-product [40]. Overexpression of GSTs and GPxs were found to increase resistance to juglone and paraquat agents that cause oxidative stress [41]. As detoxification enzymes protect organisms against oxygen toxicity, the further understanding of these mechanisms that maintain homeostasis will help in the discovery of novel ways to mitigate damage arising from free radicals [5, 16, 38, 39]. Figure 1.1 summarizes the reactions of SOD, CAT, GPx and GST during ROS detoxification.

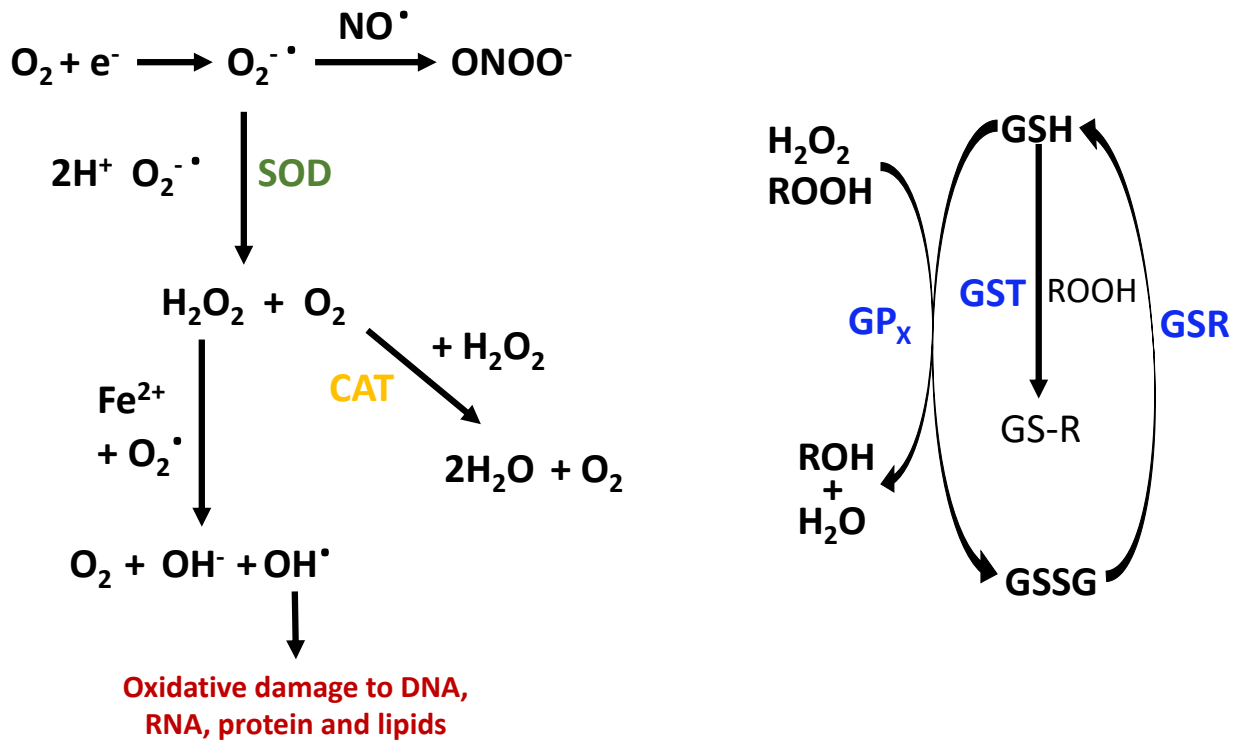


Figure 1.1 The generation of Reactive Oxygen Species and the detoxification by antioxidant enzymes.

ROS molecules form either free radicals or non-radical oxidants such as superoxide anion radicals, hydrogen peroxide, and hydroxyl radical. Antioxidant enzymes and the reactions they catalyze are shown. SOD, superoxide dismutase; CAT, catalase; GPX, glutathione peroxidase; GSR, glutathione reductase; and GST, glutathione-S-transferase. GPxs, and GSTs require glutathione (GSH) cofactor, and GSH can also scavenge for free radicals. GSR reduces the oxidized form of GSH (GSSG).

1.2.3 Aging, lifespan and longevity in *C. elegans*

Given the numerous oxidative species that are produced, biomolecules within cells are extremely vulnerable to ROS attack. Many oxidative stress response pathways tend to have overlaps with pathways affecting aging, lifespan and longevity [31]. Aging is loosely defined as the time-related deterioration of the physiological functions necessary for survival that results from progressive and unregulated accumulation of molecular and cellular damage leading to death [6,35,42–44]. Work in *C. elegans* on aging have been fruitful for finding potential disease genes and established that aging was a phenomenon that could be studied genetically. These studies have shown that aging is a regulated process with many of the nematode genes having the same functions in the regulation of aging in *Drosophila*, mice, and possibly humans.

The first forward-genetic screen found that mutations in the *age-1* gene, which enables 1-phosphatidylinositol-3-kinase activity, resulted in long-lived *C. elegans* [45]. With mutation mapping, these studies have proved that single gene mutations can have dramatic effects on an organism's lifespan. Since then, research in *C. elegans* with respect to aging has exploded. With the realization that lifespan is regulated by the insulin/IGF-1 signalling (IIS), determining which genes affect lifespan and longevity can potentially lead to the discovery of targets that may play a role in delaying the onset of many age-related diseases [46].

Recently, many studies have challenged the idea that ROS directly causes aging and presented strong evidence that ROS signalling actually combats aging [5,16,47,48]. In *C. elegans*, an increase in ROS levels leads to increased lifespan and ROS acts more as an anti-aging signalling molecule than as an oxidative damage inducing agent [5]. Nonetheless, ROS levels still need to be maintained at an appropriate level as excess ROS will continue to cause oxidative damage and contribute to cell toxicity [30, 49].

1.3 Transcriptional regulation and stress response pathways in *C. elegans*

During development, growth or responses to biological needs, eukaryotes require that gene expression, either constitutive, tissue specific or stage-specific, be mediated through transcription factors. Transcription factors are proteins that recognize specific stretches of nucleotides, called motifs, and bind to DNA to either activate, initiate, repress or cause DNA methylation and chromatin modification events [50]. Transcription factors are *trans*-regulatory elements that act on distant genes and can have a global presence to regulate their expression [51]. However, the conversion of gene sequences to mRNA and the process of protein synthesis are energetically demanding and inappropriate gene expression can have detrimental effects on cell health. Thus, transcription is a highly regulated process that governs the expression of genes essential to the development and survival of all metazoans. The precise temporal and spatial control is necessary as mutations in transcription factors and misregulation of these gene expression programs can lead to development of diseases. Many diseases arise from mutations in the regulatory regions of transcription factors, cofactors, chromatin regulators and noncoding RNAs can contribute to cancer, autoimmunity, neurological disorders, developmental syndromes, diabetes, cardiovascular disease and obesity [52,53]. Many of the MAP kinase (MAPK) and IIS pathways are involved in signalling cascades that regulate transcription factors. These pathways have been shown to be implicated in oxidative stress, aging, lifespan and longevity which can influence numerous human diseases [54]. Here, I discuss the major pathways in the *C. elegans* that are important to this thesis including the regulatory mechanisms that affect two key regulators of longevity, SKN-1/Nrf2 and DAF-16/FOXO.

1.3.1 The Insulin/Insulin-like Growth Factor signaling (IIS) pathway

The *C. elegans* IIS pathway is an integrated system and allows the nematode to respond accordingly to signals pertaining to nutrient levels, metabolism, growth, development, reproduction, aging and longevity. This pathway is conserved across other organisms and is regulated by insulin-like peptides that bind to activate the insulin/IGF-1 transmembrane receptor IGFR, known as the DAF-2 ortholog in worms [55]. Figure 1.2 compares the similarities and differences between the conserved insulin and IGF-1-like signalling pathways in nematodes, flies, and mice. The DAF-2 receptor has intrinsic tyrosine kinase activity and once activated, can trigger downstream cascades [56]. Under normal conditions DAF-2 signalling is on, and recruitment of phosphoinositide 3-kinase, AGE-1/PI3K, will activate serine/threonine kinases PDK-1, AKT-1 and AKT-2 resulting in the phosphorylation of DAF-16/FOXO. The DAF-18/PTEN lipid phosphatase counteract AGE-1/PI3K signalling. Specific phosphorylation of DAF-16/FOXO regulates its interaction with 14-3-3 regulatory proteins, PAR-5 and FTT-2, which control its subcellular localization [55]. Depending on the type of phosphorylation that DAF-16/FOXO undergoes, it can also be activated and trans-localization of DAF-16/FOXO into the nucleus can interact with additional factors, like SKN-1/Nrf2, to affect gene transcription. The IIS pathway is known to be involved in the regulation of dauer and L1 arrest. When *C. elegans* hatch, the first stage is known as L1 and here, if conditions are unfavourable, larvae will undergo developmental arrest [57]. Reduced IIS results in a dauer-constitutive phenotype and mutations in the DAF-2/IGFR slows down larval development suggesting that DAF-16/FOXO activation, as a direct result of IIS inhibition, promotes survival in starvation-induced L1 arrest and promotes dauer arrest in response to environmental stressors [55]. *daf-2/IGFR* mutants are long-lived and are also more resilient to heat stress, oxidative stress, hypoxia, osmotic stress, heavy metal stress and ultraviolet radiation [58–63].

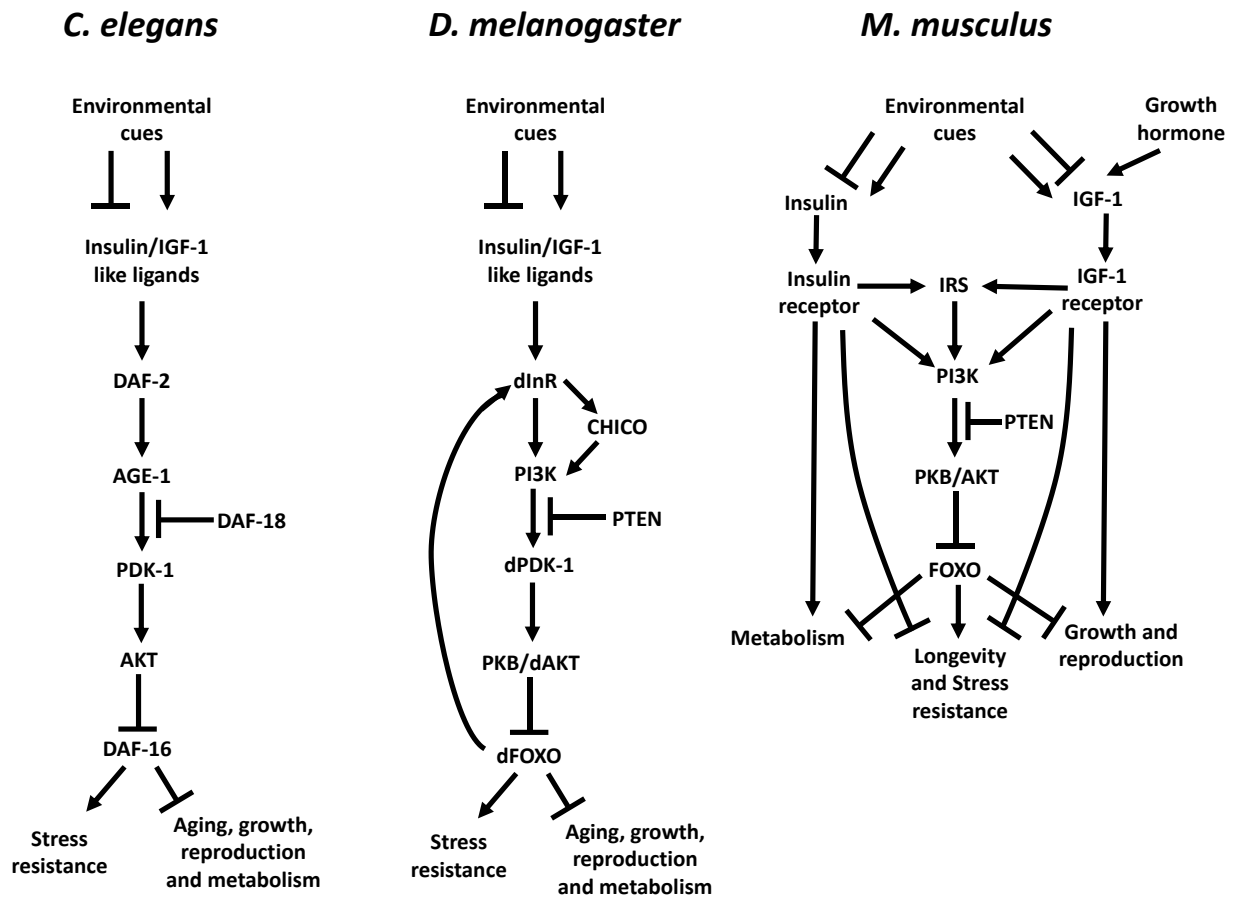


Figure 1.2 Schematic showing the conserved insulin and IGF-1-like signalling pathways in nematodes, flies, and mice. Pathways were adapted from Sutphin and Kaerberlin, 2011 [64].

1.3.2 The mTOR pathways

The mechanistic Target of Rapamycin (mTOR) is a serine/threonine kinase that regulates growth, development and behaviours through modulating protein synthesis and responses to environmental cues [65]. Also known as the ‘nutrient-sensing centres’ mTOR functions as complexes with other proteins and two mutually exclusive TOR-binding proteins, DAF-15/Raptor to form mTORC1 and RICT-1/Rictor to form mTORC2 [66]. Although mTORC1 and mTORC2 have roles in regulating larval germline and post-embryonic development, I will focus on their roles in aging, lifespan and stress responses.

mTORC1 is negatively regulated by the upstream IIS pathway, AMP-activated protein kinase (AMPK) and rapamycin (Figure 1.3) [67]. In response to the AMP/ATP energy ratio, stress conditions and low ATP levels activate AMPK to drive catabolic processes to restore cells back to a normal energy state [68]. AMPK is a conserved heterotrimeric protein complex composed of α catalytic subunits and β/γ regulatory subunits [69]. In *C. elegans*, *aak-1* and *aak-2* genes encode for the α catalytic subunits and AAK-2 was found to be the primary responder to oxidative stress [70]. Overexpression and/or activation AAK-2 contributes to resistance of *C. elegans* to heat shock and lifespan extension in a DAF-16 dependent manner [71,72]. AMPK can inhibit mTORC1 through two distinct mechanisms: phosphorylation of tumor suppressor TCS2 on conserved serine sites will cause it to complex with TCS1 and downregulate mTORC1, or AMPK can directly phosphorylate Raptor to impair mTORC1 signalling (Figure 1.3) [73–75]. Previous work surrounding the role of *C. elegans* AAKs suggest that there is a correlation between lipid metabolism, oxidative stress, aging and longevity. Rapamycin is an antifungal metabolite produced by *Streptomyces hygroscopicus* and has inhibitory effects on mTOR in mammalian, *Drosophila*, and yeast cells [76–78]. Rapamycin inhibit mTORC1 by binding the

FK506-binding protein FKBP12, which then interacts physically with the complex and decreases its activity. Much more is known about mTORC1 than mTORC2, but chronic exposure to rapamycin can sequester mTOR from mTORC2, inhibiting the assembly of the complex [79]. In *C. elegans*, the ortholog of TOR is LET-363 and the inhibition of mTORC1 and mTORC2, either through rapamycin or through food/nutrient sensing, was found extend lifespan and increased stress resistance (Figure 1.3) [65]. However, the mechanism of how mTORC1 and mTORC2 affects longevity is different [79]. An established role of mTORC1 is to regulate mRNA translation and protein synthesis. It is thought that reduced rates of translation resulting from mTORC1 inhibition could influence aging as a reduction in protein synthesis would lessen the number of damaged and/or misfolded proteins and reduce energy expended when resources are limited [67]. This would ultimately reduce the burden on organisms and lower stress levels, leading to enhanced lifespan. Transcription is also altered when translation is reduced and is partially or fully dependent on transcription factor DAF-16/FOXO [67]. SKN-1/Nrf-2 is also found to be required for lifespan extension from reduced translation suggesting that there is some overlap in DAF-16/FOXO and SKN-1/Nrf function. It is unclear how reduced translation causes these effects on transcription, although it appears that transcription factors that defend against stress are preferentially translated when translation rates are low [80].

Studies have revealed that the IIS pathway acts upstream of mTORC1 but mTORC1 can also negatively regulate IIS through protein S6 kinases (S6Ks) [81]. There is a complex relationship between the IIS and mTOR signalling that is integrated to affect aging. Similarly, the IIS pathway can also interact with mTOR through the mTORC2 complex which activates AKT to repress DAF-16/FOXO activity [82]. RICT-1 of the mTORC2 complex and the downstream phosphorylation target, SGK-1, appears to have a role in *C. elegans* aging [67]. During cold

stress, DAF-16/FOXO is a target of SGK-1 and its activity is enhanced in neurons and intestines to promote lifespan (Figure 1.3). Loss of the mTORC2 component *rict-1* was also found to increase SKN-1/Nrf nuclear occupancy and extend lifespan independently of DAF-16/FOXO [81,83]. Thus, current evidence supports the idea that mTORC signalling pathways act as evolutionarily conserved regulators of longevity and increase lifespan by mechanisms that are overlapping but distinct from IIS.

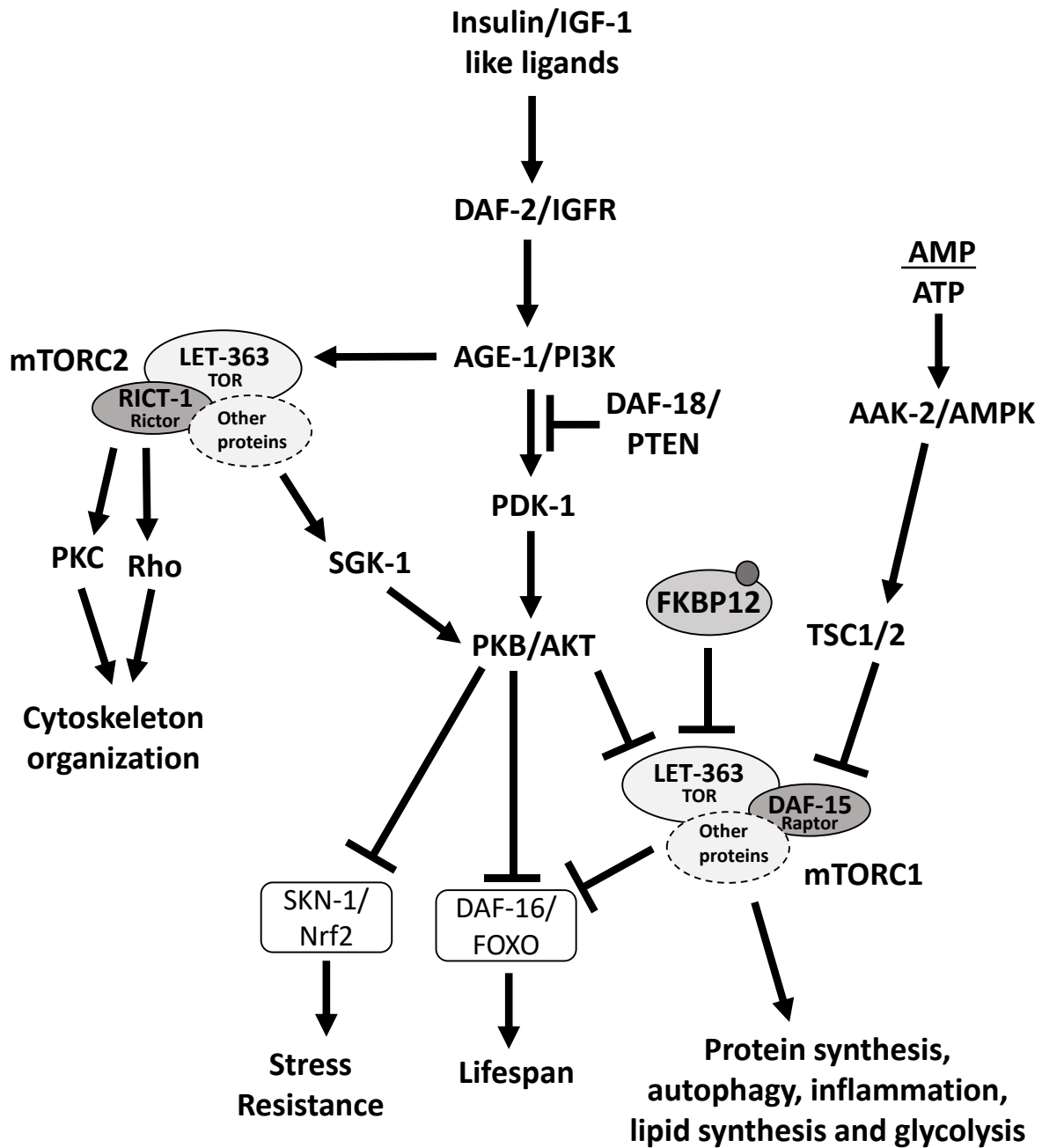


Figure 1.3 Pathways affecting mechanistic TOR1 and TOR2 complexes and their downstream targets and biological processes. Adapted and modified from Blackwell *et al.*, 2019 [84].

1.3.3 The MAPK pathways

Mitogen-activated protein kinase (MAPK) signalling pathways serve as transducers relaying extracellular signals to cellular responses and allow for adaptation to environmental changes or stressful conditions. There are many MAPK signalling cascades that exist but the three main MAPK families are the extracellular signal-regulated kinase (ERK), the c-Jun N-terminal kinase (JNK) and the p38 MAPK, and each is essential for various biological processes [85]. The signalling cascade begins with a stimuli that is relayed, amplified and integrated by the MAPK pathway through the activation of three enzymes in series: a MAPK kinase kinase (MAPKKK, a MAPK kinase (MAPKK) and MAP Kinase (MAPK) to elicit a physiological response such as cell proliferation, differentiation, inflammatory response and apoptosis [85].

The **ERK pathway** is perhaps the most well characterized of the MAPK pathways. Stimulation of tyrosine kinase receptors (RTKs) can activate the MAPK phosphorylation cascade starting with the MAPKKK RAF1, then MAPKK MEK1 and MEK2 and lastly MAPK ERK-1 and ERK-2. Their enzymatic activity is enhanced during their phosphorylated state and activated ERK-1 and ERK-2 can enter the nucleus where they can transactivate transcription factors to regulate gene expression [86]. Activated G-coupled protein receptors can also lead to the phosphorylation of RTKs and Ras signalling, called Ras-ERK, to activate MAPK networks [87]. In *C. elegans*, the ERK/MAPK is highly conserved, and the cascade consists of *lin-45*/RAF1, *mek-2*/MEK1/2 and *mpk-1*/ERK1/2. The ERK/MAPK-mediated signalling pathway promotes longevity through direct phosphorylation of SKN-1 by MPK-1 at sites that affect its nuclear translocation in intestinal cells of *C. elegans*. Activated SKN-1 in turn, regulate the DAF-2/DAF-16 IIS signalling through a positive feedback loop by repressing the expression of insulin-like

peptides [88]. This observation suggests that SKN-1 and MPK-1 acts upstream of DAF-2 to extend lifespan with overlap occurring between MAPK and IIS.

The **c-Jun N-terminal kinase (JNK)** family is a subgroup of the MAPK superfamily, and the signal transduction cascade can be activated by cytokines and exposure to environmental stress [89]. The JNK is implicated in the regulation of critical biological processes such as cancer, development, apoptosis and cell survival [89]. In mammals, JNK components were found to interact with IIS through the insulin receptor substrate 1 (IRS-1) or through protein kinase B (AKT) and in *Drosophila*, it was observed to be involved in life span regulation and stress resistance [90]. In *C. elegans*, the mammalian JNK and JNK kinase orthologs are JNK-1 and JKK-1 respectively [91]. When lifespan was examined in loss-of-function *jnk-1* and *jkk-1* mutants, there was a significant decrease in lifespan suggesting that the JNK pathway positively regulated processes leading to longevity [92]. Further studies found that phosphorylation of JNK-1 was required for lifespan extension and works through direct binding and subsequent activation of DAF-16/FOXO [92]. Overexpression of JNK-1 confers stress resistance to heat and oxidative stress and affects nuclear translocation of DAF-16 [92]. Interestingly, combining a hypomorphic mutation in the IIS pathway with *jnk-1* overexpression produced further increased lifespan which suggested that there was a parallel network between MAPK and IIS that converge onto DAF-16 [92].

Similar to the previously discussed MAPK pathways, the **p38 MAP kinase** is also evolutionarily conserved across species and play an important role in adaptation, homeostasis, neuronal symmetry development, and specialized responses to stress [93]. In *C. elegans*, *sek-1* encodes a MAPK kinase and *nsy-1* encodes the upstream MAPKK kinase. The p38 MAPK pathway respond to a variety of stressors and inflammatory cytokines. Extensive research on the

p38 MAPK pathway has shown that oxidative stress inducing compounds, such as arsenite, paraquat and *tert*-Butyl hydroperoxide, can activate this signal transduction pathway [93]. In *sek-1* mutants, treatment with arsenite resulted in defective PMK-1 activation suggesting that the SEK-1 MAPKK is an essential upstream activator of PMK-1 [93]. During oxidative stress, the p38 MAPK pathway regulates the nuclear localization of SKN-1 through phosphorylation by PMK-1 and results in the induction of antioxidant genes such as *gst-4* and *gcs-1* [93,94]. This suggests that SKN-1 is a direct target of PMK-1. More recently, the p38 MAPK ortholog, *pmk-1*, appears have functions in immune responses that is required against microbial pathogen attacks [95,96]. A schematic of the three described MAPK pathways is shown in Figure 1.4.

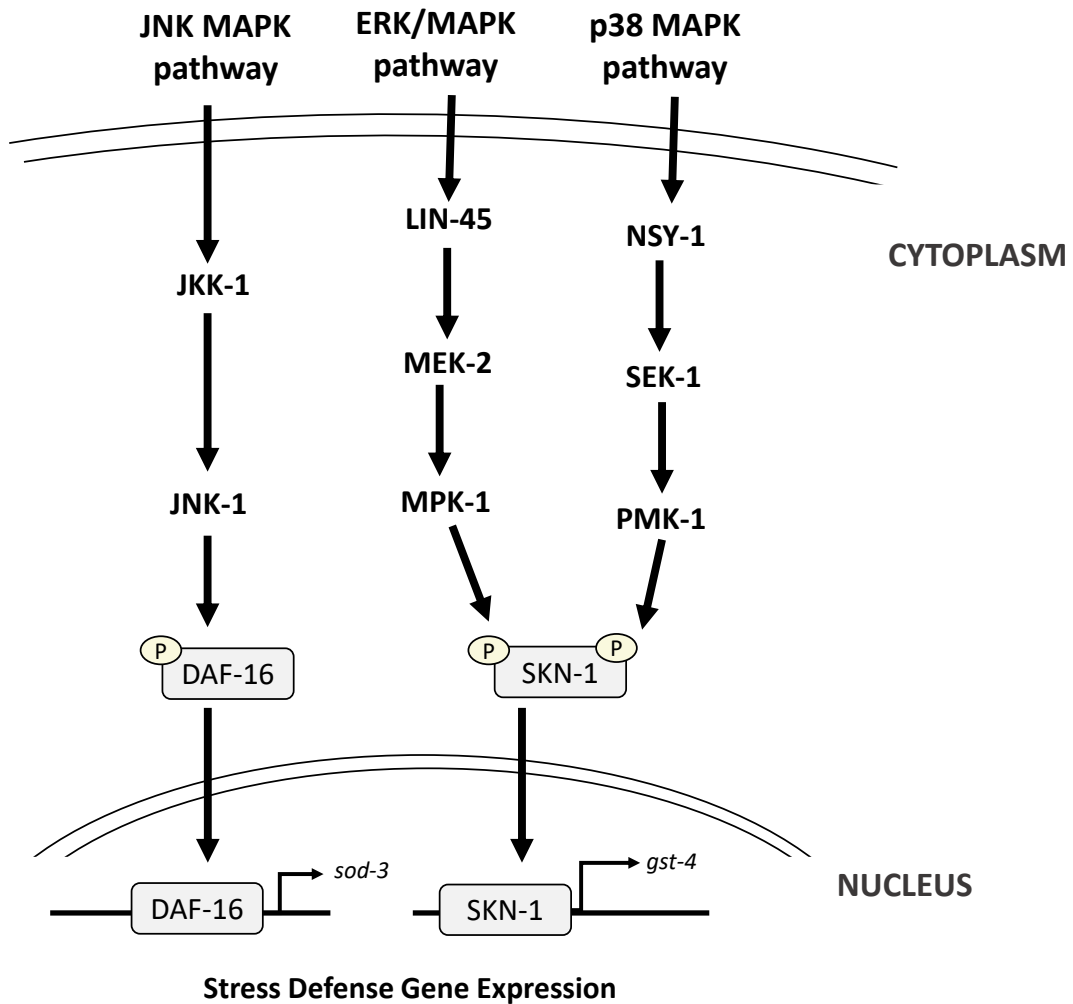


Figure 1.4 Schematic representation of JNK, ERK and p38 MAP Kinase pathway that regulate SKN-1 and DAF-16 in the *C. elegans* oxidative stress response.

Respective components of the individual MAPK pathways adapted from Inoue *et al.*, 2005 [93], Tullet *et al.*, 2017 [97], Okuyama *et al.*, 2010 [88], Wu *et al.*, 2016 [98], Blackwell *et al.*, 2015 [99], and Spatola *et al.*, 2019 [100].

1.3.4 microRNA gene silencing pathway

microRNAs (miRNAs) belong to a class of regulatory RNAs called small, non-coding RNAs (sncRNAs). miRNAs act to downregulate protein levels of target mRNAs by acting as “guide molecules” for the miRNA induced silencing complex (miRISC). In *C. elegans*, miRNA primary transcripts are processed by Dicer/DCR-1 before complexing with argonaut protein (ALG-1) prior to loading onto the miRISC. These miRISC complexes can then bind to target mRNAs at their complimentary 3'UTRs to repress gene expression (Figure 1.5) [101,102]. Although miRNAs have been heavily studied for their roles in developmental regulation, recent studies in *C. elegans* have found that miRNAs change their expression during aging, suggesting that miRNA expression may also regulate lifespan [103]. miRNAs negatively regulate gene expression at the post-transcriptional level and miRNAs have partial or perfect sequence complementarity to their mRNA targets [104]. For example, *lin-4* miRNA accumulates in the early larval stage of *C. elegans* to suppress the expression of its target gene, thereby regulating an important developmental transition stage [102]. However, during adulthood, overexpression of *lin-4* miRNA and *lin-4* loss-of-function mutants exhibited longer lifespan and higher resistance to heat shock. Further research found that *lin-4* miRNA actually regulates lifespan in worms through the IIS pathway suggesting that mRNA and miRNA-mediated negative regulation can influence longevity [102]. Gene expression profiling in *C. elegans* found that genomic instability and unfavourable transcription activation was directly proportional to aging with many genes encoding for heat shock proteins and stress resistance factors decreasing in aged animals [105,106]. Other studies found that SKN-1 expression also appears to be inhibited by miRNAs and *mir-228*, *mir-84* and *mir-241* negatively regulate SKN-1 during immune responses and dietary restriction induced longevity [106,107].

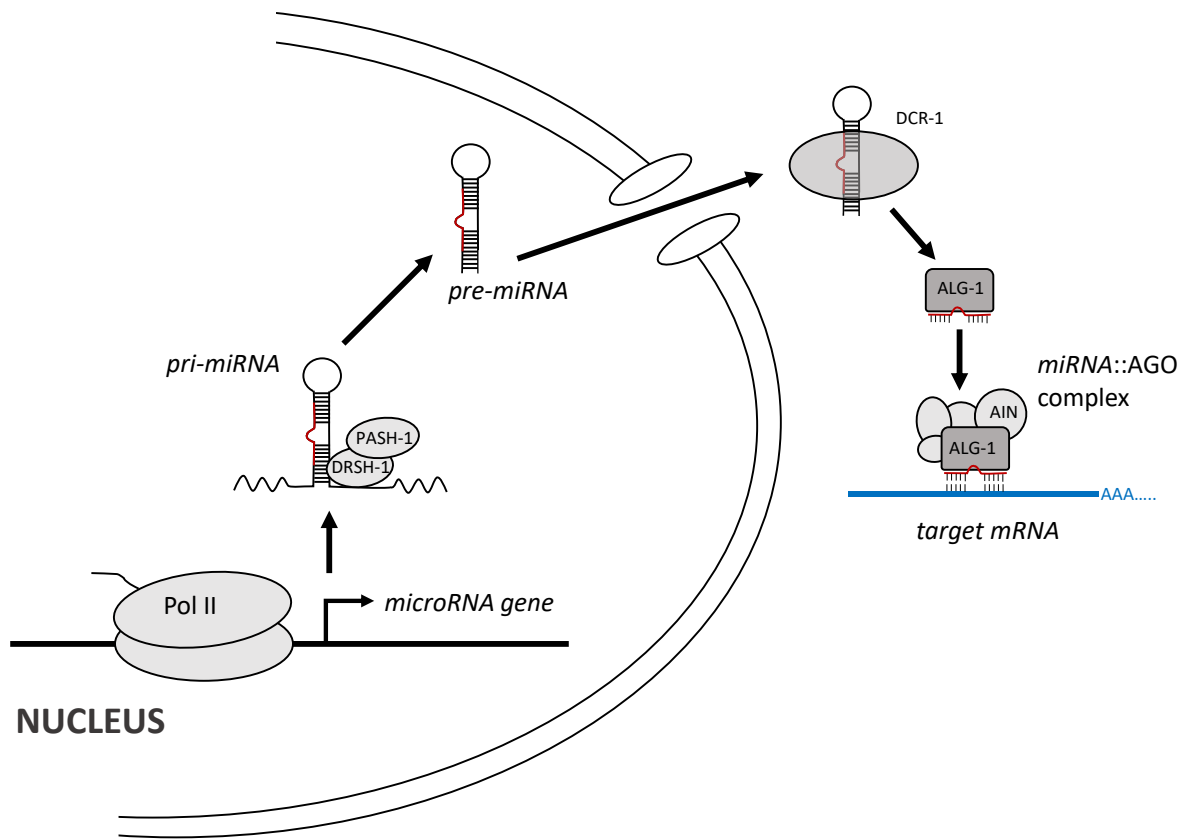
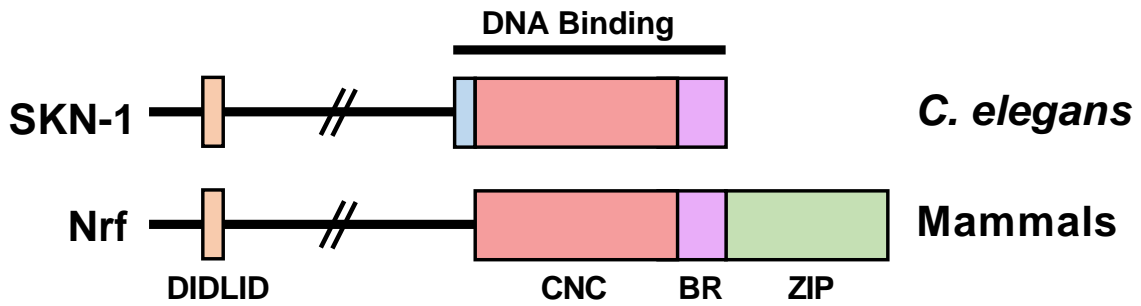


Figure 1.5 MicroRNA processing and function in *C. elegans*. The microRNA gene is transcribed in the nucleus and microRNA primary transcripts (pri-miRNA) is processed by DRSH-1 and PASH-1. The precursor mRNA (pre-mRNA) hairpin is exported and additional processing by DCR-1 generates the mature miRNA. The miRNA binds to Argonaute protein (ALG-1) and is loaded into a core microRNA-induced Silencing Complex (miRISC) to target mRNAs via complimentary sites at the 3'UTRs. Adapted and modified from Ambros and Ruvkun, 2018 [101].

1.4 SKN-1/Nrf2 and its involvement in the oxidative stress response

As previously mentioned, SKN-1/Nrf2 is one of the master regulators of transcription and perform a wide range of developmental, protective and maintenance functions. In *C. elegans*, one of the well-known functions of the Nrf2 ortholog, SKN-1, is to promote oxidative stress resistance through the regulation of the antioxidant defense system. Since the nematode demonstrates functional conservation and regulates the same target genes found in other species, it offers exceptional predictive value for understanding how mammalian Nrf/CNC proteins are regulated. The Nrf (NF-E2-related factor)/CNC family of transcription factors are basic-leucine zipper (bZIP) transcription factors that require their Maf (musculoaponeurotic fibrosarcoma) partner to form heterodimers for stable DNA binding [98–101]. The mammalian Nrf/CNC is defined by the presence of the CNC (Cap ‘n’ Collar) and the basic region (BR) domains for DNA-binding, however, SKN-1 lacks the ZIP dimerization molecule. In *C. elegans*, the SKN-1 CNC domain has evolved to form a helical structure that recognizes SKN-1 cognate sites and allows for DNA binding that is comparable to that of a bZIP dimer (Figure 1.6A) [112,113]. Also conserved is a 14-residue motif called the DIDLID element that is important for transcription activation and interaction with other proteins [114]. There are four mammalian Nrf/CNC proteins, Nrf1, Nrf-2, Nrf3 and p45 NF-E2, and of these, Nrf2 is heavily studied [109]. The *C. elegans* SKN-1 has four isoforms generated through alternative splicing [29]. *skn-1a-c* expressed *in vivo* and *skn-1d* expression is predicted but not confirmed (Figure 1.6B) [114]. The SKN-1A and SKN-1C isoforms mainly function to mediate stress responses while SKN-1B functions in the two ASI chemosensory neurons for dietary restriction-induced longevity [115,116]. The expression of SKN-1 is located in the nuclei of precursor cells of the intestines during embryogenesis and in the larval/adult stage of life, SKN-1 is expressed in the cytoplasm but accumulates in the nuclei under stress [117,118].

A



B

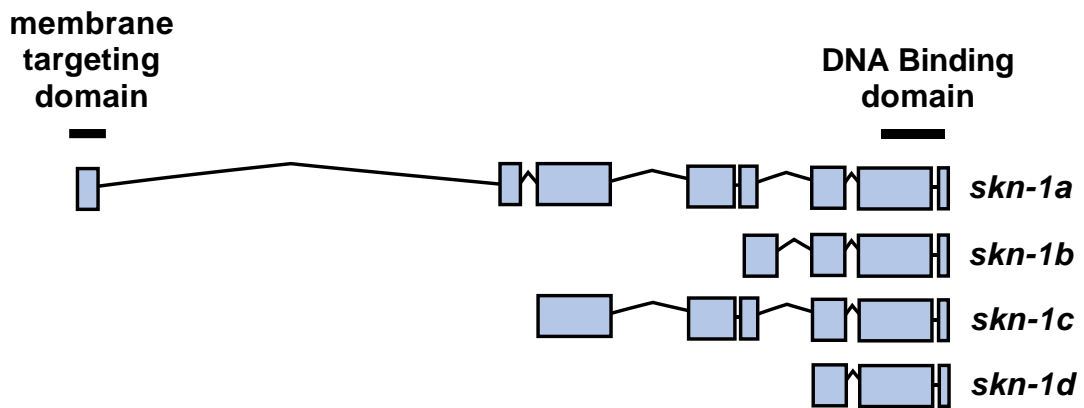


Figure 1.6 SKN-1 is the *C. elegans* ortholog of the highly conserved mammalian Nrf/CNC proteins.

(A) SKN-1 and Nrf/CNC both contain the DIDLID and DNA-binding regions. Although SKN-1 lacks the ZIP domain (green), SKN-1 interacts directly with specific DNA sequences through the BR and short element (light blue) in the minor groove. (CNC: Cap'n'Collar in red; BR: Basic Region in pink) (B) *C. elegans* have three isoforms of the *skn-1* gene, while *skn-1a-c* has been confirmed *in vivo*, *skn-1d* is predicted.

1.4.1 The Mechanism of SKN-1 function and regulation

One of the post embryonic functions of SKN-1/Nrf2 is to regulate Phase II (PII) detoxification genes needed to defend against acute oxidative stress. Because SKN-1/Nrf are under negative regulation to prevent constitutive activation, elucidating what mechanisms are important for proper SKN-1/Nrf function will help provide further insight to what factors influence disease states and identify potential targets for therapy.

In *C. elegans*, SKN-1 is activated through different MAPK pathways by specific MPK-1 and PMK-1 kinase phosphorylation and its nuclear translocation promotes the transcription of PII detoxification genes [97,99,119]. This results in expression of target genes associated with stress resistance although the mechanism by which SKN-1 promotes the activation of antioxidant genes to achieve longevity and increased lifespan is still poorly defined. Other protein kinases, such as AKT-1/2, SGK-1 and GSK-3, have been shown to be implicated in SKN-1 inhibition [98,115].

BRAP2 (BRCA-1 Associated Protein 2) was first found to bind nuclear localization motifs of the human tumour suppressor BRCA1 and have many roles in different pathways [120]. BRAP2 is a negative regulator of the Ras/MAPK pathway which can be activated when a ligand binds to RTKs followed by phosphorylation and recruitment of the GEF-Grb2 adaptor protein complex that triggers Ras signalling (Figure 1.7) [121]. When BRAP2 binds Ras-GTP, BRAP2 is auto-ubiquitinated and auto-degraded through its E3 ligase activity [121,122]. Other regulatory roles of BRAP2 include ubiquitination of protein phosphatases for degradation and cytoplasmic retention of proteins [123].

The *C. elegans* BRAP-2 is an E3 ubiquitin ligase and its activity is conserved in the worm orthologs of the Ras-MAPK signalling (Figure 1.7). Recent studies have shown that BRAP-2

also functions in the oxidative stress response and mutations in *brap-2* can be lethal or cause developmental arrest in larval worms [120]. BRAP-2 negatively regulates the ERK/MAPK pathways and in *brap-2(ok1492)* mutants, loss of BRAP-2 leads to an increase in phosphorylated MAPK activity and affects downstream regulation of SKN-1 [88]. Thus, BRAP-2 plays a crucial role in modulating stress response pathways.

Like Nrf2, SKN-1 can still be negatively regulated by other proteins and through ubiquitin mediated proteolysis. Keap1 is an actin-binding protein that interacts with Nrf2. Under basal conditions, Nrf2 is bound in the cytoplasm to Keap1, which prevents the induction of PII enzymes [124]. To date, a true *C. elegans* Keap-1 ortholog has yet to be identified, however, the WD40 repeat protein, WDR-23, functions as a direct repressor of SKN-1 [29]. Under normal physiological conditions, WDR-23 is a ubiquitin ligase adaptor protein that simultaneously binds to SKN-1, CUL-4 and DDB-1 [29,124–126]. The CUL-4/DDB-1 complex regulates various nuclear processes ranging from DNA damage, to DNA replication and chromatin remodeling, but CUL-4/DDB-1 binding to substrates, in this case WDR-23, will trigger selective ubiquitylation and basal protein degradation of SKN-1 (Figure 1.7) [124,127,128]. SKN-1 in *C. elegans* and Nrf2 in mammals are regulated by distinct ubiquitin ligases that function in different cellular compartments. SKN-1 proteasomal degradation occurs in the nucleus while Nrf2 ubiquitination and degradation is cytosolic [125]. Upon exposure to endogenously or exogenously derived oxidants, *C. elegans* SKN-1 is released from WDR-23 repression and accumulates in the nuclei to activate genes that protect cells from any resulting damage [124]. *wdr-23* loss of function mutations leads to constitutive activation of *gst-4* and upregulation of glutathione synthesis through *gcs-1* promotes longevity and stress resistance [29]. Upstream of WDR-23 are SKR-1/2 (SKP1- related) proteins, which are homologs of human SKP1 and a

member of the SCF (SKP1-CUL1-F-box protein) complex, target substrate proteins for ubiquitin-mediated degradation by the proteasome [129–132]. *C. elegans* have numerous SKR proteins and SKR-1/2 was previously shown to be required for longevity in *daf-2* mutants [98]. RNAi knock down of *skr-1/2* mimicked *skn-1* RNAi patterns that do not require PMK-1 dependant SKN-1 activation [120,133,134]. GST pulldown analysis indicated that SKR-1/2 interacts and functions as an upstream modulator of WDR-23 to positively regulate SKN-1 activity [98]. SKN-1 can be activated by various mechanisms, with BRAP-2, WDR-23 and SKR-1/2 being just some of the upstream mediators that play a crucial role in modulating the levels of PII detoxification enzymes during stress response.

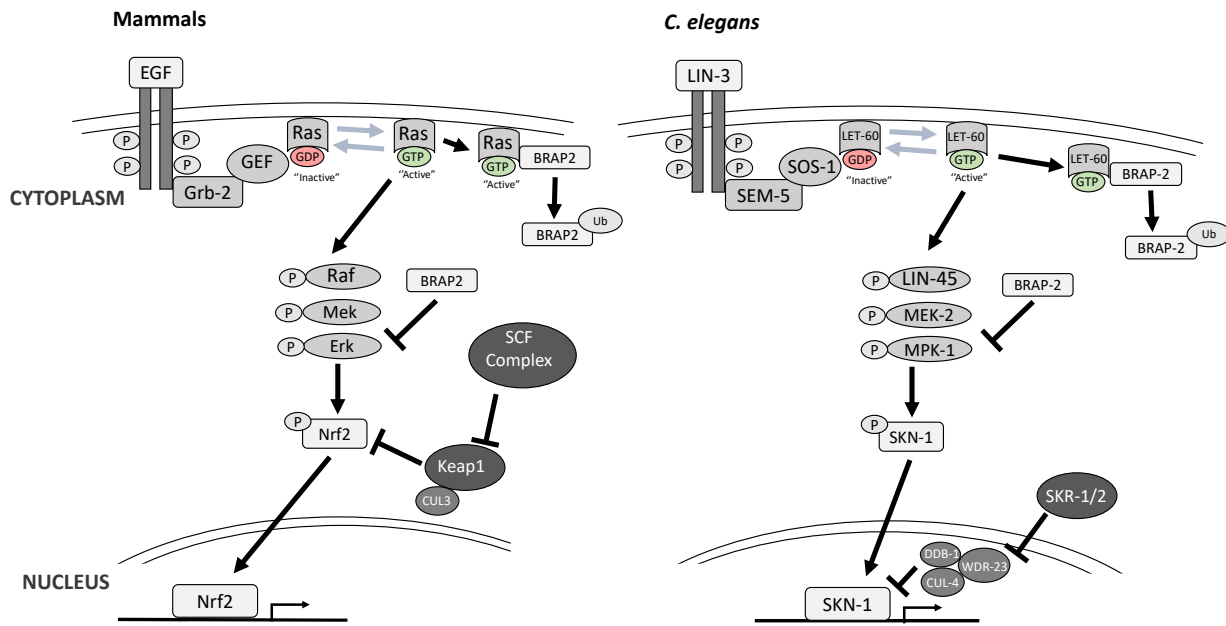


Figure 1.7 Comparison of the Ras-MAPK signalling and the proteasomal degradation pathway that regulates Nrf2/SKN-1 in mammals and *C. elegans*.

Adapted and modified from Kolch 2005 [121], Spatola *et al.*, 2019 [100] and Ji *et al.*, 2019 [135].

1.5 DAF-16/FOXO and its role in the oxidative stress response

DAF-16/FOXO is another master key regulator of responses related to stress resistance. FOXOs belong to the class O of the Forkhead transcription factors with their distinct Forkhead box DNA-binding domain (Figure 1.8A) [136]. In mammals, there are four FOXO genes, FOXO1, FOXO3, FOXO4 and FOXO6, while the *C. elegans* only have one FOXO gene named *daf-16* [137]. *daf-16* encodes eight isoforms, *daf-16a* to *daf-16h*, although *daf-16a*, and *daf-16d/f/h* appear to be the major isoforms that are involved in dauer arrest and longevity (Figure 1.8C) [138]. Both the human FOXO and the *C. elegans* DAF-16 share high similarity in their function, pathways, and sequences especially in the Forkhead DNA binding domain. DAF-16A has the same RxRxxS/T phosphorylation motif as the FOXO proteins while the DAF-16D/F/H isoforms contain a QxRxxS motif instead (Figure 1.8B) [139,140]. The *C. elegans* DAF-16 can recognize the TTGTTTACT sequence named the DAF-16 Binding Element (DBE), which is a core consensus sequence found at numerous phase I (PI) genes. DAF-16 also has the DAF-16 Associate Element (DAE) with a GATA site that can recognize the CTTATCA sequence present at promoters of PII detoxification genes [141–143]. AMPK, JNK, mTOR and IIS pathways are involved in aging and longevity with DAF-16/FOXO being an important downstream target that integrates the different signalling from these pathways.

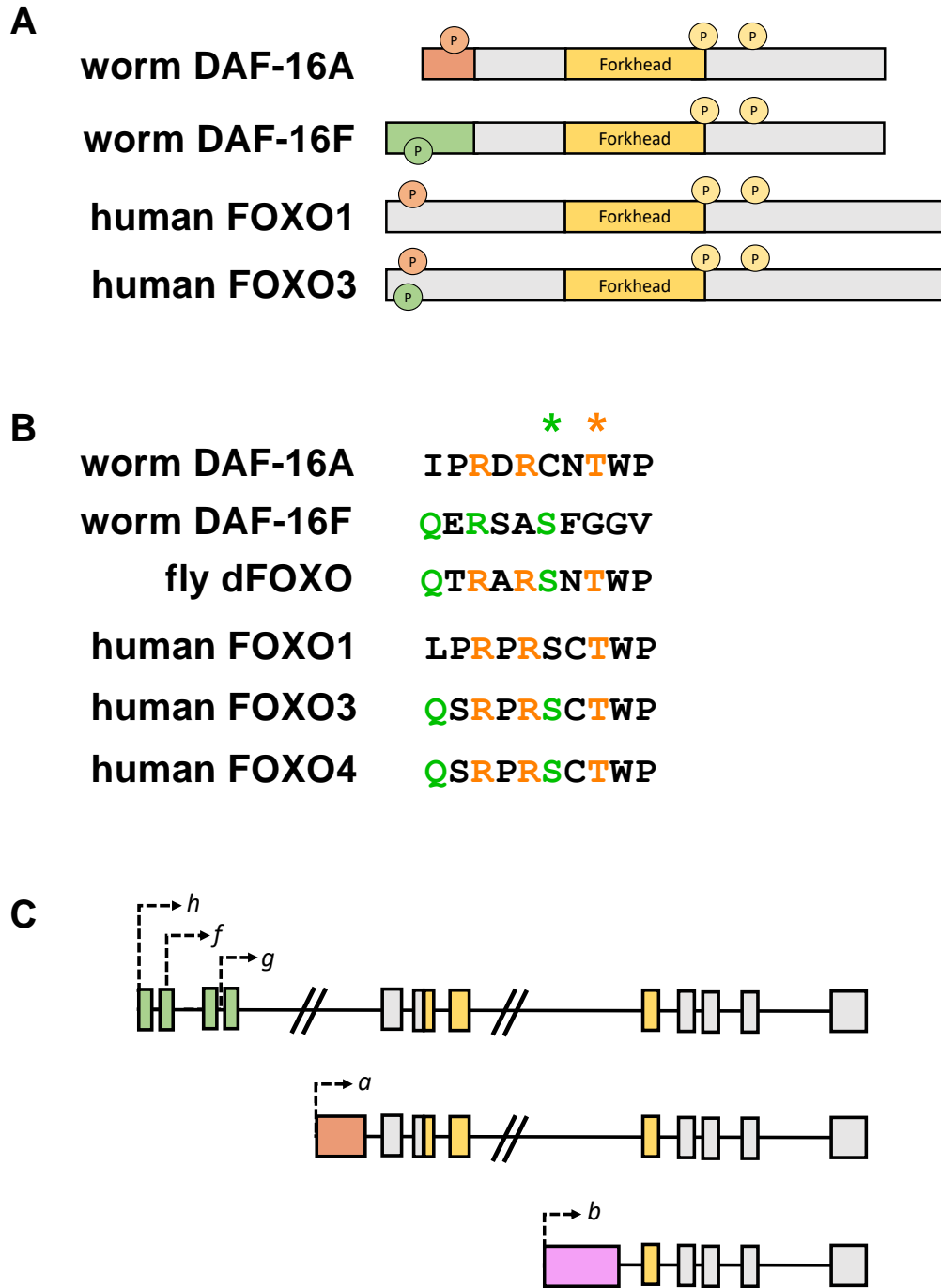


Figure 1.8 Schematic comparing the *C. elegans* DAF-16 and human FOXO.

(A) DAF-16A/F isoforms and human FOXO1 and FOXO3 with their conserved Forkhead domain. (B) DAF-16A and DAF-16F share two highly conserved RxRxxS/T Akt-family consensus phosphorylation motifs (orange) and QxRxxS motif (green) with human FOXO and *Drosophila* dFOXO. (C) The different *daf-16* isoforms *h/f/g/a/b*. Information obtained from WormBase and modified from Murphy and Hu, 2018 [55] and Chen *et al.*, 2015 [144].

1.5.1 The mechanism of DAF-16 function and activation

DAF-16 (the sole ortholog of the FOXO family of transcription factors) is responsible for activating genes involved in ageing, longevity, lipogenesis, heat shock survival and oxidative stress resistance via the nutrient sensing IIS pathway [145]. The IIS pathway is conserved across species with the *C. elegans*' DAF-16 being a common downstream mediator of longevity and lifespan extension. During food deprivation and unfavourable conditions, DAF-16 also causes *C. elegans* to undergo a dormancy transformation known as “dauer” [138]. This aging-controlling and growth pathway is regulated by insulin-like peptide (ILPs) [146–148]. Under normal conditions, IIS is on to negatively regulate DAF-16. Upon DAF-2/IGFR activation, the signaling cascade results in the recruitment of various kinases that phosphorylates DAF-16. This causes DAF-16 to be sequestered in the cytosol by 14-3-3 regulatory proteins and retention in the cytoplasm renders it inactive [148]. Thus, worms with any mutation in the signalling cascade, for example at the DAF-2 receptor - denoted as *daf-2* mutants, are long-lived with increased lifespan. Activation of DAF-16 and subsequent nuclear localization of DAF-16 can trigger transcriptional activity of genes that promote stress resistance and prolong lifespan. This switch from a pro-growth/reproductive state to a maintenance mode results in worm longevity [149,150]. When DAF-16 responds to stressors, such as heat, anoxia, oxidative, starvation and exposure to pathogenic bacteria, genes such as *sod-3*, *dod-3* and *mtl-1* are activated [149]. DAF-16 is also activated by acute levels of ROS, thus, DAF-16's sensitivity to changes in ROS levels suggests that ROS can potentially have regulatory functions to modulate specific enzyme activities [22,149].

1.6 The evolution of the pluripotency marker mammalian REX1/ZFP42

Human REX1 (Reduced Expression Protein 1), also referred to as ZFP42, is a zinc finger transcription factor that contains four repeats of the C₂H₂, Cys-His, motifs (Figure 1.9A) [151]. This protein is encoded by the *ZFP42* gene and is a member of the YY1 (Ying Yang 1) subfamily of transcription factors. YY1 is a Gli-Kruppel type zinc finger protein with a DNA-binding domain at the C-terminus and modulating domains at the N-terminus that allows for protein-protein interaction with other key factors [152]. YY1 can act as an activator, repressor or initiator depending on the other regulatory elements found at the YY1-binding sites [152,153]. YY1 is a highly conserved family and similar genes are found in other vertebrate species. Phylogenetic analyses of YY1 found that duplication events and retroposition was responsible for generating YY2 (Ying Yang 2) and REX1 paralogs in humans [154]. Similar events in *Drosophila* resulted in proteins, Pleiohomeotic (PHO) and Pho-like (PHOL), that were found to be very similar to YY1, while fish genomes, zebrafish and pufferfish, have two active copies of YY1 (Figure 1.9B) [154]. YY1, YY2 and REX1 have co-evolved to have essential roles in development and cell cycle control. Analysis of the DNA-binding motifs found that majority of the DNAs bound by YY1 and YY2 had the consensus sequence CGCCATnTT while the DNAs bound by REX1 were slightly different, and categorized into two groups, Type 1: GGCAGCCATTA and Type 2: GGCCATTA [154]. Although there are differences in the consensus sequences that would result in different binding specificities, the core -CCAT- motif is retained in all three genes suggesting that conservation of at least two zinc fingers were responsible for maintaining a similar core target motif [154].

REX1 was discovered independently and before the identification of YY1 and YY2 when its expression profile was found to be abruptly downregulated as embryonic stem cells began to differentiate [151]. The initial studies were conducted in F9 teratocarcinoma stem cells where

REX1 was found to be expressed at high levels but the mRNA of *Rex1* steadily decreased in the presence of retinoic acid which resulted in differentiation of cells in early mouse embryos [151]. *Rex1* has been found to be critical in maintaining the proliferative state of pluripotent stem cells while simultaneously preventing differentiation during embryo development. *Rex1* expression was also found to be inversely correlated with MAPK signalling, with activation of the ERK and p38 MAPK pathways inhibiting *Rex1* [155–157]. REX1 activity is controlled by transcription factors OCT3/4 in humans [158]. *oct3/4* has a dual role, that is, it can both repress and activate the *Rex1* promoter. At low levels, OCT3/4 proteins activates the *Rex1* promoter while high levels of OCT3/4 will repress the promoter activity [158]. This implies that the regulation of REX1 depends on various upstream transcription factors and networks involving protein kinases. Since then, *Rex1* is now primarily used as a marker for the undifferentiated state of pluripotent stem cells.

1.7 Current understanding of Transcription Factor ZTF-17: The *C. elegans* Zinc Finger Putative Transcription Factor family

The *C. elegans* ZTF-17 still remains an uncharacterized transcription factor, although the mammalian homolog REX1/ZFP42 and *Drosophila* ortholog PHOL are a pluripotency factors involved in regulating development [159]. The *ztf-17* gene encodes for a protein that is 705 amino acids (aa) in size and is part of the zinc finger putative transcription factor family (WormBase). Figure 1.9C is schematic representation showing that ZTF-17 has two C₂H₂ type zinc finger protein domains located at position 268 and 319 and a Low Complexity Region (LCR) of ~10aa in length at position 627 in its protein sequence (SMART: Simple Modular Architecture Research Tool). LCRs are protein sequences that have little diversity in their aa composition, and it is suspected that the position of LCRs within the sequence is important in

determining the binding properties and biological roles of proteins [160]. Centrally-located LCRs have been shown to be implicated in transcription while terminal LCRs are enriched with translation and stress-response related functions [160]. Based on ZTF-17's overall Gene Ontology, it is believed that ZTF-17 enables RNA polymerase II transcription via *cis*-regulatory region and sequence-specific DNA binding activity (WormBase). While some characteristics of ZTF-17 as a transcription factor have been described, the role of ZTF-17 outside of development is less elucidated. Using *C. elegans* as a model organism, my aim is to look at the different pathways involved in lifespan extension and longevity by looking at the MAPK and IIS pathways. I hope to further the understanding of the transcriptional regulator, ZTF-17, which I suspected to be multi-functional and represses the expression of genes involved in the oxidative stress response.

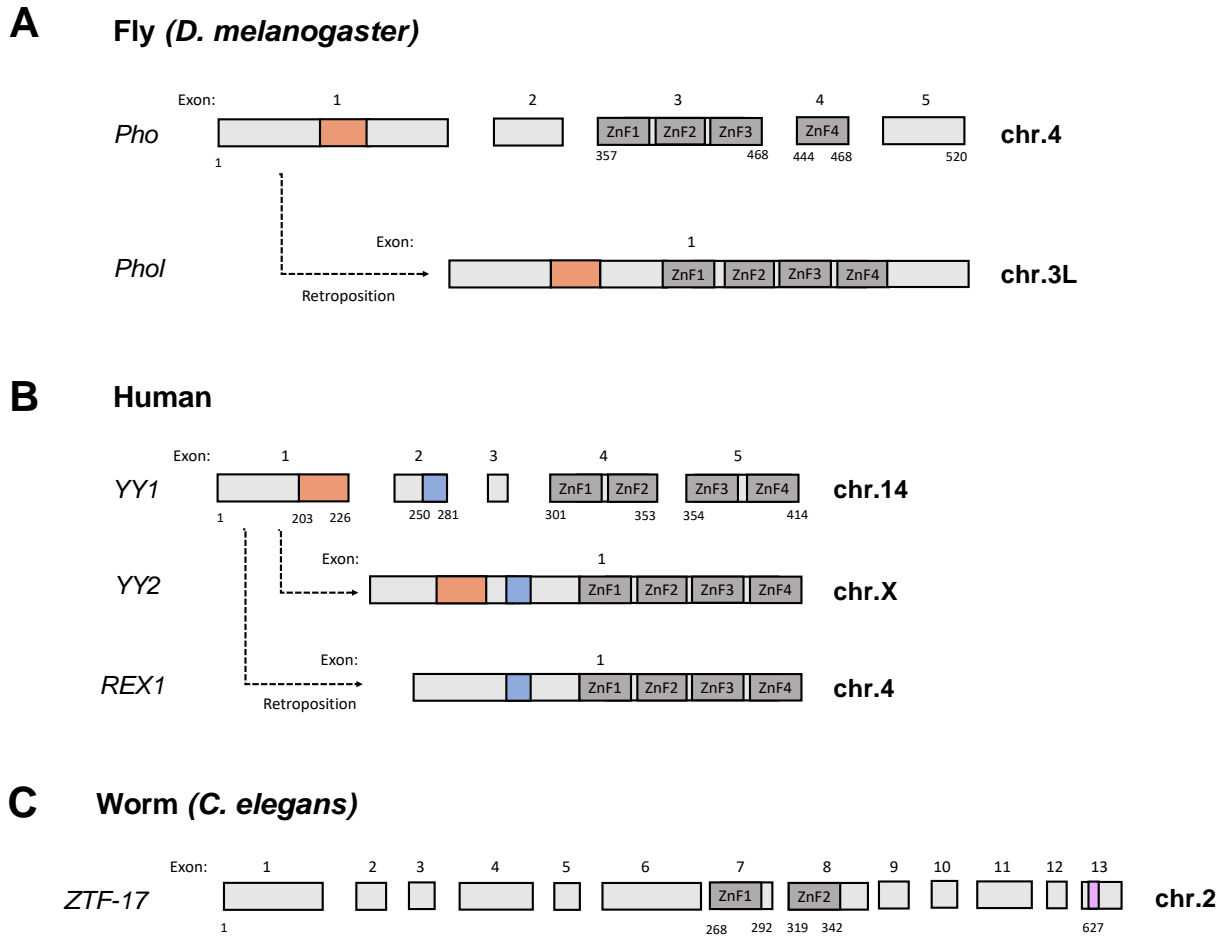


Figure 1.9 Exon structures of PHO and PHOL in *D. melanogaster*, YY1, YY2 and REX1 in humans, and ZTF-17 in *C. elegans*.

(A-B) The protein coding regions of PHO and YY1 are made up of five distinct exons. PHOL, YY2 and REX1 arises from retroposition-driven duplication in flies and humans and the entire coding region of each is localized within one exon in different chromosomal positions. Conserved domains are colour coded: Domain I (orange), Domain II (blue) and Zinc Finger domains (dark gray). (C) Genomic illustration of *ztf-17* in *C. elegans* which is made up of 13 exons consisting of two Zinc Fingers and a Low Complexity Region (pink).

1.7.1 ZTF-17 positively regulates *lin-39*

Hox genes are important during development as they are responsible for the differential gene expression required for specifying structures along the anteroposterior axis of bilaterians [161]. The discovery of *Hox* genes were originally found to be clustered in *Drosophila* and encoded transcription factors that contained a DNA-binding and homeodomain [162]. *Hox* genes are conserved across species and also known as “selector” genes, that is, they can choose certain pathways for development to take place and results in the specific formation of structures, limbs and organs at the correct places on the body plan of animals [161]. Thus, mutations in *Hox* genes, called homeotic mutations, can result in changes from one structure to another or body parts forming in the wrong location. There are six *Hox* genes in *C. elegans*, *lin-39*, *mab-5* and *egl-5* are required for proper embryonic development while *ceh-13*, *nob-1* and *php-3* are required during post-embryonic development [163–167]. Of the *Hox* genes mentioned, *lin-39* is required for correct development in the midbody region and is responsible for vulva development arising from vulval precursor cell (VPC) fate specification in the L3 stage [161,168]. *In vivo* analysis of *lin-39* levels and enhanced yeast one-hybrid (eY1H) experiments identified 16 *C. elegans* transcription factors that bound to specific *lin-39* genomic DNA [169]. Of those transcription factors, the orphan nuclear hormone receptor NHR-43, hypodermal fate regulator LIN-26 and GATA factor ELT-6 positively regulated *lin-39* expression during the transition from embryonic precursors to VPCs [168]. Additionally, three other factors, zinc finger proteins ZTF-17, BED-3 and T box factor TBX-9, also positively regulated *lin-39* expression [168]. ZTF-17 was found to be bound to DNA ~2kb upstream of *lin-39* and *ztf-17* RNAi treated animals had decreased *lin-39* expression at the L3 stage suggesting that ZTF-17 may be a positive larval regulator of *lin-39* [168].

1.7.2 *mir-77* is a candidate target gene of ZTF-17

As mentioned previously, miRNAs are an important component in gene expression for numerous biological processes ranging from sex determination to embryonic development, but certain miRNAs in *C. elegans* can contribute to lifespan regulation and stress responses [104,170]. A particular interest lies with *mir-77*, an miRNA that was identified as a target of ZTF-17 through eY1H assays that mapped interactions between transcription factors and regulatory genomic regions within *C. elegans* [169]. *mir-77* was found to have very low or absent expression in early developmental stages but then upregulated after the mid-L4 and young adult stages only to be downregulated again with aging [171,172]. Alterations in expression of miRNAs over time implied that there was a potential role of *mir-77* to regulate processes, such as reproduction, metabolism, and aging, in adult worms. Interestingly, *mir-77* was also found to be a target of zinc finger proteins LIN-26, SEM-2, SEM-4 and homeobox protein ALR-1, which all have roles in *C. elegans* larval development like ZTF-17 [169]. This suggests that there may be a link where transcription factors that regulate early development, could also have dual roles in regulating stress resistance and aging mechanisms.

1.8 Rationale, hypotheses and objectives of this thesis

The current understanding of ZTF-17 is limited and information about its function as a transcription factor is scarce in the literature. Previous work published by our lab has shown that *C. elegans* BRAP-2 was involved in preventing inappropriate responses when there were elevated ROS levels, and that BRAP-2 was a key regulator of PII detoxification. In an attempt to identify novel regulatory components of oxidative stress, an RNAi screen for transcription factors affecting *gst-4::gfp* was done and here, it was revealed that animals lacking *ztf-17* gene expression appeared to have enhanced GFP expression. This suggested that ZTF-17 was capable

of negatively regulating PII detoxification genes. New evidence from preliminary experiments also suggest that ZTF-17 may have a role in modulating the expression of DAF-16 target genes, for instance *sod-3*. Since the ZPF42/REX1 homolog appears to repress transcription of genes involved in mammalian development, I aim to investigate whether ZTF-17 possessed similar repressor like functions in *C. elegans* [159].

Some possibilities to explain why the absence of *ztf-17* resulted in increased *gst-4* expression include: (a) removing the repressive effects of ZTF-17 on promoters allowed SKN-1 to bind and activate PII detoxification genes, (b) ZTF-17 affects upstream regulators of SKN-1, like PMK-1, or MPK-1, such that removal of ZTF-17 causes enhanced SKN-1 activity, (c) ZTF-17 is required for expression of miRNAs that regulates *skn-1* mRNA, or (d) some other undefined mechanism.

At this stage of investigation, I suspected ZTF-17 to have repressor like functions in the oxidative stress response. Thus, the objective of my project was to contribute to the understanding of the oxidative stress response pathways in *C. elegans* by investigating the role of ZTF-17. My aim is to characterize ZTF-17's role by precisely determining the signalling pathways through which ZTF-17 regulates stress resistance genes and derive a mechanism for its function using molecular and genetic approaches. I plan on investigating the signalling pathways that link ZTF-17 to SKN-1, DAF-16 or any of the associated regulatory components. Based on my recent findings, I hypothesize that transcription factor ZTF-17 is a repressor that attenuates the expression of detoxification genes required for the oxidative stress response in *C. elegans*. I also hypothesize that the absence of ZTF-17 will relieve the inhibitory effects on antioxidant gene expression by increasing the effects of SKN-1 and DAF-16 in activating its target promoters thus, allowing stress resistance to be enhanced.

1.9 References

1. Benoît D'Autréaux & Toledano, M. B. ROS as signalling molecules: mechanisms that generate specificity in ROS homeostasis. *Nat Rev Mol Cell Biol* **8**, 813–824 (2007).
2. Finkel, T. & Holbrook, N. J. NATURE - Finkel 2000 - Oxidative stress and biology of ageing. *Nature* **408**, 239–247 (2000).
3. Finkel, T. Signal transduction by reactive oxygen species. *J. Cell Biol.* **194**, 7–15 (2011).
4. Fleeson, W. *et al.* No {Title}. *J. Pers. Soc. Psychol.* **1**, 1188–1197 (2017).
5. Van Raamsdonk, J. M. & Hekimi, S. Reactive Oxygen Species and Aging in *Caenorhabditis elegans* : Causal or Casual Relationship? *Antioxid. Redox Signal.* **13**, 1911–1953 (2010).
6. Hekimi, S., Lapointe, J. & Wen, Y. Taking a ‘good’ look at free radicals in the aging process. *Trends Cell Biol.* **21**, 569–576 (2011).
7. Berks, M. The *C. elegans* genome sequencing project. *Genome Res.* **5**, 99–104 (1995).
8. Schrimpf, S. P. *et al.* Comparative functional analysis of the *Caenorhabditis elegans* and *Drosophila melanogaster* proteomes. *PLoS Biol.* **7**, 0616–0627 (2009).
9. Kaletta, T. & Hengartner, M. O. Finding function in novel targets: *C. elegans* as a model organism. *Nat. Rev. Drug Discov.* **5**, 387–399 (2006).
10. O'Brien, Kevin P.; Westerlund, Isabelle; Sonnhammer, E. L. L. OrthoDisease: a database of human disease orthologs. *Hum. Mutat.* **24**, 112–119 (2004).
11. Nigon, V. & Félix, M. History of research on *C. elegans* and other free-living nematodes as model organisms. *Online Rev. C. elegans Biol.* (2018).
12. Dues, D. J. *et al.* Aging causes decreased resistance to multiple stresses and a failure to activate specific stress response pathways. *Aging (Albany, NY).* **8**, 777–795 (2016).
13. Ishii, N. Oxidative stress and aging in *Caenorhabditis elegans*. *Free Radic. Res.* **33**, 857–864 (2000).
14. Harman, D. Aging: a theory based on free radical and radiation chemistry. *J Gerontol.* **11**, 298–300 (1956).
15. Apfeld, J. & Alper, S. What Can We Learn About Human Disease from the Nematode *C. elegans*? *Methods Mol. Biol.* **1706**, 53–75 (2018).
16. Van Raamsdonk, J. M. & Hekimi, S. Superoxide dismutase is dispensable for normal animal lifespan. *Proc. Natl. Acad. Sci.* **109**, 5785–5790 (2012).
17. Van Raamsdonk, J. M. & Hekimi, S. Deletion of the mitochondrial superoxide dismutase *sod-2* extends lifespan in *Caenorhabditis elegans*. *PLoS Genet.* **5**, (2009).
18. Monaghan, P., Metcalfe, N. B. & Torres, R. Oxidative stress as a mediator of life history trade-offs: Mechanisms, measurements and interpretation. *Ecol. Lett.* **12**, 75–92 (2009).
19. Balaban, R. S., Nemoto, S. & Finkel, T. Mitochondria, oxidants, and aging. *Cell* **120**, 483–495 (2005).
20. Carocho, M. & Ferreira, I. C. F. R. A review on antioxidants, prooxidants and related controversy: Natural and synthetic compounds, screening and analysis methodologies and future perspectives. *Food Chem. Toxicol.* **51**, 15–25 (2013).
21. Surai, P. F. *Natural antioxidants and immunity. Natural Antioxidants in Avian Nutrition and Reproduction* (2002).
22. Russell, E. G. & Cotter, T. G. New Insight into the Role of Reactive Oxygen Species (ROS) in Cellular Signal-Transduction Processes. *Int Rev Cell Mol Biol* 221–254 (2015) doi:<https://doi.org/10.1016/bs.ircmb.2015.07.004>.

23. Holmström, K. M. & Finkel, T. Cellular mechanisms and physiological consequences of redox-dependent signalling. *Nat. Rev. Mol. Cell Biol.* **15**, 411–421 (2014).
24. Rhee, S. G. H₂O₂, a Necessary Evil for Cell Signaling. *Science (80-)*. **312**, 1882–1883 (2006).
25. Dröge, W. Free radicals in the physiological control of cell function. *Physiol. Rev.* **82**, 47–95 (2002).
26. Ruchko, M. V. *et al.* Hypoxia-induced oxidative base modifications in the VEGF hypoxia-response element are associated with transcriptionally active nucleosomes. *Free Radic. Biol. Med.* **46**, 352–359 (2009).
27. Murphy, M. P. How mitochondria produce reactive oxygen species. *Biochem. J.* **417**, 1–13 (2009).
28. Tawe, W., Eschbach, R., Walter, R. & Henkle-Duehrsen, K. Identification of stress-responsive genes in *Caenorhabditis elegans* using RT-PCR differential display. *Nucleic Acids Res.* **26**, 1621–1627 (1998).
29. Tang, L. & Choe, K. P. Characterization of *skn-1/wdr-23* phenotypes in *Caenorhabditis elegans*; pleiotrophy, aging, glutathione, and interactions with other longevity pathways. *Mech. Ageing Dev.* **149**, 88–98 (2015).
30. Hu, Q., D’Amora, D. R., MacNeil, L. T., Walhout, A. J. M. & Kubiseski, T. J. The *Caenorhabditis elegans* Oxidative Stress Response Requires the NHR-49 Transcription Factor. *G3* **8**, 3857–3863 (2018).
31. Hu, Q., D’Amora, D. R., Macneil, L. T., Walhout, A. J. M. & Kubiseski, T. J. The Oxidative Stress Response in *Caenorhabditis elegans* Requires the GATA Transcription Factor ELT-3 and SKN-1/Nrf2. *Genetics* **206**, 1909–1922 (2017).
32. Davies, K. J. A. Oxidative stress, antioxidant defenses, and damage removal, repair, and replacement systems. *IUBMB Life* **50**, 279–289 (2000).
33. Trachootham, D., Lu, W., Ogasawara, M. A., Valle, N. R. Del & Huang, P. Redox regulation of cell survival. *Antioxidants Redox Signal.* **10**, 1343–1374 (2008).
34. Gems, D. & Doonan, R. Antioxidant defense and aging in *C. elegans*: Is the oxidative damage theory of aging wrong? *Cell Cycle* **8**, 1681–1687 (2009).
35. Gems, D. & Partridge, L. Genetics of Longevity in Model Organisms: Debates and Paradigm Shifts. *Annu. Rev. Physiol.* **75**, 621–644 (2013).
36. Doonan, R. *et al.* Against the oxidative damage theory of aging: Superoxide dismutases protect against oxidative stress but have little or no effect on life span in *Caenorhabditis elegans*. *Genes Dev.* **22**, 3236–3241 (2008).
37. Petriv, O. I. & Rachubinski, R. A. Lack of Peroxisomal Catalase Causes a Progeric Phenotype in *Caenorhabditis elegans*. *J. Biol. Chem.* **279**, 19996–20001 (2004).
38. Rodriguez, M., Basten Snoek, L., De Bono, M. & Kammenga, J. E. Worms under stress: *C. elegans* stress response and its relevance to complex human disease and aging. *Trends Genet.* **29**, 367–374 (2013).
39. Sharma, Mohini, Stuti Gupta, Kalpana Singh, Mohit Mehndiratta, Amar Gautam, Om P. Kalra, R. S. and J. K. G. Association of glutathione-S-transferase with patients of type 2 diabetes mellitus with and without nephropathy. *Diabetes Metab. Syndr. Clin. Res. Rev.* **10**, 194 (2016).
40. Lubos, E., Loscalzo, J. & Handy, D. E. Glutathione peroxidase-1 in health and disease: From molecular mechanisms to therapeutic opportunities. *Antioxidants Redox Signal.* **15**, 1957–1997 (2011).

41. Burmeister, C. *et al.* Oxidative stress in *Caenorhabditis elegans* : protective effects of the Omega class glutathione transferase (GSTO-1) . *FASEB J.* **22**, 343–354 (2008).
42. Gilbert, S. F. *Developmental Biology. 6th edition. Aging: The Biology of Senescence. Sunderland (MA): Sinauer Associates* (2000).
43. Kirkwood, T. B. L. Understanding the odd science of aging. *Cell* **120**, 437–447 (2005).
44. Vijg, J. & Campisi, J. Puzzles, promises and a cure for ageing. *Nature* **454**, 1065–1071 (2008).
45. Klass, M. R. A method for the isolation of longevity mutants in the nematode *Caenorhabditis elegans* and initial results. *Mech. Ageing Dev.* **22**, 279–286 (1983).
46. Longo, V. D. *et al.* Interventions to slow aging in humans: Are we ready? *Aging Cell* **14**, 497–510 (2015).
47. Wang, Y., Ozer, D. & Hekimi, S. Mitochondrial function and lifespan of mice with controlled ubiquinone biosynthesis. *Nat. Commun.* **6**, (2015).
48. Lapointe, J. & Hekimi, S. When a theory of aging ages badly. *Cell. Mol. Life Sci.* **67**, 1–8 (2010).
49. Zhao, L. & Wang, J. Uncovering the mechanisms of *Caenorhabditis elegans* ageing from global quantification of the underlying landscape. *J. R. Soc. Interface* **13**, (2016).
50. Farnham, P. J. Insights from genomic profiling of transcription factors. *Nat. Rev. Genet.* **10**, 605–616 (2009).
51. Nowick, K., Gernat, T., Almaas, E. & Stubbs, L. Differences in human and chimpanzee gene expression patterns define an evolving network of transcription factors in brain. *Proc. Natl. Acad. Sci. U. S. A.* **106**, 22358–22363 (2009).
52. Reinke, Valerie, Krause, Michael, Okkema, P. Transcriptional Regulation of Gene Expression in *C. elegans*. *WormBook* 1–34 (2017)
doi:10.1895/wormbook.1.45.2.Transcriptional.
53. Lee, T. I. & Young, A. R. Transcriptional Regulation and its Misregulation in Disease. *Cell* **152**, 1237–1251 (2003).
54. Gami, M. S. & Wolkow, C. A. Studies of *Caenorhabditis elegans* DAF-2/insulin signaling reveal targets for pharmacological manipulation of lifespan. *Aging Cell* **5**, 31–37 (2006).
55. Murphy, C. T. & Hu, P. J. Insulin/insulin-like growth factor signaling in *C. elegans*. *Wormb. Online Rev. C. elegans Biol.* (2018).
56. Taniguchi, C. M., Emanuelli, B. & Kahn, C. R. Critical nodes in signalling pathways: insights into insulin action. *Nat. Rev. Mol. Cell Biol.* **7**, 85–96 (2006).
57. Ruaud, A. F., Katic, I. & Bessereau, J. L. Insulin/insulin-like growth factor signaling controls non-dauer developmental speed in the nematode *Caenorhabditis elegans*. *Genetics* **187**, 337–343 (2011).
58. Honda, Y. & Honda, S. The daf-2 gene network for longevity regulates oxidative stress resistance and Mn-superoxide dismutase gene expression in *Caenorhabditis elegans*. *FASEB J.* 1385–1393 (1999).
59. Murakami, S., and Johnson, T. . A genetic pathway conferring life extension and resistance to UV stress in *Caenorhabditis elegans*. *Genetics* **143**, 1207–1218 (1996).
60. Scott, B.A., Avidan, M.S., and Crowder, C. M. Regulation of hypoxic death in *C. elegans* by the insulin/IGF receptor homolog DAF-2. *Science (80-)*. **296**, 2388–2391 (2002).
61. Lithgow, G. J., White, T. M., Hinerfeld, D. A. & Johnson, T. E. Thermotolerance of a Long-lived Mutant of *Caenorhabditis elegans*. *J. Gerontol.* **49**, B270–B276 (1994).
62. Lamitina, S.T., and Strange, K. Transcriptional targets of DAF-16 insulin signaling

- pathway protect *C. elegans* from extreme hypertonic stress. *Am. J. Physiol. Cell Physiol.* **288**, C467-474 (2005).
63. Barsyte, D., Lovejoy, D.A., and Lithgow, G. . Longevity and heavy metal resistance in *daf-2* and *age-1* long-lived mutants of *Caenorhabditis elegans*. *FASEB J.* **15**, 627–634 (2001).
 64. Sutphin, G. L. & Kaeberlein, M. *Comparative genetics of aging. Handbook of the Biology of Aging* (Elsevier Inc., 2011). doi:10.1016/B978-0-12-378638-8.00010-5.
 65. Saxton, R. A. & Sabatini, D. M. mTOR Signaling in Growth, Metabolism, and Disease. *Cell* **168**, 960–976 (2017).
 66. Hara, K. *et al.* Raptor, a binding partner of target of rapamycin (TOR), mediates TOR action. *Cell* **110**, 177–189 (2002).
 67. Kaeberlein, M., Johnson, S. C. & Rabinovitch, P. S. mTOR is a key modulator of ageing and age-related disease. *Nature* **493**, 338–345 (2013).
 68. Carling, D. *et al.* Mammalian AmpActivated Protein-Kinase Is Homologous to Yeast and Plant Protein-Kinases Involved in the Regulation of Carbon Metabolism. *J. Biol. Chem.* **269**, 11442–11448.
 69. Mihaylova, M. & Shaw, R. The AMPK signalling pathway coordinates cell growth, autophagy and metabolism. *Nat Cell Biol* **13**, 1016–1023 (2011).
 70. Apfeld, J., O'Connor, G., McDonagh, T., DiStefano, P. & Curtis, R. The AMP-activated protein kinase AAK-2 links energy levels and insulin-like signals to lifespan in *C. elegans*. *Genes Dev* **18**, 3004–3009 (2004).
 71. Lee, H. *et al.* The *Caenorhabditis elegans* AMP-activated protein kinase AAK-2 is phosphorylated by LKB1 and is required for resistance to oxidative stress and for normal motility and foraging behavior. *J. Biol. Chem.* **283**, 14988–14993 (2008).
 72. Wong, C. & Roy, R. AMPK regulates developmental plasticity through an endogenous small rna pathway in *caenorhabditis elegans*. *Int. J. Mol. Sci.* **21**, 1–9 (2020).
 73. Moreno-Arriola, E., El Hafidi, M., Ortega-Cuéllar, D. & Carvajal, K. AMP-activated protein kinase regulates oxidative metabolism in *Caenorhabditis elegans* through the NHR-49 and MDT-15 transcriptional regulators. *PLoS One* **11**, 1–20 (2016).
 74. Gwinn, D. M. *et al.* AMPK Phosphorylation of Raptor Mediates a Metabolic Checkpoint. *Mol. Cell* **30**, 214–226 (2008).
 75. Huang, J. & Manning, B. D. The TSC1–TSC2 complex: a molecular switchboard controlling cell growth. *Biochem J.* **412**, 179–190 (2008).
 76. Kaira, K. *et al.* L-type amino acid transporter 1 and CD98 expression in primary and metastatic sites of human neoplasms. *Cancer Sci.* **99**, 2380–2386 (2008).
 77. Lin, Y. H. *et al.* Diacylglycerol lipase regulates lifespan and oxidative stress response by inversely modulating TOR signaling in *Drosophila* and *C. elegans*. *Aging Cell* **13**, 755–764 (2014).
 78. Huang, S., Bjornsti, M. A. & Houghton, P. J. Rapamycins: Mechanism of action and cellular resistance. *Cancer Biol. Ther.* **2**, 222–232 (2003).
 79. Vellai, T. *et al.* Influence of TOR kinase on lifespan in *C. elegans*. *Nature* **426**, 620 (2003).
 80. Harding, H. P. *et al.* Regulated translation initiation controls stress-induced gene expression in mammalian cells. *Mol. Cell* **6**, 1099–1108 (2000).
 81. Takano, A. *et al.* Mammalian Target of Rapamycin Pathway Regulates Insulin Signaling via Subcellular Redistribution of Insulin Receptor Substrate 1 and Integrates Nutritional

- Signals and Metabolic Signals of Insulin. *Mol. Cell. Biol.* **21**, 5050–5062 (2001).
82. Guertin, D. A. *et al.* Ablation in Mice of the mTORC Components raptor, rictor, or mLST8 Reveals that mTORC2 Is Required for Signaling to Akt-FOXO and PKC α , but Not S6K1. *Dev. Cell* **11**, 859–871 (2006).
 83. Mizunuma, M., Neumann-Haefelin, E., Moroz, N., Li, Y. & Blackwell, T. K. mTORC2-SGK-1 acts in two environmentally responsive pathways with opposing effects on longevity. *Aging Cell* **13**, 869–878 (2014).
 84. Keith Blackwell, T., Sewell, A. K., Wu, Z. & Han, M. TOR signaling in caenorhabditis elegans development, metabolism, and aging. *Genetics* **213**, 329–360 (2019).
 85. Wei, Z. & Liu, H. T. MAPK signal pathways in the regulation of cell proliferation in mammalian cells. *Cell Res.* **12**, 9–18 (2002).
 86. Stokoe, D., Macdonald, S., Cadwallader, K., Symons, M. & Hancock, J. Activation of Raf as a result of recruitment to the plasma membrane. *Science (80-.)*. **264**, 1463–1467 (1999).
 87. Pierce, K., Luttrell, L. & Lefkowitz, R. New mechanisms in heptahelical receptor signaling to mitogen activated to mitogen activated protein kinase cascades. *Oncogene* **20**, 1532–1539 (2001).
 88. Okuyama, T. *et al.* The ERK-MAPK pathway regulates longevity through SKN-1 and insulin-like signaling in Caenorhabditis elegans. *J. Biol. Chem.* **285**, 30274–30281 (2010).
 89. Davis, R. J. Signal transduction by the JNK group of MAP kinases. *Cell* **103**, 239–252 (2000).
 90. Wang, M. C., Bohmann, D. & Jasper, H. JNK signaling confers tolerance to oxidative stress and extends lifespan in Drosophila. *Dev. Cell* **5**, 811–816 (2003).
 91. Kawasaki, M. *et al.* A Caenorhabditis elegans JNK signal transduction pathway regulates coordinated movement via type-D GABAergic motor neurons. *EMBO J.* **18**, 3604–3615 (1999).
 92. Oh, S. W. *et al.* JNK regulates lifespan in Caenorhabditis elegans by modulating nuclear translocation of forkhead transcription factor/DAF-16. *Proc. Natl. Acad. Sci. U. S. A.* **102**, 4494–4499 (2005).
 93. Inoue, H. *et al.* The C. elegans p38 MAPK pathway regulates nuclear localization of the transcription factor SKN-1 in oxidative stress response. *Genes Dev.* **19**, 2278–2283 (2005).
 94. DH, K. *et al.* A conserved p38 MAP kinase pathway in Caenorhabditis elegans innate immunity. *Science (80-.)*. **297**, 623–626 (2002).
 95. Couillault, C. *et al.* TLR-independent control of innate immunity in Caenorhabditis elegans by the TIR domain adaptor protein TIR-1, an ortholog of human SARM. *Nat. Immunol.* **5**, 488–494 (2004).
 96. Kim, D. H. *et al.* A Conserved p38 MAP Kinase Pathway in Caenorhabditis elegans Innate Immunity. *Science (80-.)*. **297**, 623–626 (2002).
 97. Tullet, J. M. A. *et al.* The SKN-1/Nrf2 transcription factor can protect against oxidative stress and increase lifespan in C. elegans by distinct mechanisms. *Aging Cell* **16**, 1191–1194 (2017).
 98. Wu, C. W., Deonaraine, A., Przybysz, A., Strange, K. & Choe, K. P. The Skp1 Homologs SKR-1/2 Are Required for the Caenorhabditis elegans SKN-1 Antioxidant/Detoxification Response Independently of p38 MAPK. *PLoS Genet.* **12**, 1–30 (2016).
 99. Blackwell, T. K., Steinbaugh, M. J., Hourihan, J. M., Ewald, C. Y. & Isik, M. SKN-1/Nrf, stress responses, and aging in Caenorhabditis elegans. *Free Radic. Biol. Med.* **88**, 290–301

- (2015).
100. Spatola, B. N., Lo, J. Y., Wang, B. & Curran, S. P. Nuclear and cytoplasmic WDR-23 isoforms mediate differential effects on GEN-1 and SKN-1 substrates. *Sci. Rep.* **9**, 1–11 (2019).
 101. Ambros, V. & Ruvkun, G. Recent molecular genetic explorations of caenorhabditis elegans microRNAs. *Genetics* **209**, 651–673 (2018).
 102. Lee, R. C., Feinbaum, R. L. & Ambros, V. The C. elegans Heterochronic Gene lin-4 Encodes Small RNAs with Antisense Complementarity to lin-14. *Cell* **75**, 843–854 (1993).
 103. Kato, M., Chen, X., Inukai, S., Zhao, H. & Slack, F. J. Age-associated changes in expression of small, noncoding RNAs, including microRNAs, in C. elegans. *RNA* **17**, 1804–1820 (2011).
 104. Abbott, A. L. Uncovering new functions for MicroRNAs in caenorhabditis elegans. *Curr. Biol.* **21**, R668–R671 (2011).
 105. McCarroll, S. A. *et al.* Comparing genomic expression patterns across species identifies shared transcriptional profile in aging. *Nat. Genet.* **36**, 197–204 (2004).
 106. Golden, T. R. & Melov, S. Microarray analysis of gene expression with age in individual nematodes. *Aging Cell* **3**, 111–124 (2004).
 107. Liu, F. *et al.* Nuclear Hormone Receptor Regulation of MicroRNAs Controls Innate Immune Responses in C. elegans. *PLoS Pathog.* **9**, 1–14 (2013).
 108. Kensler, T. W., Wakabayashi, N. & Biswal, S. Cell Survival Responses to Environmental Stresses Via the Keap1-Nrf2-ARE Pathway. *Annu. Rev. Pharmacol. Toxicol.* **47**, 89–116 (2007).
 109. Sykiotis, G. & Bohmann, D. Stress-activated cap'n'collar transcription factors in aging and human disease. *Sci Signal.* **47**, 89–116 (2007).
 110. Hayes, J. D. & Dinkova-Kostova, A. T. The Nrf2 regulatory network provides an interface between redox and intermediary metabolism. *Trends Biochem. Sci.* **39**, 199–218 (2014).
 111. Taguchi, K., Motohashi, H. & Yamamoto, M. Molecular mechanisms of the Keap1-Nrf2 pathway in stress response and cancer evolution. *Genes to Cells* **16**, 123–140 (2011).
 112. Carroll, A. S. *et al.* SKN-1 domain folding and basic region monomer stabilization upon DNA binding. *Genes Dev.* **11**, 2227–2238 (1997).
 113. Blackwell, T., Bowerman, B., Priess, J. & Weintraub, H. Formation of a monomeric DNA binding domain by Skn-1 bZIP and homeodomain elements. *Science.* **266**, 621–628 (1994).
 114. Walker, A. K. *et al.* A conserved transcription motif suggesting functional parallels between Caenorhabditis elegans SKN-1 and Cap'n'Collar-related basic leucine zipper proteins. *J. Biol. Chem.* **275**, 22166–22171 (2000).
 115. Tullet, J. M. A. *et al.* Direct Inhibition of the Longevity-Promoting Factor SKN-1 by Insulin-like Signaling in C. elegans. *Cell* **132**, 1025–1038 (2008).
 116. Staab, T. A. *et al.* The Conserved SKN-1/Nrf2 Stress Response Pathway Regulates Synaptic Function in Caenorhabditis elegans. *PLoS Genet.* **9**, (2013).
 117. Hyde, R., Taylor, P. M. & Hundal, H. S. Amino acid transporters: roles in amino acid sensing and signalling in animal cells. *Biochem. J.* **373**, 1–18 (2003).
 118. Alison, K., Ventura, N., Kahn, N. & Johnson, T. E. Activation of SKN-1 by Novel Kinases in Caenorhabditis elegans. *Free Radic Biol Med.* **43**, 1560–1566 (2007).
 119. An, J. H. & Blackwell, T. K. SKN-1 links C. elegans mesendodermal specification to a

- Conserved Oxidative Stress Response. *Genes Dev.* **17**, 1882–1893 (2003).
120. Koon, J. C. & Kubiseski, T. J. Developmental arrest of *Caenorhabditis elegans* BRAP-2 mutant exposed to oxidative stress is dependent on BRC-1. *J. Biol. Chem.* **285**, 13437–13443 (2010).
 121. Kolch, W. Coordinating ERK/MAPK signalling through scaffolds and inhibitors. *Nat. Rev. Mol. Cell Biol.* **6**, 827–837 (2005).
 122. Matheny, S. A. *et al.* Ras regulates assembly of mitogenic signalling complexes through the effector protein IMP. *Nature* **427**, 256–260 (2004).
 123. Asada, M. *et al.* Brap2 functions as a cytoplasmic retention protein for p21 during monocyte differentiation. *Mol Cell Biol* **24**, 8236–8243 (2004).
 124. Choe, K. P., Przybysz, A. J. & Strange, K. The WD40 Repeat Protein WDR-23 Functions with the CUL4/DDB1 Ubiquitin Ligase To Regulate Nuclear Abundance and Activity of SKN-1 in *Caenorhabditis elegans*. *Mol. Cell. Biol.* **29**, 2704–2715 (2009).
 125. Choe, K. P., Leung, C. K. & Miyamoto, M. M. Unique structure and regulation of the nematode detoxification gene regulator SKN-1: implications to understanding and controlling drug resistance. *Drug Metab. Rev.* **44**, 209–223 (2012).
 126. Itoh, K. *et al.* Keap1 represses nuclear activation of antioxidant responsive elements by Nrf2 through binding to the amino-terminal Neh2 domain. *Genes Dev.* **13**, 76–86 (1999).
 127. Higa, L. & Zhang, H. Stealing the spotlight: CUL4-DDB1 ubiquitin ligase docks WD40-repeat proteins to destroy. *Cell Div.* **2**, 1–9 (2007).
 128. Lee, J. & Zhou, P. DCAFs, the Missing Link of the CUL4-DDB1 Ubiquitin Ligase. *Mol. Cell* **26**, 775–780 (2007).
 129. Feldman, R. M. R., Correll, C. C., Kaplan, K. B. & Deshaies, R. J. A complex of Cdc4p, Skp1p, and Cdc53p/cullin catalyzes ubiquitination of the phosphorylated CDK inhibitor Sic1p. *Cell* **91**, 221–230 (1997).
 130. Cardozo, T. & Pagano, M. The SCF ubiquitin ligase: Insights into a molecular machine. *Nat. Rev. Mol. Cell Biol.* **5**, 739–751 (2004).
 131. Chang, B. *et al.* SKP1 connects cell cycle regulators to the ubiquitin proteolysis machinery through a novel motif, the F-box. *Cell* **86**, 263–274 (1996).
 132. Skowyra, D., Craig, K. L., Tyers, M., Elledge, S. J. & Harper, J. W. F-box proteins are receptors that recruit phosphorylated substrates to the SCF ubiquitin-ligase complex. *Cell* **91**, 209–219 (1997).
 133. Sbodio, J. I., Snyder, S. H. & Paul, B. D. Redox Mechanisms in Neurodegeneration: From Disease Outcomes to Therapeutic Opportunities. *Antioxid Redox Signal.* (2018).
 134. Sena, L. A. & Chandel, N. S. Physiological roles of mitochondrial reactive oxygen species. *Mol. Cell* **48**, 158–167 (2012).
 135. Ji, J. *et al.* Harmine suppresses hyper-activated Ras-MAPK pathway by selectively targeting oncogenic mutated Ras/Raf in *Caenorhabditis elegans*. *Cancer Cell Int.* **19**, 1–16 (2019).
 136. Accili, D. & Arden, K. C. FoxOs at the crossroads of cellular metabolism, differentiation, and transformation. *Cell* **117**, 421–426 (2004).
 137. Albert, P. S., Brown, S. J. & Riddle, D. L. Sensory control of dauer larva formation in *Caenorhabditis elegans*. *J. Comp. Neurol* **198**, 435–451 (1981).
 138. Riddle, D. L., Swanson, M. M. & Albert, P. S. Interacting genes in nematode (*Caenorhabditis elegans*) dauer larva formation. *Nature* **290**, 668–671 (1981).
 139. Kwon, E. S., Narasimhan, S. D., Yen, K. & Tissenbaum, H. A. A new DAF-16 isoform

- regulates longevity. *Nature* **466**, 498–502 (2010).
140. Murphy, C. T. & Hu, P. J. Insulin/insulin-like growth factor signaling in *C. elegans*. *WormBook* (2013).
 141. Murphy, C. T. *et al.* Genes that act downstream of DAF-16 to influence the lifespan of *Caenorhabditis elegans*. *Nature* **424**, 277–284 (2003).
 142. Schuster, E. *et al.* DamID in *C. elegans* reveals longevity-associated targets of DAF-16/FoxO. *Mol. Syst. Biol.* **6**, 1–6 (2010).
 143. McElwee, J. J., Schuster, E., Blanc, E., Thomas, J. H. & Gems, D. Shared transcriptional signature in *Caenorhabditis elegans* dauer larvae and long-lived *daf-2* mutants implicates detoxification system in longevity assurance. *J. Biol. Chem.* **279**, 44533–44543 (2004).
 144. Chen, A. T. Y. *et al.* Longevity genes revealed by integrative analysis of isoform-specific *daf-16/FoxO* mutants of *caenorhabditis elegans*. *Genetics* vol. 201 (2015).
 145. Zheng, S., Liao, S., Zou, Y., Qu, Z. & Liu, F. *ins-7* gene expression is partially regulated by the DAF-16/IIS signaling pathway in *Caenorhabditis elegans* under celecoxib intervention. *PLoS One* **9**, (2014).
 146. López-Otín, C., Blasco, M. A., Partridge, L., Serrano, M. & Kroemer, G. The hallmarks of aging. *Cell* **153**, 1194 (2013).
 147. Fontana, L., Partridge, L. & Longo, V. D. Extending healthy life span—from yeast to humans. *Science*. **328**, 321–326 (2010).
 148. Martins, R., Lithgow, G. J. & Link, W. Long live FOXO: Unraveling the role of FOXO proteins in aging and longevity. *Aging Cell* **15**, 196–207 (2016).
 149. Senchuk, M. M. *et al.* Activation of DAF-16/FOXO by reactive oxygen species contributes to longevity in long-lived mitochondrial mutants in *Caenorhabditis elegans*. *PLoS Genet.* **14**, 1–27 (2018).
 150. Longo, V. D., Lieber, M. R. & Vijg, J. Turning anti-ageing genes against cancer. *Nat. Rev. Mol. Cell Biol.* **9**, 903–910 (2008).
 151. Hosler, B. A., LaRosa, G. J., Grippo, J. F. & Gudas, L. J. Expression of REX-1, a gene containing zinc finger motifs, is rapidly reduced by retinoic acid in F9 teratocarcinoma cells. *Mol. Cell. Biol.* **9**, 5623–5629 (1989).
 152. Shi, Y., Lee, J. S. & Galvin, K. . Everything you ever wanted to know about Yin Yang 1. *Biochim. Biophys. Acta* **1334**, F49–F66 (1997).
 153. Thomas, M. J. & Seto, E. Unlocking the mechanisms of transcription factor YY1: are chromatin modifying enzymes the key? *Gene* **236**, 197–208 (1999).
 154. Kim, J. Do, Faulk, C. & Kim, J. Retroposition and evolution of the DNA-binding motifs of YY1, YY2 and REX1. *Nucleic Acids Res.* **35**, 3442–3452 (2007).
 155. Bhandari, D. R. *et al.* REX-1 Expression and p38 MAPK Activation Status Can Determine Proliferation/Differentiation Fates in Human Mesenchymal Stem Cells. *PLoS One* **5**, (2010).
 156. Guallar, D. *et al.* Expression of endogenous retroviruses is negatively regulated by the pluripotency marker Rex1/Zfp42. *Nucleic Acids Res.* **40**, 8993–9007 (2012).
 157. Luk, S. *et al.* Deficiency in Embryonic Stem Cell Marker Reduced Expression 1 Activates Mitogen-Activated Protein Kinase Kinase 6-Dependent p38 Mitogen-Activated Protein Kinase Signaling to Drive Hepatocarcinogenesis. *Hepatol. Md.* **72**, 183–197 (2020).
 158. Ben-shushan, E., Thompson, J. R., Gudas, L. J. & Bergman, Y. Rex-1, a Gene Encoding a Transcription Factor Expressed in the Early Embryo, Is Regulated via Oct-3/4 and Oct-6 Binding to an Octamer Site and a Novel Protein, Rox-1, Binding to an Adjacent Site. *Mol.*

- Cell. Biol.* **18**, 1866–1878 (1998).
159. Makhlouf, M. *et al.* A prominent and conserved role for YY1 in Xist transcriptional activation. *Nat. Commun.* **5**, 1–12 (2014).
 160. Coletta, A. *et al.* Low-complexity regions within protein sequences have position-dependent roles. *BMC Syst. Biol.* **4**, 1–13 (2010).
 161. Foronda, D., De Navas, L. F., Garaulet, D. L. & Sánchez-Herrero, E. Function and specificity of Hox genes. *Int. J. Dev. Biol.* **53**, 1409–1419 (2009).
 162. Duboule, D. The rise and fall of Hox gene clusters. *Development* **134**, 2549–2560 (2007).
 163. Ferreira, H. B., Zhang, Y., Zhao, C. & Emmons, S. W. Patterning of *Caenorhabditis elegans* posterior structures by the Abdominal-B homolog, *egl-5*. *Dev. Biol.* **207**, 215–228 (1999).
 164. Wang, B. B. *et al.* A homeotic gene cluster patterns the anteroposterior body axis of *C. elegans*. *Cell* **74**, 29–42 (1993).
 165. Brunschwig, K. *et al.* Anterior organization of the *Caenorhabditis elegans* embryo by the labial-like Hox gene *ceh-13*. *Development* **126**, 1537–1546 (1999).
 166. Van Auken, K., Weaver, D. C., Edgar, L. G. & Wood, W. B. *Caenorhabditis elegans* embryonic axial patterning requires two recently discovered posterior-group Hox genes. *Proc. Natl. Acad. Sci. U. S. A.* **97**, 4499–4503 (2000).
 167. Wittmann, C. *et al.* The expression of the *C. elegans* labial-like Hox gene *ceh-13* during early embryogenesis relies on cell fate and on anteroposterior cell polarity. *Development* **124**, 4193–4200 (1997).
 168. Liu, W. J., Reece-Hoyes, J. S., Walhout, A. J. & Eisenmann, D. M. Multiple transcription factors directly regulate Hox gene *lin-39* expression in ventral hypodermal cells of the *C. Elegans* embryo and larva, including the hypodermal fate regulators LIN-26 and ELT-6. *BMC Dev. Biol.* **14**, 1–21 (2014).
 169. Reece-Hoyes, J. *et al.* Enhanced yeast one-hybrid (eY1H) assays for high-throughput gene-centered regulatory network mapping. *Nat Methods* **8**, 1059–1064 (2011).
 170. McJunkin, K. & Ambros, V. A microRNA family exerts maternal control on sex determination in *C. Elegans*. *Genes Dev.* **31**, 422–437 (2017).
 171. Kato, M., de Lencastre, A., Pincus, Z. & Slack, F. J. Dynamic expression of small non-coding RNAs, including novel microRNAs and piRNAs/21U-RNAs, during *Caenorhabditis elegans* development. *Genome Biol.* **10**, 1–15 (2009).
 172. De Lencastre, A. *et al.* MicroRNAs both promote and antagonize longevity in *C. elegans*. *Curr. Biol.* **20**, 2159–2168 (2010).

**CHAPTER 2: INVESTIGATION OF THE
CAENORHABDITIS ELEGANS TRANSCRIPTION
FACTOR ZTF-17 AND ITS ROLE IN THE
OXIDATIVE STRESS PATHWAYS**

2.1 Introduction

Reactive oxygen species (ROS) are by-products of endogenous cellular metabolism and are thought to be a major contributor to the onset of age-associated diseases [1,2]. ROS are chemically reactive oxygen containing molecules that causes oxidative stress when there is an imbalance between these free radicals and antioxidants [3]. As ROS readily react with other macromolecules in the cell, if left untreated, oxidative damage resulting from accumulated ROS can target DNA, RNA, protein and lipids causing extensive damage to tissues and lead to cell death [4,5]. Although ROS production is inevitable, organisms have devised complex defense mechanisms that protect against ROS. Biological processes that eliminate excess free radicals can neutralize the harmful effects of ROS. Alternatively, organisms can promote the expression of stress resistance genes as a mechanism to cope with oxidative damage. Two important transcription factors, Nrf2 and FOXO, were discussed for their roles as key regulators of antioxidant responses and stress resistance [6–9].

The Nrf (Nuclear factor erythroid 2-related factor) family of transcription factors are evolutionarily conserved and have critical roles in mediating various responses to cellular stress, one of which is to activate antioxidant proteins [8]. Likewise, FOXOs belong to the class O of the Forkhead box transcription factors that participate in many cellular process that range from cell cycle regulation, apoptosis and metabolism to functions related to stress resistance and longevity [10].

In *C. elegans*, DAF-16 and SKN-1 are the worm homologs, respective of FOXO and Nrf2, with well established roles in detoxifying toxic compounds. Although extensive research has been done to elucidate the importance of DAF-16 and SKN-1, the molecular mechanisms of their function and upstream regulation is still poorly understood. An RNAi screen done by MacNeil *et*

al., searched for candidate transcription factors affecting the SKN-1 signalling pathway using *gst-4p::gfp* expression as a reporter since *gst-4* is a direct target of SKN-1. The screen revealed that among the transcription factors identified, loss of *ztf-17* was found to promote the expression of *gst-4*. From this initial RNAi screen, I took a genetic approach to study other target genes involved in the PI and PII detoxification process, looking at genes that were typically upregulated and/or downregulated during stress. Here, I discovered that ZTF-17 has a regulator role as a repressor of the SKN-1 and DAF-16 signalling pathways that confer stress resistance in *C. elegans*. Using *ztf-17(tm963)* mutants, a strain generated to contain a 315bp deletion mutation between the 36673-36988bp sequences of the coding region, I found that these homozygous viable mutants displayed enhanced expression of SKN-1 dependent genes, such as *gst-4* and *gcs-1*, but also had elevated expression of stress resistance genes that were under DAF-16 control, such as *sod-3*. My results indicated that ZTF-17 may act as a novel regulatory component that facilitates crosstalk between different pathways involving repression of SKN-1 and DAF-16 or its target genes. Further analysis indicated that although loss of functional ZTF-17 resulted in enhanced expression of SKN-1 and DAF-16 dependent genes, under stress inducing conditions, *ztf-17(tm963)* mutants appear to only have enhanced short-term resilience to oxidative stressors and are more susceptible to heat stress than wildtype. Taken together all my findings, I suggest a model for the potential function of ZTF-17 where it acts as a negative regulator of SKN-1 and/or SKN-1 dependent genes. As a direct result of modulating SKN-1, ZTF-17 also has a secondary role that affects DAF-16 function and DAF-16 related target genes.

2.2 Materials and Methods

2.2.1 Maintenance of *C. elegans* Worm Strains

The *Caenorhabditis* Genetics Center at The University of Minnesota and the National Bioresource Project (Tokyo, Japan) were the source of all the worm strains obtained for this project. *C. elegans* were maintained on aseptically poured NGM petri plates seeded with *E. coli* OP-50 bacterial food source under standard conditions outlined by the protocol designed by Sydney Brenner [11]. All experiments used N2 as wildtype and were carried at 20°C unless otherwise specified in the corresponding sections. All temperature sensitive strains were maintained at 15°C. The list of worm strains used in this project can be found in Table 6.

2.2.2 Generation of *ztf-17(tm963)* Transgenic Worms

Backcrossed YF210 [*ztf-17(tm963)*] worms that were homozygous for the gene deletion were used to generate the following worm strains: YF209 [*ztf-17(tm963); dvIs(gst-4p::gfp)*], YF219 [*ztf-17(tm963); muls84(sod-3p::gfp)*], YF218 [*ztf-17(tm963); zIs356(daf-16p::gfp)*] and YF217 [*ztf-17(tm963); daf-2(e1370)*]. A detailed schematic of the *ztf-17(tm963)* backcross can be found in Supplementary Figure S1.

To generate *ztf-17(tm963); dvIs(gst-4p::gfp)* worms, male *him-5(e1490)* mutants were crossed with L3/L4 stage *dvIs19(gst-4p::gfp)* hermaphrodites. Male progenies expressing *dvIs19(gst-4p::gfp)* under fluorescence microscopy were selected then crossed with L3/L4 stage *ztf-17(tm963)*, these worms were considered the parental worms (P1). P1 progenies – denoted as F1, were allowed to hatch from eggs and grow to early L4 stage. Individual F1 hermaphrodites that expressed GFP fluorescence were then picked onto NGM plates and allowed to lay eggs, the progenies were denoted as F2. The genotype of the individual F1 worms were determined by SW-PCR (Single Worm Polymerase Chain Reaction) with CT5 and CT6 primers specific for the *ztf-17(tm963)* deletion region. F1 worms that were homozygous for the *ztf-17(tm963)* mutation were selected and their F2 progenies were screened by SW-PCR to confirm all worms were

homozygous for the *ztf-17(tm963)* gene deletion and expressed *dvIs19(gst-4p::gfp)*. If plates contained both worms that expressed GFP and worms that did not, those were excluded from the screen. F3 and subsequent generations were maintained on NGM plates after genotyping. Similar approaches were done to generate the *ztf-17(tm963); muls84(sod-3p::gfp)* and *ztf-17(tm963); zIs356(daf-16p::gfp)* worm strains. TJ356 [*zIs356(daf-16p::gfp)*] worms exhibit the rolling phenotype denoted as rollers. Rollers were used to select for worms that carried *zIs356(daf-16p::gfp)*. A detailed schematic of these crosses can be found in the Supplementary Figure S2 and primers used for genotyping can be found in Table 7.

To generate the *ztf-17(tm963); daf-2(e1370)* double mutants, *him-5(e1490)* mutants were crossed with L3/L4 stage *ztf-17(tm963)* hermaphrodites. Male progenies were crossed with L3/L4 stage *daf-2(e1370)* at 15°C, these worms were considered the parental worms (P1). P1 progenies – denoted as F1, were allowed to hatch from eggs and grow to early L4 stage. Individual F1 hermaphrodites were picked onto NGM plates and allowed to lay eggs at 15°C, the progenies were denoted as F2. The genotype of the individual F1 worms were determined by SW-PCR. F1 worms that were homozygous for the *ztf-17(tm963)* mutation were selected and their F2 progenies were screened by SW-PCR to confirm all worms were homozygous for the *ztf-17(tm963)* gene deletion. Another SW-PCR was done in F2 and subsequent generations to amplify the region containing the *daf-2(e1370)* mutation. DNA sequencing was done at ATCG DNA/Sequencing Facility at SickKids (Toronto) to confirm that all worms were also homozygous for the *daf-2(e1370)* mutation. After genotyping, subsequent generations were maintained on NGM plates at 15°C. A detailed schematic of these *ztf-17(tm963)* and *daf-2(e1370)* cross can be found in the Supplementary Data Figure S3.

2.2.3 Single Worm-Polymerase Chain Reaction

The SW-PCR was used to verify the genotype of the worm strains generated using the standard single-worm PCR protocol. Single worms were picked and transferred to PCR strips containing 4ul of Single Worm Lysis buffer (1X Thermopol buffer (NEB E5000S) with 1 μ l (800 U, ~20 ug) of Proteinase K (NEB P8107S) per 20 μ l PCR reaction). PCR tubes were frozen overnight at -80 °C then heated in a thermocycler at 65°C for 1 hour. The reaction was stopped by incubating at 95°C for 15 minutes to inactivate the proteinase K. A PCR master mix was prepared containing: 1X Thermopol Buffer, 0.5 mM primers, 0.2 mM/each dNTPs and 1 μ l Taq polymerase (NEB E5000S) per 200 μ l of PCR master mix. Each PCR reaction was performed in the thermocycler for 30-35 cycles with appropriate annealing and extension temperatures according to primer sets used. The PCR products were verified by gel electrophoresis using the Gel XL Ultra V-2 gel box (Labnet International Inc) on a 1% agarose gel.

2.2.4 Confocal Microscopy and GFP Fluorescence Analysis

GFP expression was visualized in transgenic worms containing specific *gfp* reporters. L4 live animals were picked and mounted onto 2% agarose cushions secured on glass microscope slides. Animals were anesthetized using 2 mM Levamisole (Sigma L9756). Images of fluorescent animals were captured using tile scan and Z-stack parameters on a Zeiss Observer Z1 Spinning Disk Confocal Microscope and analyzed with the ZEN 2.6 Software ®. Whole worm fluorescence was quantified using ImageJ Software by tracing around each worm and the difference between the raw intensity readings per worm minus the area of the background fluorescence was recorded and used for analysis.

2.2.5 Worm Synchronization

Worm strains used for RNA isolation and qRT-PCR were synchronized to L4 or early adult stage prior to harvesting. 3-4 healthy worms were picked on to OP-50 seeded NGM plates and

starved for ~5 days until mostly L1 worms remained. Worms were then chunked from agar plates and moved onto new seeded NGM plates and allowed to grow to L4/early adult stage for ~2 days. Synchronized worms were now ready for use in downstream experiments. For YF217 [*ztf-17(tm963); daf-2(e1370)*] and CB1370 [*daf-2(e1370)*] temperature sensitive strains, worm synchronization was completed according to the protocol by Sulston and Hodgkin with modifications [12]. *ztf-17(tm963); daf-2(e1370)* and CB1370 [*daf-2(e1370)*] animals were synchronized to L1 stage at 15°C then allowed to continue developing at 15°C until early L4 stage. L4 stage animals were then shifted to 25°C and allowed to develop for 24hr. Worms were then washed with M9 buffer gently and collected for RNA extraction and subsequent qRT-PCR experiments.

2.2.6 RNAi (RNA interference)

This project utilized the transcription factor RNAi library created by the Walhout laboratory at the University of Massachusetts. The RNAi-mediated knock down of specific genes was performed by feeding worm strains with HT115 *E. coli* expressing either the bacterial plasmid pL4440 control or the dsRNA homologous to the target gene cloned into pL4440. HT115 was transformed using standard protocol (NEB) and grown on NGM plates containing 0.4 mM IPTG, 100 µg/mL Ampicillin and 12.5 µg/mL Tetracycline. Worms were synchronized on RNAi plates until animals reached L4 stage then were used for GFP quantification by confocal microscopy or harvested for RNA extraction depending on the experiment that followed.

2.2.7 RNA Extraction and Quantitative Real Time PCR

Prior to RNA extraction, L4 synchronized worms were harvested by gently washing with M9 buffer then transferred from plates to microfuge tubes. Worms were centrifuged at 500 x g for 2 minutes then washed three additional times with M9 buffer. Worm pellets were then stored at -

80°C overnight or indefinitely until RNA isolation. RNA extraction was done by adding 250µl of TRI reagent (Sigma 93289) to ~200µl of frozen worms followed by a brief vortex to dissolve the pellet. 250µl of absolute ethanol was added to each sample and then placed on a vortex shaker for 15 minutes at 4°C. The solution was then transferred to a Zymo column (Zymo R2060) and RNA extraction continued according to the manufacturer's protocol. Total RNA concentration was measured using the Fisher Thermo NanoDrop2000 and 500ng of RNA was used to synthesize cDNA by reverse transcription using the OneScript® Plus cDNA Synthesis Kit (abm G236) following the manufacturer's protocol. qRT-PCR was performed to measure the mRNA expression levels in different worm strains using specific qPCR primers, either BrightGreen 2X qPCR MasterMix (abm MasterMix-S) or BlasTaq™ 2X qPCR MasterMix (abm G891) and the Qiagen Rotor-gene Q system. qRT-PCR from at least three independent experiments were obtained and the comparative method with $\Delta\Delta C_t$ values were used to analyze data sets. Relative mRNA expression levels for experimental worm strains were normalized to N2 wildtype using either of the following endogenous control genes *act-1*, *cdc-42*, *tba-1* or *pmp-3*. List of forward and reverse primers used for qRT-PCR can be found in Table 8.

2.2.8 Oxidative Stress Assays

Survival assays were done using a sodium arsenite (As) solution and *tert*-Butyl hydroperoxide (tBHP) plates to determine if there was a functional difference in sensitivity to oxidative stress inducing compounds in *ztf-17(tm963)* deletion mutants vs. N2 wildtype worms. The experimental set up for both assays followed the protocol outlined by Ewald *et al.* [13] with minor modifications. In the As-assay, using a 24-well plate, synchronized L4 *ztf-17(tm963)* mutants and N2 worms were placed into wells containing either 500µl of 5mM As or 500µl of M9 buffer for control. In the tBHP-assay, 15.4mM tBHP plates were prepared the day before

conducting the assay. The assay was performed by placing synchronized L4 *ztf-17(tm963)* mutants and N2 worms on tBHP plates. Worms placed on normal NGM plates were used as controls. In both the As- and tBHP-assays, worms were scored every hour for survival and worms that showed no movement or were unresponsive to poking were deemed dead. Data was collected for three independent experiments conducted in triplicates for analysis.

2.2.9 Thermotolerance Assay and Heat Stress Treatment

Synchronized L4 *muls84(sod-3p::gfp)* and *ztf-17(tm963); muls84(sod-3p::gfp)* worms were heat stressed at 35°C in an incubator for 2 hours. Worms were then prepared for confocal microscopy and fluorescence intensity was compared to untreated *muls84(sod-3p::gfp)* and *ztf-17(tm963); muls84(sod-3p::gfp)* at 20°C.

Synchronized L4 *ztf-17(tm963)* mutants and N2 worms grown on OP-50 seeded NGM plates were heat stressed at 35°C for 2 hours prior to harvesting for RNA extraction and downstream qRT-PCR experiments. Untreated synchronized L4 *ztf-17(tm963)* mutants and N2 worms were also collected at 20°C. Data from three independent experiments were collected and used to analyze differences observed between the untreated and the heat stressed treatment groups.

The thermotolerance assay was conducted to determine the functional differences between *ztf-17(tm963)* mutants and N2 wildtype worms stressed at 35°C. Synchronized L4 *ztf-17(tm963)* mutants and N2 worms were transferred to new OP-50 seeded NGM plates warmed to 35°C. Worms were heat stressed in an incubator set to 35°C and scored hourly for survival until a treatment group reached 100% mortality. *ztf-17(tm963)* mutants and N2 worms grown on NGM plates kept at 20°C were used as the untreated control group. Worms that ceased to move or were unresponsive to probing by a worm pick were deemed dead. Data from three independent experiments with triplicates were used for analysis.

2.2.10 DAF-16 Nuclear Localization Assay

L4 stage TJ356 [(*zIs356(daf-16p::gfp)*)] and *ztf-17(tm963); zIs356(daf-16p::gfp)* animals were picked and mounted on 2% agarose cushions prepared for fluorescence microscopy. Microscopy was done on a Zeiss Observer Z1 Spinning Disk Confocal Microscope using the tile scan and Z-stack features then images were processed by the Zen Blue 2.6 Software ®. The GFP signal localization was quantified by analyzing each worm and categorizing if animals had cytosolic, intermediate or nuclear DAF-16::GFP. Cytosolic referred to animals without nuclear localized GFP signal, intermediate refers to animals with both nuclear and cytosolic GFP and nuclear refers to animals with solely nuclear GFP signal. Results were analyzed and displayed as a percentage of the worm sample size in each group.

2.2.11 Primer Design and Subcloning

All primers for this project were designed using the Primer3 and BLAST (NCBI) programs using the *C. elegans* genome to ensure primer pair specificity. Primer pairs were chosen based on optimal T_m, GC%, self complementarity and validated to ensure there were no off-target hits. Primers CT1-CT12 were used to genotype *ztf-17(tm963)* deletion mutants.

qRT-PCR primers were designed using the coding region of the gene of interest in the *C. elegans* genome and PCR products were < 200bp. Primers were validated prior to use.

The following constructs were designed by subcloning DAF-16A into pPA-RL-GW, DAF-16A into p3xFLAG-CMV-7.1, ZTF-17 into HA₂-pcDNA3.1, ZTF-17 into pFL-V5-GW, ZTF-22 into pPA-RL-GW, ZTF-17 into pSL301 and SOD-3 into pGL4.10. Specific primer pairs for each subcloning experiment were designed so that the insert would have ~25bp overhangs that overlapped with the restrictive enzyme sites on the vector sequence and on the gene insert itself. PCR was done using either Q5® High-Fidelity DNA Polymerase (NEB M0491S) or Platinum

SuperFi II DNA Polymerase–High-Fidelity PCR Enzyme (Invitrogen 12361010) to amplify both the vectors and the inserts followed by DpnI digestion (NEB R0176S) and PCR purification using the GeneJET PCR Purification Kit (Thermo Scientific K0701). Subcloning of the constructs were carried out using the NEBuilder® HiFi DNA Assembly Master Mix (NEB E2621S) according to the manufacturer’s protocol in DH5 α competent cells. DNA was purified using the GeneJet Plasmid Miniprep Kit (Thermo Scientific K0502) and DNA content was quantified using the Fisher Thermo NanoDrop2000. All constructs were sent to ATCG DNA/Sequencing Facility at SickKids (Toronto) to ensure that the cloned DNA product was in frame, had correct orientation and had no mutations that would affect the coding region. All plasmids used to generate constructs can be found in Table 9.

2.2.12 Cell Culture and Transfection

HEK293T cells were cultured in Gibco™ Dulbecco’s Modified Eagle’s Medium (DMEM) (Fisher Scientific 11995065) supplemented with 10% Fetal Bovine Serum (FBS). Cells were maintained at 37°C with 5% CO₂ levels and passaged using Gibco™ Trypsin-EDTA (0.25%) (Fisher Scientific 25200056) once confluency reached 70-90% on 10cm treated petri dishes specific for tissue/cell culture work.

2.2.13 Luciferase Assay

HEK293T cells were passaged at 70%-80% confluency and cells were seeded onto 24-well treated plates. Cells were incubated overnight and co-transfected the next day with Opti-MEM, DNA constructs and Lipofectamine 3000 (Invitrogen L3000001) based on the manufacturer’s protocol. 48 hr post-transfection, cells were lysed and prepared for luminescence readings using the Firefly & *Renilla* Luciferase Single Tube Assay Kit (Biotium 300811) based on the manufacturer’s guidelines. Luminescence was quantified on the Synergy™ H4 Hybrid Multi-

Mode Microplate Reader (BioTek) and the ratios between the Firefly and *Renilla* Luciferases were used to normalize all the data sets to the experimental control group. Each transfection was done in duplicates and data was derived from three independent experiments.

2.2.14 Dual Luminescence-Based Co-Immunoprecipitation (DULIP) Assay

HEK293T cells were passaged at 70%-80% confluency and cells were seeded onto 6-well treated plates. Cells were incubated overnight and co-transfected the next day with Opti-MEM, DNA constructs and Lipofectamine 3000 (Invitrogen L3000001) based on the manufacturer's protocol. 48 hr post-transfection, cells were lysed and Co-Immunoprecipitation was performed according the methods described by Trepte *et al.* [14]. The Firefly & *Renilla* Luciferase Single Tube Assay Kit (Biotium 300811) was used to quantify luminescence based on the manufacturer's protocol and luminescence readings were obtained on the Synergy™ H4 Hybrid Multi-Mode Microplate Reader (BioTek). Data was obtained from three independent experiments and the Normalized Interaction Ratio (NIR) and the corrected NIR was calculated according the methods described by Trepte *et al.* [14].

2.2.15 *ztf-17(+)* Overexpression Construct and Transgenic Worm Strains

ZTF-17 was subcloned into pSL301 according to the methods described in previous sections. Standard protocol for *C. elegans* microinjection were followed to generate transgenic animals. A DNA injection mix containing the *ztf-17(+)* overexpressing construct was prepared and healthy N2 worms at stage L3/L4 were co-injected with 25ng/μl of the red fluorescent marker, *sur-5p::mCherry*, into the gonad using the microINJECTOR™ System (Tritech Research MINJ1000). Worms were allowed to grow on OP-50 seeded NGM plates and F1 progeny with the red fluorescent marker were selected for. F2 and subsequent generations have a percent chance of expressing the array, but typically, inherited arrays will be consistently expressed ~30-

60% in most cases [15]. Two worm strains were kept, *ztf-17(+)* line 1 (YF214) and *ztf-17(+)* line 2 (YF213). Worm strains were maintained by picking red fluorescent worms. To prepare worms for qRT-PCR, ~20 red fluorescent worms were picked. These parental worms were allowed to lay eggs on OP-50 seeded NGM plates. Progenies were then grown until most of the population reached L4 stage before being harvested for RNA isolation and downstream qRT-PCR experiments.

2.2.16 SapTrap Assembly

The ZTF-17 localization experiment was carried out based on the SapTrap Assembly methods outlined by Dickinson *et al.* and Schwartz *et al.* [16–18] with some modifications. The SapTrap Assembly was divided up into two constructs. The ZTF-17 SEC Repair Template and the pDD162 Cas9-sgRNA plasmid (Figure 3.2) was modified to contain a specific Site Directed Mutagenesis (SDM) using TK284 and Cas9 Rev Primer. The 3' and 5' Homology arms for ZTF-17 were designed as gene fragments and PCR was done generate the remaining components using the Platinum SuperFi II DNA Polymerase–High-Fidelity PCR Enzyme (Invitrogen 12361010). Subcloning procedures outlined in section 2.2.11 were used to assemble the constructs. Primers and plasmids used for the SapTrap Assembly can be found in Table 7 and 9.

2.2.17 Statistical Analysis

Figures were generated and statistical analyses were completed on the GraphPad Prism8 Software. Depending on the nature of the experiment and data, Multiple *t*-tests, Two-tailed Unpaired Student's *t*-test or One-way ANOVA were used to determine statistical significance. For the survival assays, the Log-rank (Mantel-Cox) test and the online survival analysis program OASIS® were used in conjunction to calculate statistics. P-values are represented as the following to denote significance on figures; **** P < 0.0001, *** P < 0.001, ** P < 0.01, * P < 0.05. Error bars represent ± Standard Error of the Mean unless otherwise specified.

2.3 Results

2.3.1 Animals homozygous for the *ztf-17* gene deletion displayed increased expression of antioxidant genes found in phase I and II detoxification pathways.

My current understanding of the *C. elegans* ZTF-17 stemmed from the initial RNAi-mediated knock down of transcription factors done by the MacNeil Lab at McMaster University [19]. In the screen, when *ztf-17* RNAi was used, loss of *ztf-17* resulted in an increase in *gst-4p::gfp* suggesting that it could be a potential negative regulator of *gst-4*. To further test whether *ztf-17* was able to influence express levels of genes related to detoxification, I first validated the preliminary results obtained from the RNAi screen using a *ztf-17(tm963)* mutant strain containing a 315bp deletion within its sequence. The *ztf-17(tm963)* mutant worms were first backcrossed with N2 wildtype worms to remove any background mutations that might have been present (Supplementary Figure S1). I then generated transgenic animals carrying the *gst-4p::gfp* reporter construct with the *ztf-17(tm963)* deletion and analyzed the GFP expression in both N2 and mutant worms. I found that there was a significant increase in the amount of GFP quantified by confocal microscopy in the intestinal and hypodermal cells of the *ztf-17(tm963)* mutants. Figure 2.1A shows the anatomy of the worm with the major structures in hermaphrodites and Figure 2.1B indicated that there was approximately a ~2.4-fold increase in the *gst-4p::gfp* signals compared to N2 worms. I also generated another transgenic worm strain carrying the reporter construct, *sod-3p::gfp*, and interestingly, *ztf-17(tm963)* mutants also expressed elevated levels of GFP. The difference was ~4.3-fold increase in whole worm fluorescence when compared to N2 (Figure 2.1B, D). To confirm that the enhanced GFP fluorescence observed in both the reporter constructs were due to the *ztf-17* deletion, I measured the mRNA levels of both *gst-4* and *sod-3* by qRT-PCR to complement the transgenic studies and found that the results were consistent

with the observations seen during fluorescence microscopy. In Figure 2.2, *ztf-17(tm963)* mutants showed a ~3.8-fold increase in *gst-4* and a ~2.8-fold increase in *sod-3* mRNA levels. Previous studies confirmed that BRAP-2 and WDR-23 were negative regulators of detoxification enzymes and thus *brap-2(ok1492)* and *wdr-23(tm1817)* mutants were good candidates to use as positive controls [20,21]. *brap-2(ok1492)* had at least an 18-fold increase in *gst-4* while *wdr-23(tm1817)* had an astonishing 119-fold increase. For the *sod-3* expression levels, *brap-2(ok1492)* had a similar increase in *sod-3* as *ztf-17(tm963)* with ~3.7-fold increase, while no significant changes were observed in *wdr-23(tm1817)* for *sod-3* expression (Figure 2.2). These findings further confirmed ZTF-17's role in repressing the expression of PI and PII stress resistance genes.

Since *gst-4* is one of the primary target genes of SKN-1 and *sod-3* is under DAF-16 transcriptional control, I wanted to further test if ZTF-17 could modulate other PI and PII target genes. I tested three PII detoxification enzymes, *gst-4*, *gcs-1* and *sdz-8*, by qRT-PCR. Figure 2.3A-D represents the qRT-PCR results normalized to reference genes *act-1*, *cdc-42*, *tba-1* and *pmp-3* respectively. I decided to analyze the data against four different internal controls and was glad to find that in all the data sets, the trends were consistent. *gst-4* and *gcs-1* expression were significantly enhanced in *ztf-17(tm963)* mutants while *sdz-8* expression levels were inconsistent and showed no significant changes (Figure 2.3B). *brap-2(ok1492)* and *wdr-23(tm1817)* mutants also showed an increase in *gst-4* expression as expected. Only *wdr-23(tm1817)* showed consistent increases in *sdz-8* whereas *brap-2(ok1492)* showed no significant changes. *gcs-1* expression levels in *wdr-23(tm1817)* were enhanced in three out of the four normalized data sets (Figure 2.3A-C) whereas *brap-2(ok1492)* mutants had no significant changes in *gcs-1* expression.

Following the qRT-PCR results obtained from the PII genes, I chose four DAF-16 target genes (*sod-3*, *ctl-1*, *ctl-2* and *ins-7*) and measured by qRT-PCR the differences between N2 and

ztf-17(tm963) mutants. Figure 2.4A-D represent the data normalized to the internal controls. *cdc-42* was shown to be the most consistent out of the reference genes used and thus was selected as the internal control for subsequent qRT-PCR experiments.

sod-3 and *ins-7* expression levels were enhanced in *ztf-17(tm963)* mutants while *ctl-2* expression remained relatively unchanged (Figure 2.4A-C). *ctl-1* expression levels were higher in *ztf-17(tm963)* when compared to N2 worms (Figure 2.4A). *ctl-1* and *ctl-2* both functions to protect organisms from toxic effects of hydrogen peroxide by increasing the amount of catalase activity in dauer larvae and *ctl-1* expression is suspected to be regulated by DAF-16 [22]. *ins-7* is one of the insulin-like genes in *C. elegans* and is downregulated in *daf-2* loss of function mutants while upregulated in *daf-16* null mutants [23]. Suppression of *ins-7* expression in the intestine lowers INS-7 levels in other tissues, which in turn triggers DAF-16 activity [23]. Interestingly, the expression of *ins-7*, which is typically downregulated when DAF-16 is activated, was upregulated in the *ztf-17(tm963)* mutants (Figure 2.4A-D). Studies from other labs have also indicated that although *ins-7* is negatively regulated by DAF-16 activity, it could also be positively regulated by other DAF-16-independent mechanisms [23]. Another possibility is that the ablation of ZTF-17 itself released the suppression of *ins-7* that would take place under normal conditions or that there is a some feedback mechanism. These findings require further work to fully investigate the effects of the *ztf-17* gene deletion on DAF-16 target genes. Overall, the results obtained from the transgenic studies and from measuring the mRNA levels of various antioxidant genes indicate that ZTF-17 has an active role in repressing genes involved in the oxidative stress response but may also function in more than one pathway to confer resistance.

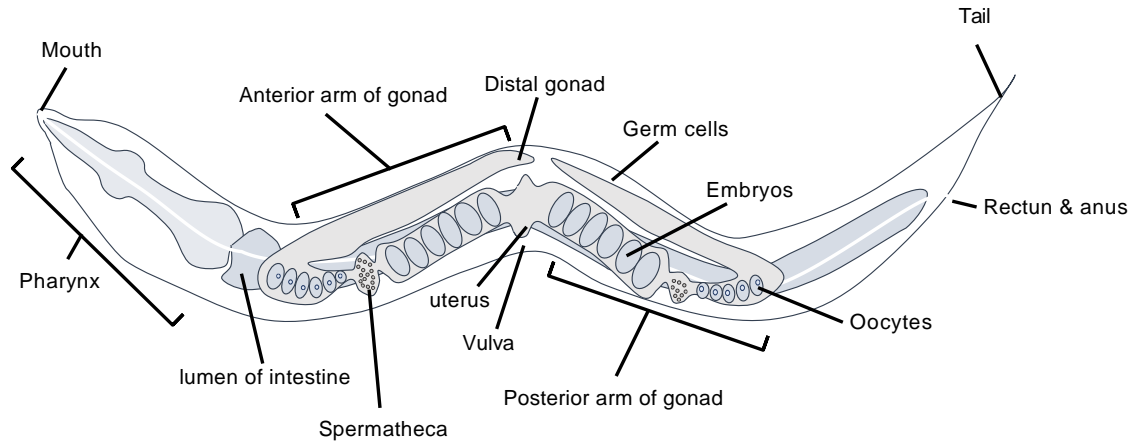
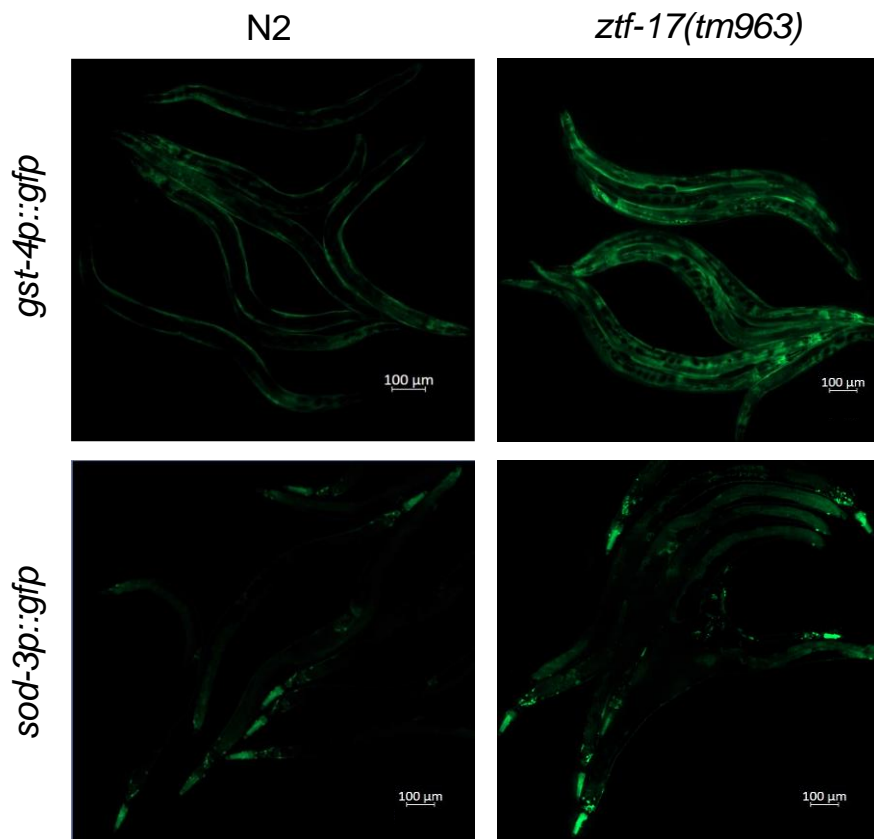
A**B**

Figure legend found on the next page.

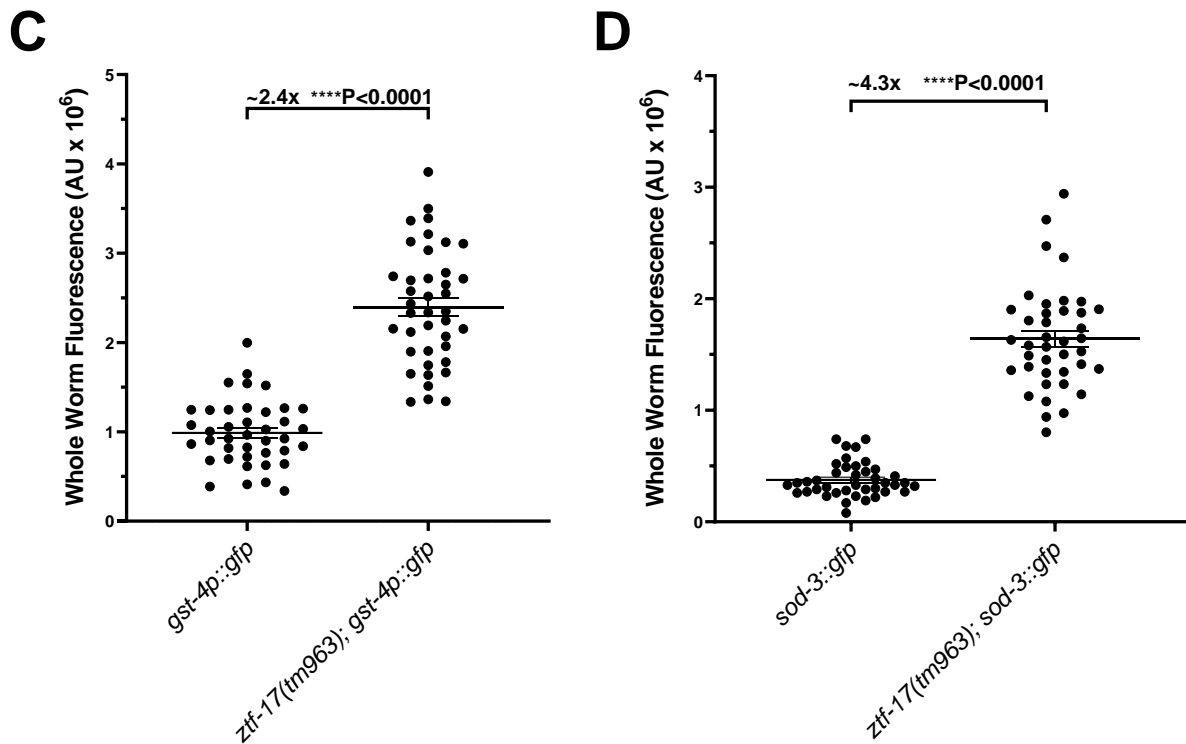


Figure 2.1 *ztf-17(tm963)* mutants display increased *gst-4p::GFP* and *sod-3p::GFP* expression compared to N2 wildtype worms.

(A) Schematic of the *C. elegans* anatomy with the major features of a hermaphrodite worm. (B) Whole worm GFP fluorescence was visualized in transgenic animals with the *ztf-17(tm963)* deletion. Fluorescence was captured using the Zeiss Observer Z1 Spinning Disk Confocal Microscope. (C-D) Fluorescence intensity was quantified using ImageJ Software. Results for n=40 worms are shown as individual points as the difference between the intensity readings per worm minus the background fluorescence. The mean fluorescence intensity is displayed as a solid black line for each worm strain. GFP levels of *ztf-17(tm963)* mutants were ~ 2.4x and ~4.3x that of wildtype worms for *gst-4p::GFP* and *sod-3p::GFP* respectively. Statistical analyses were performed using Two-tailed Unpaired Student's *t*-test; **** P < 0.0001.

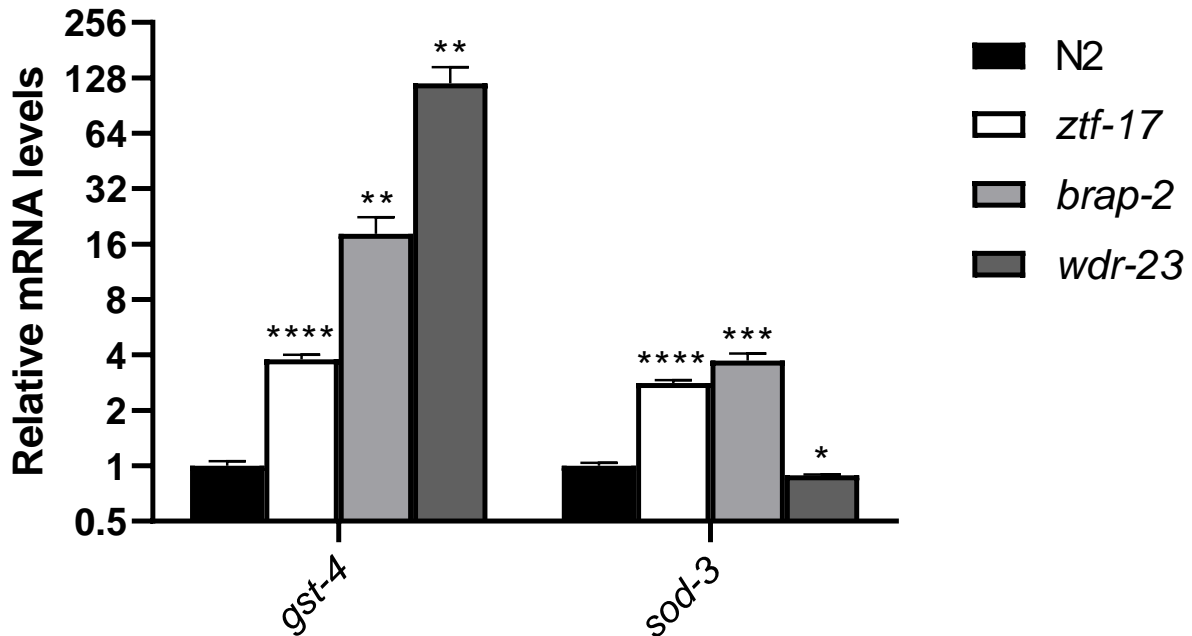


Figure 2.2 *ztf-17(tm963)* mutants showed enhanced expression of *gst-4* and *sod-3* mRNA levels under non-oxidative stress inducing conditions.

qRT-PCR was done to monitor the amplification of *gst-4* and *sod-3* antioxidant genes. Worms were synchronized to L4 stage then harvested for RNA isolation. *gst-4* mRNA expression levels were ~3.8x higher while *sod-3* mRNA expression levels were ~2.8x higher in *ztf-17(tm963)* worms when compared to N2 wildtype worms. *brap-2(ok1492)* and *wdr-23(tm1817)* mutant strains served as positive controls. Results were derived from 3 independent trials and normalized to reference gene *act-1*. Statistical analysis was carried out using Multiple *t*-tests with the Holm-Sidak multiple comparisons test. Error bars represent \pm SEM; **** $P < 0.0001$, *** $P < 0.001$, ** $P < 0.01$, * $P < 0.05$.

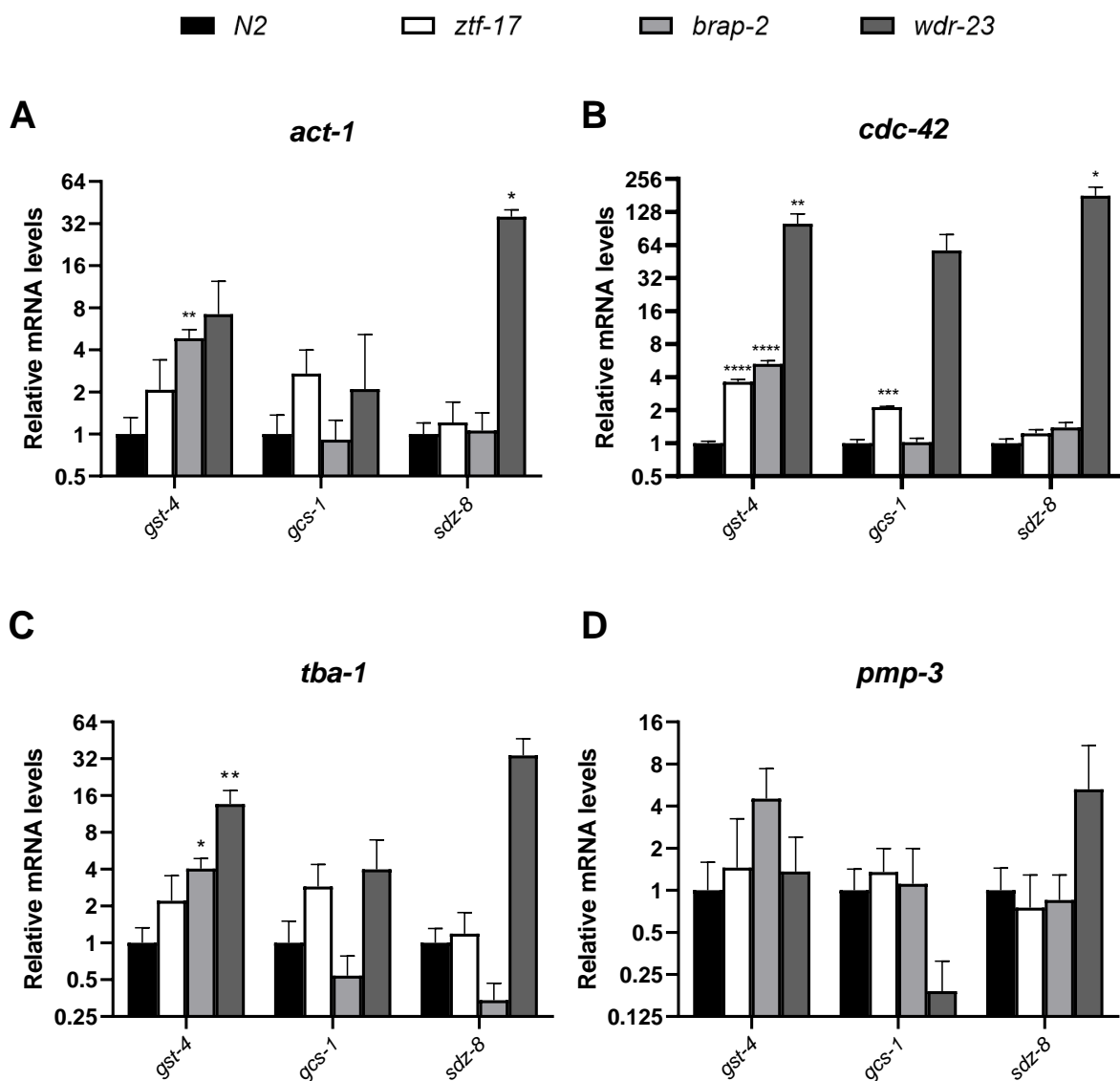


Figure 2.3 Phase II detoxification genes, *gst-4* and *gcs-1* had higher mRNA expression levels in *ztf-17(tm963)* mutants under normal conditions.

qRT-PCR was done to monitor the amplification of phase II antioxidant genes. Worms were synchronized to L4 stage then harvested for RNA isolation. *gst-4* and *gcs-1* mRNA expression levels were significantly enhanced in *ztf-17(tm963)* mutants when compared to *N2* wildtype worms. (A) Relative mRNA levels were normalized to *act-1* reference gene. (B) Relative mRNA levels were normalized to *cdc-42* reference gene. (C) Relative mRNA levels were normalized to *tba-1* reference gene. (D) Relative mRNA levels were normalized to *pmp-3* reference gene. Results for all experiments were derived from 3 independent trials. Statistical analysis was carried out using Multiple *t*-tests with the Holm-Sidak multiple comparisons test. Error bars represent \pm SEM; **** $P < 0.0001$, *** $P < 0.001$, ** $P < 0.01$, * $P < 0.05$.

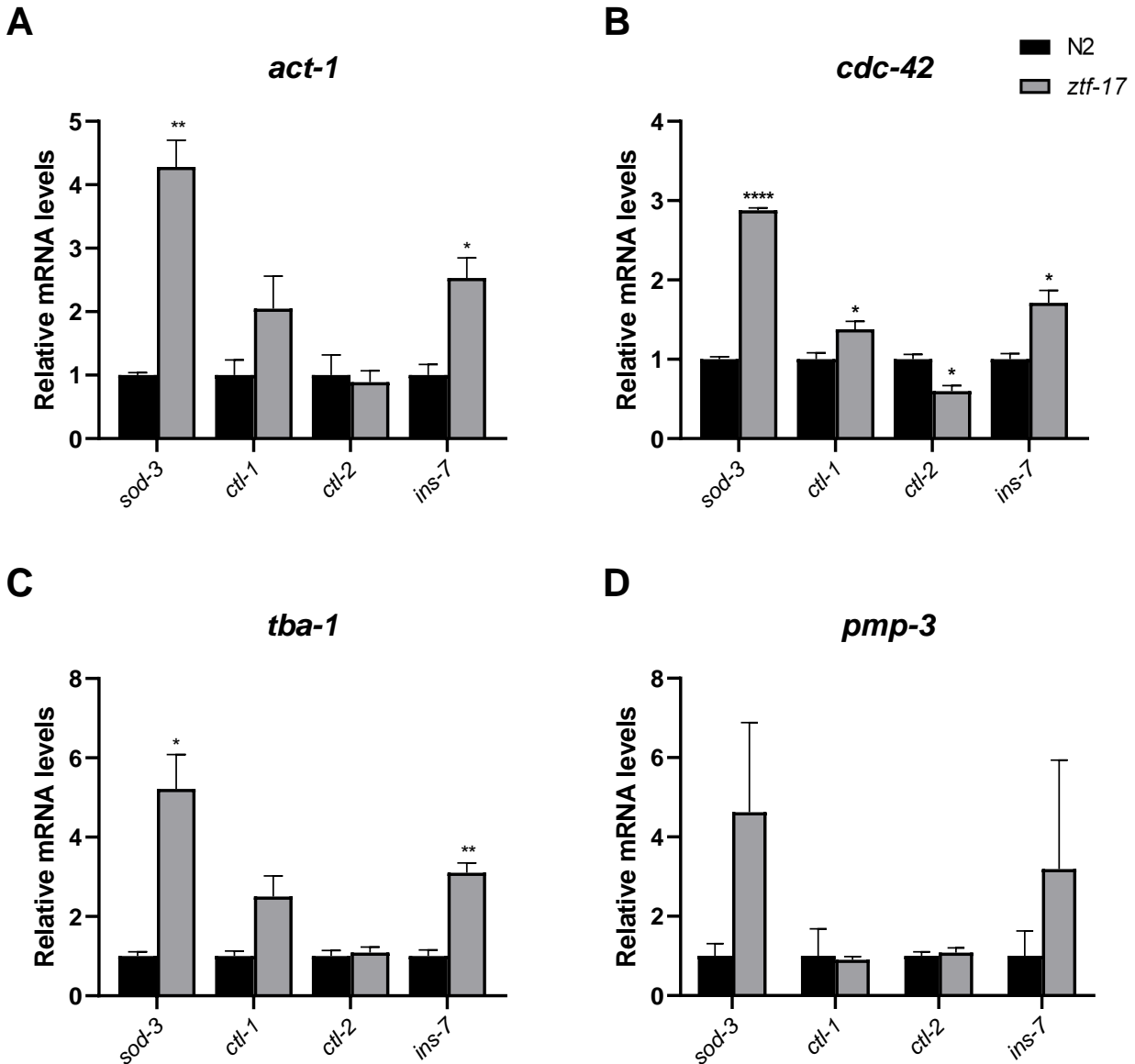


Figure 2.4 DAF-16 target genes, *sod-3*, *ctl-1* and *ins-7*, mRNA expression levels were higher in *ztf-17(tm963)* mutants under normal conditions.

qRT-PCR monitoring amplification of DAF-16 target genes. Worms were synchronized to L4 stage then harvested for RNA isolation. *sod-3*, *ctl-1* and *ins-7* mRNA expression levels were significantly enhanced in *ztf-17(tm963)*, represented as grey bars, when compared to N2 wildtype worms, represented as black bars. (A) Relative mRNA levels were normalized to *act-1* reference gene. (B) Relative mRNA levels were normalized to *cdc-42* reference gene. (C) Relative mRNA levels were normalized to *tba-1* reference gene. (D) Relative mRNA levels were normalized to *pmp-3* reference gene. Results for all experiments were derived from 3 independent trials. Statistical analysis was carried out using Multiple *t*-tests with the Holm-Sidak multiple comparisons test. Error bars represent \pm SEM; *****P* < 0.0001, ****P* < 0.001, ***P* < 0.01, **P* < 0.05.

2.3.2 Loss of *ztf-17* via RNAi-mediated knockdown resulted in an upregulation of *gst-4* and *sod-3*.

To validate the initial RNAi screen done, I wanted to see if worms treated with *ztf-17* RNAi would yield similar results as the *ztf-17(tm963)* deletion mutants. If the results aligned, then it would help me gain confidence that the upregulation of *gst-4* and *sod-3* are the result of the *ztf-17* gene deletion and not due to another variable that affected the worm when the *ztf-17(tm963)* strain was generated. I first conducted this experiment in N2 worms. I treated N2 with either pL4440 or specific RNAi for *ztf-17* and *wdr-23* by feeding prior to harvesting for qRT-PCR. Worms were feed HT115 RNAi-containing bacterial plates seeded with the dsDNA required for the specific gene knockdown of *ztf-17*. An empty vector, pL4440, was used as my control and *wdr-23* RNAi was used as a positive control. As parental worms grown on RNAi plates, they ingest the dsDNA and pass on the RNAi-mediated knockdown to their progenies. Figure 2.5A show the qRT-PCR results normalized to *cdc-42* reference gene from N2 worms treated with RNAi. I saw that although *gst-4* and *sod-3* mRNA levels were slightly enhanced in worms treated with *ztf-17* RNAi, the difference observed was not statistically significant (Figure 2.5A). As expected, my positive control showed a significant increase in *gst-4* but *sod-3* levels decreased with *wdr-23* RNAi treatment. Since the RNAi-mediated knockdown qRT-PCR results from treated N2 worms were not as robust as the results obtained from the *ztf-17(tm963)* mutants, I decided to use *rrf-3(pk1426)* worms to conduct the RNAi qRT-PCR experiments again. *rrf-3(pk1426)* is a worm strain that has a mutation making them hypersensitive to RNAi and thus, might respond better to *ztf-17* RNAi [24]. Figure 2.5B show the results for the qRT-PCR using *rrf-3(pk1426)* worms normalized to *cdc-42* reference gene. There was a significant increase of ~2.1-fold in *sod-3* expression levels for worms treated with *ztf-17* RNAi, however the increase

observed in *gst-4* was very similar to that of worms that were treated with the pL4440 empty vector control and was not statistically significant. The results obtained for the *wdr-23* RNAi treated *rrf-3(pk1426)* mutants were as expected, with ~39-fold increase in *gst-4* and reduced *sod-3* expression. To ensure that the lack of differences seen in the qRT-PCRs were not due to genomic contamination during RNA extraction, I examined the melting curves of all the RNAi qRT-PCRs done and found only one peak for each gene amplification during the experiments. The qRT-PCR products were also separated on an agarose gel, and the DNA fragment sizes matched the expected products suggesting no signs of genomic contamination. Lastly, I sequenced the *ztf-17* RNAi and made sure that it indeed did target the *ztf-17* gene. I suspect that the reason for the lack of difference seen between wildtype worms treated with *ztf-17* RNAi and my *ztf-17(tm963)* deletion mutants might be because RNAi by feeding does not always result in complete silencing of the target gene. RNAi also has varying degrees of effectiveness depending on the gene and the tissue it is expressed in. I believe that post treatment with *ztf-17* RNAi, there is still some residual ZTF-17 activity remaining which might explain the RNAi results.

To further confirm that the elevated levels of *sod-3* and *gst-4* were from loss of *ztf-17*, I looked at the differences in GFP expression when *sod-3p::gfp* and *gst-4p::gfp* worms were treated with specific RNAi. In Figure 2.6A-C, worms expressing *sod-3p::GFP* were treated with pL4440, *ztf-17* RNAi or *wdr-23* RNAi and GFP fluorescence was captured by confocal microscopy. Figure 2.6D showed the whole worm fluorescence quantification and analysis of GFP signals revealing that *ztf-17* RNAi treated worms had ~3.2-fold increase in fluorescence intensity compared to pL4440 treated worms. Worms exposed to *wdr-23* RNAi had slightly less fluorescence compared to my control worms which were consistent with the qRT-PCR results obtained from previous experiments (Figure 2.6D).

Figure 2.7A-E are the images taken of *gst-4p::gfp* worms treated with pL4440, *brap-2* RNAi, *wdr-23* RNAi, *ztf-17* RNAi and *ztf-22* RNAi respectively through confocal microscopy. When I compared the whole worm fluorescence, I found that there was a significant increase in GFP expression when worms were treated with *ztf-17* RNAi (~4.7-fold increase) and *ztf-22* RNAi (~6.1-fold increase) than that of worms treated with pL4440. My positive controls, *brap-2* RNAi and *wdr-23* RNAi treated worms, also had significantly enhanced GFP expression (Figure 2.7F).

Since the *ztf-22* RNAi was shown to affect *gst-4*, I wanted to investigate whether there was a link between *ztf-22* and *ztf-17* as both had similar expression patterns (in the body wall musculature, gonad, intestine, pharynx, and ventral nerve cord of *C. elegans*) and encodes for a protein that had a zinc finger DNA binding domain [25–27]. Though there is limited information in the literature on *ztf-17* and *ztf-22*, *in vivo* analysis found that *ztf-22* transcripts were enriched near the TRA-1 transcription factor binding sites that determined sex during *C. elegans* development, while *ztf-17* may regulate miRNAs involved in larval developmental [28–30]. Perhaps a connection between ZTF-17 and ZTF-22 also exist in the oxidative stress response pathways. I wanted to see if loss of both *ztf-17* and *ztf-22* would result in noticeable changes in *gst-4p::GFP* expression. Figure 2.8A are confocal microscopy images of *ztf-17(tm963)* and *ztf-22(gk3296)* transgenic worms expressing *gst-4p::GFP*. After worms were fed RNAi, targeting *ztf-17* and *ztf-22*, or the empty vector pL4440, loss of both transcription factors (deletion mutant and RNAi treatment) resulted in further enhancement of *gst-4p::GFP*. There was ~2x increase in GFP when *ztf-17(tm963);gst-4p::gfp* worms were fed *ztf-22 RNAi* and ~1.2x increase when *ztf-22(gk3296);gst-4p::gfp* worms were fed *ztf-17 RNAi*. This difference was in comparison to the fluorescence intensity of worms that were fed only the pL4440 plasmid (Figure 2.8B). The results suggest that ZTF-17 and ZTF-22 may work in parallel pathways but together to affect the

expression of *gst-4* as loss of one transcription factor does not appear to affect the repressive effects of the other.

Since the reporter construct *gst-4p::gfp* fluorescence appeared to be further enhanced when both transcription factors were knocked down via RNAi, I suspected that they may function in different pathways but I did not want to ignore if there was a possibility that ZTF-17 and ZTF-22 might work together to repress *gst-4* gene expression. To determine if there was an interaction between ZTF-17 and ZTF-22, a DULIP assay was done to test the protein-protein interaction (PPI) between ZTF-17 (prey) and ZTF-22 (bait). HEK293T cells were transfected with the DNA constructs expressing said proteins and analysis of the co-immunoprecipitations (Co-IP) were done. Figure 2.9A is a schematic diagram of the *Renilla* luciferase (RL) and Firefly luciferase (FL) activity in each of the Co-IPs. Figure 2.9B-C are the readings for the RL and FL found in the cell lysates and the precipitated protein complexes. ZTF-17's interaction with ZTF-22 was first represented as a Normalized Interaction Ratio (NIR), then corrected by subtracting the NIRs obtained from the mCherry controls. The corrected NIR (cNIR) is the true PPI between ZTF-17 and ZTF-22 (Figure 2.9D). When the DULIP assay was optimized, a cNIR that is ≥ 3 was determined to separate positive and negative PPIs [14]. The cNIR determined for ZTF-17 and ZTF-22 was found to be ~ 0.07 . Thus, the data suggested that based on this assay, the detection of ZTF-17 and ZTF-22 interaction was low. Taken together these results, although ZTF-17 and ZTF-22 both act on *gst-4*, the proteins may work independently of each other or function in different pathways leading to the same outcome of regulating genes involved in the oxidative stress response.

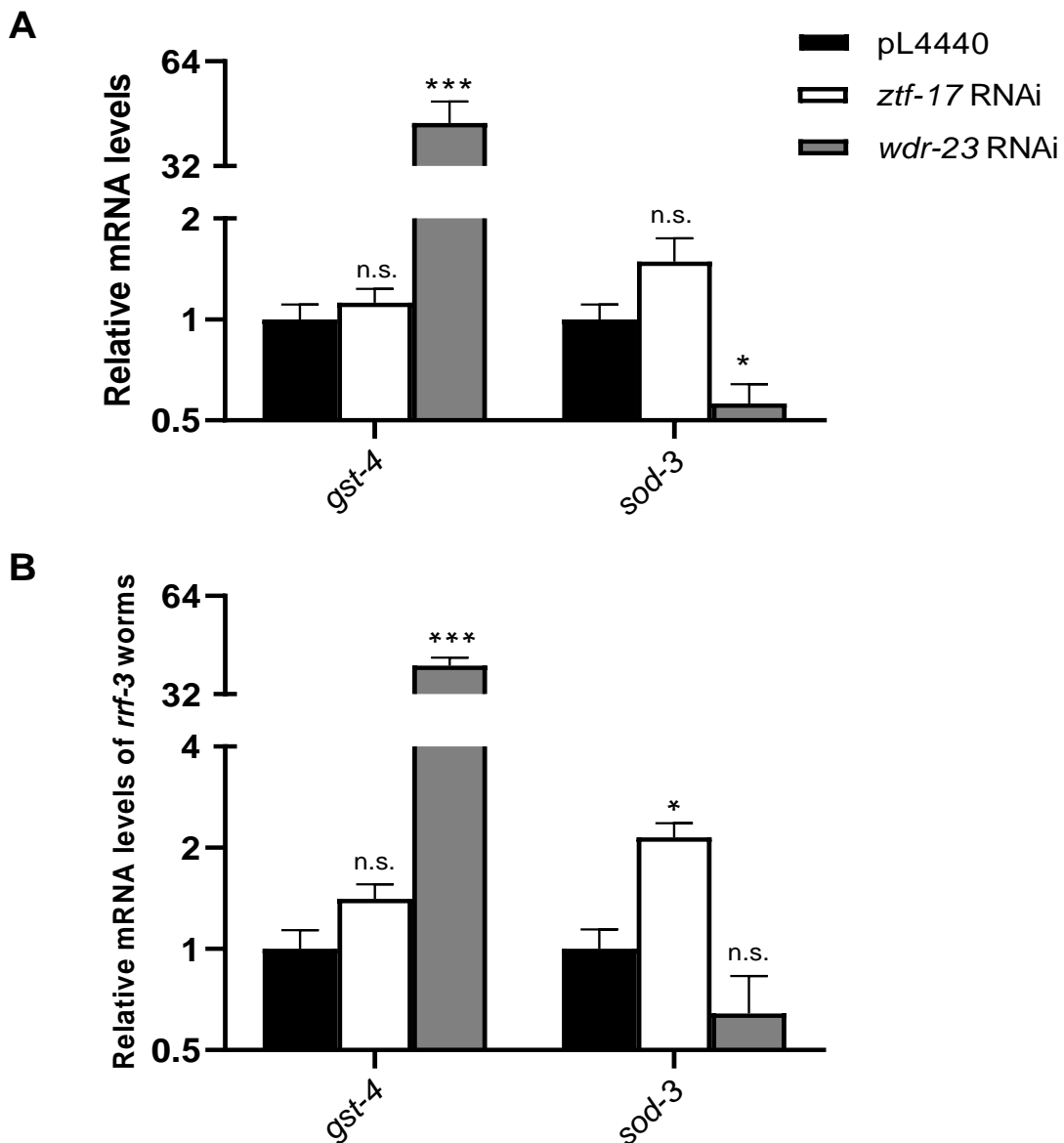


Figure 2.5 mRNA expression levels of *gst-4* during RNAi-mediated knockdown of *ztf-17* showed no significant differences but there was enhanced *sod-3* expression.

qRT-PCR was done to measure mRNA expression levels of *gst-4* and *sod-3* in worms treated with either pL4440 empty vector, *ztf-17* RNAi or *wdr-23* RNAi. (A) Relative mRNA expression levels of *gst-4* and *sod-3* were not significantly different in N2 worms when treated with *ztf-17* RNAi. (B) Relative mRNA expression levels of *gst-4* were slightly enhanced in hypersensitive *rrf-3(pk1426)* mutants treated with *ztf-17* RNAi while *sod-3* mRNA levels showed ~2.1x increase. Results were derived from 5 independent trials and normalized to reference gene *cdc-42* mRNA. Statistical analysis was carried out using Multiple *t*-tests with the Holm-Sidak multiple comparisons test. Error bars represent \pm SEM; *** $P < 0.001$, ** $P < 0.01$, * $P < 0.05$.

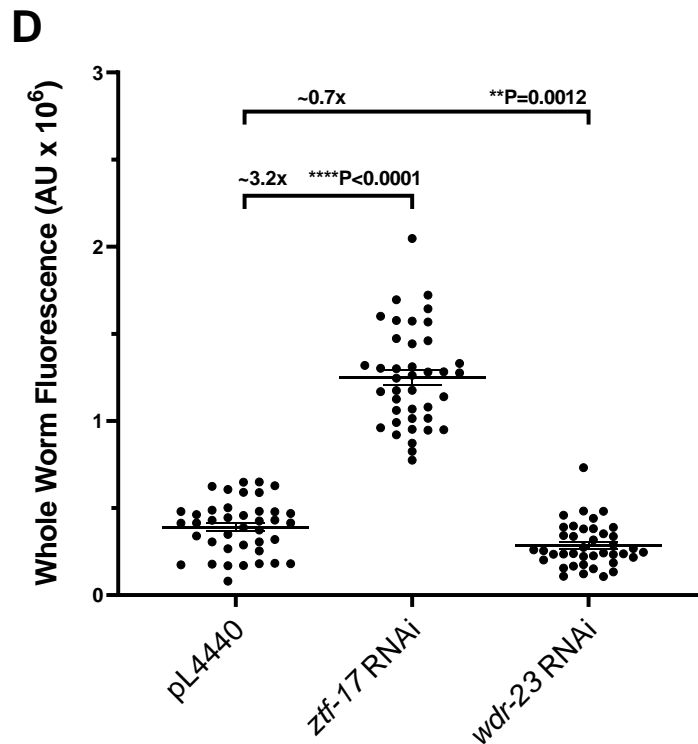
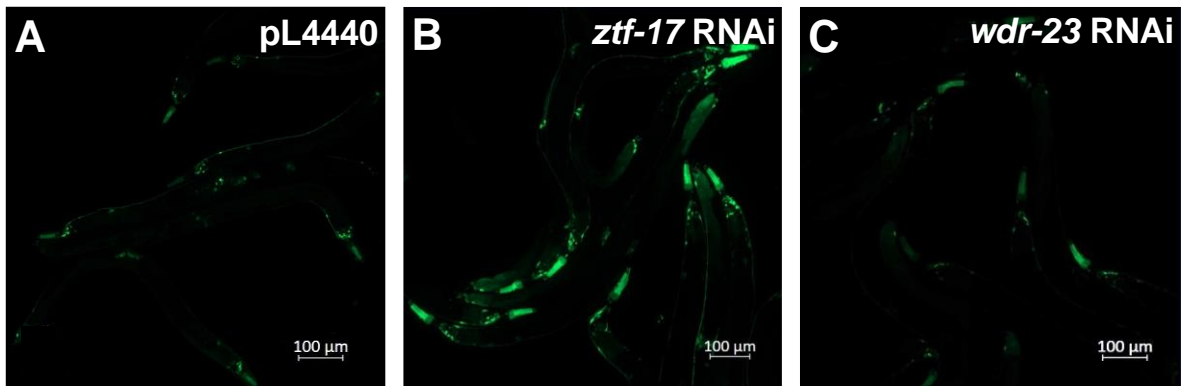


Figure 2.6 *ztf-17* RNAi increases the basal expression levels of *sod-3p::GFP* under non-oxidative stress-inducing conditions.

(A-C) Whole worm GFP fluorescence was captured using the Zeiss Observer Z1 Spinning Disk Confocal Microscope. *sod-3p::GFP* expressing worms were fed with HT115 *E. coli* cells that expressed either pL4440 (empty vector) or dsRNA that targeted specific mRNA for 48 hours prior to visualization. *wdr-23* RNAi was used as a positive control. (D) Worms treated with *ztf-17* RNAi had ~3.2x increased GFP fluorescence signal compared to pL4440 treated worms. *wdr-23* RNAi treated worms showed a slight decrease in GFP signals. Results for n=40 worms are shown as individual points as the difference between the intensity readings per worm minus the background fluorescence. The mean fluorescence intensity is displayed as a solid black line for each worm strain. Statistical analyses were performed using Two-tailed Unpaired Student's *t*-test; **** P < 0.0001.

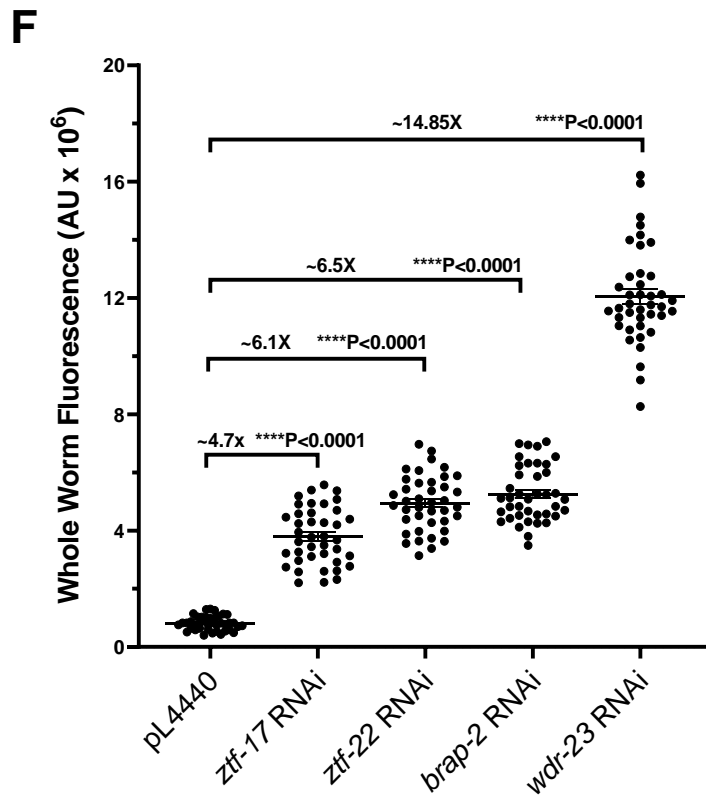
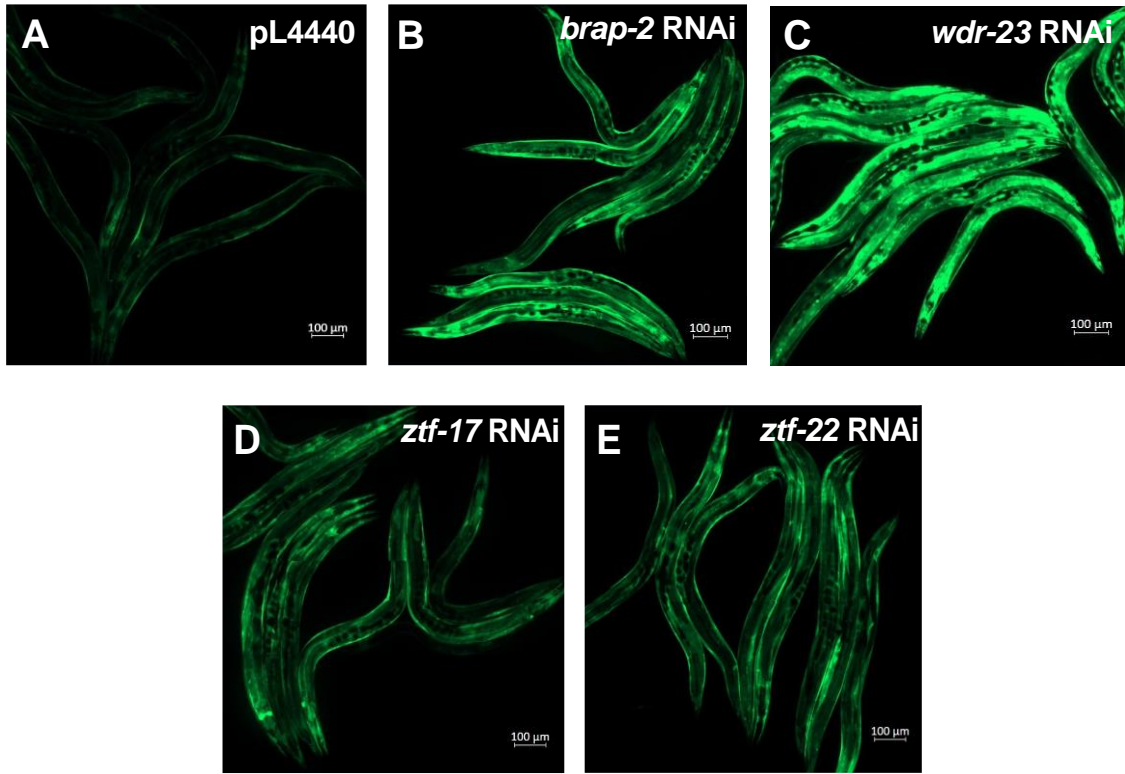


Figure legends can be found on the next page.

Figure 2.7 *ztf-17* RNAi and *ztf-22* RNAi increases the basal expression levels of *gst-4p::GFP* under non-oxidative stress-inducing conditions.

(A-E) Whole worm GFP fluorescence was captured using the Zeiss Observer Z1 Spinning Disk Confocal Microscope. *gst-4p::GFP* expressing worms were fed with HT115 *E. coli* cells that expressed either pL4440 (empty vector) or dsRNA that targeted specific mRNA for 48 hours prior to visualization. *brap-2* RNAi and *wdr-23* RNAi were used as positive controls. (F) Both *ztf-17* and *ztf-22* RNAi-mediated knock-down significantly increased the intensity of the GFP fluorescence of *gst-4* with ~4.7x and ~6.1x increase, respectively. Results for n=40 worms are shown as individual points as the difference between the intensity readings per worm minus the background fluorescence. The mean fluorescence intensity is displayed as a solid black line for each worm strain. Statistical analyses were performed using Two-tailed Unpaired Student's *t*-test; **** P < 0.0001.

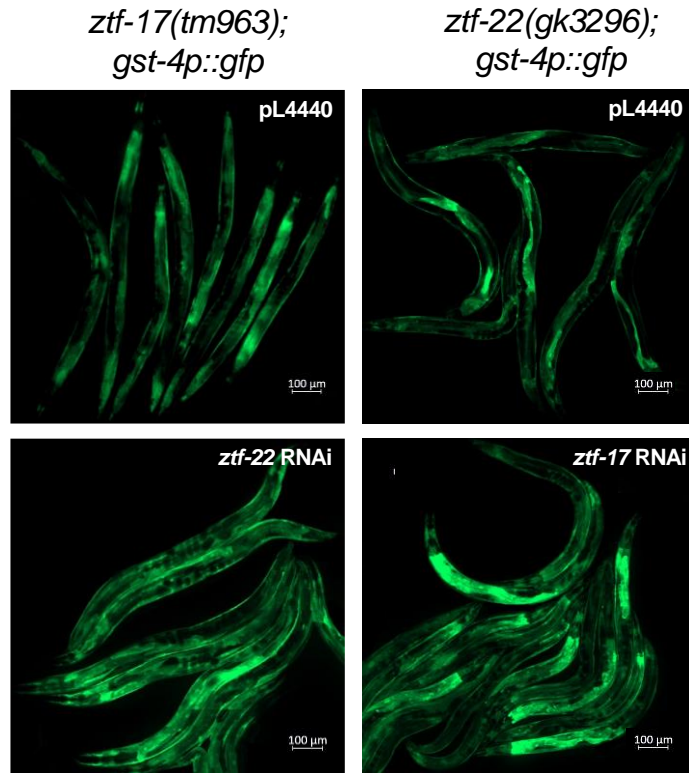
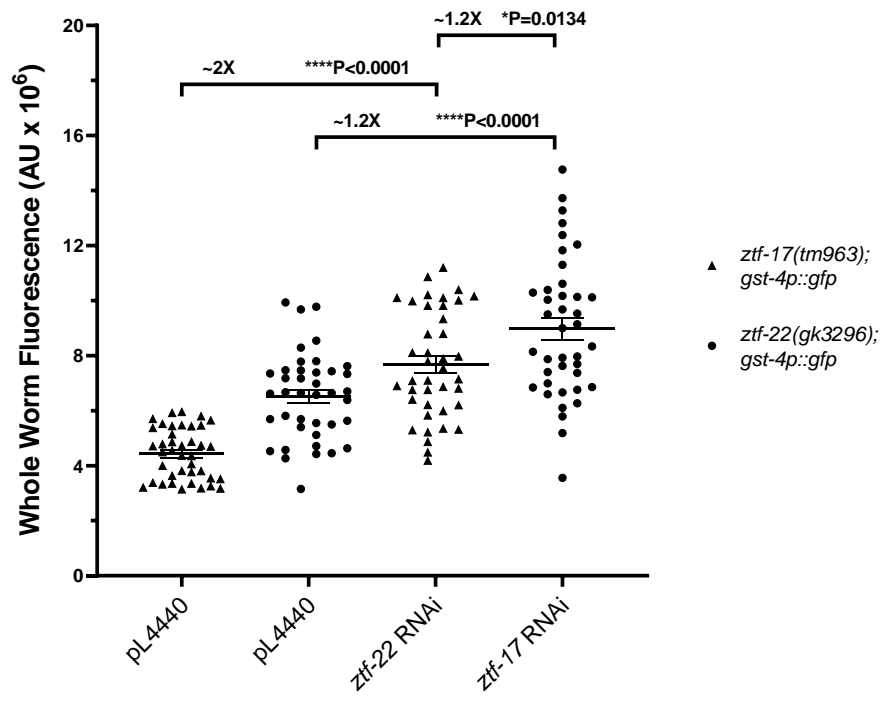
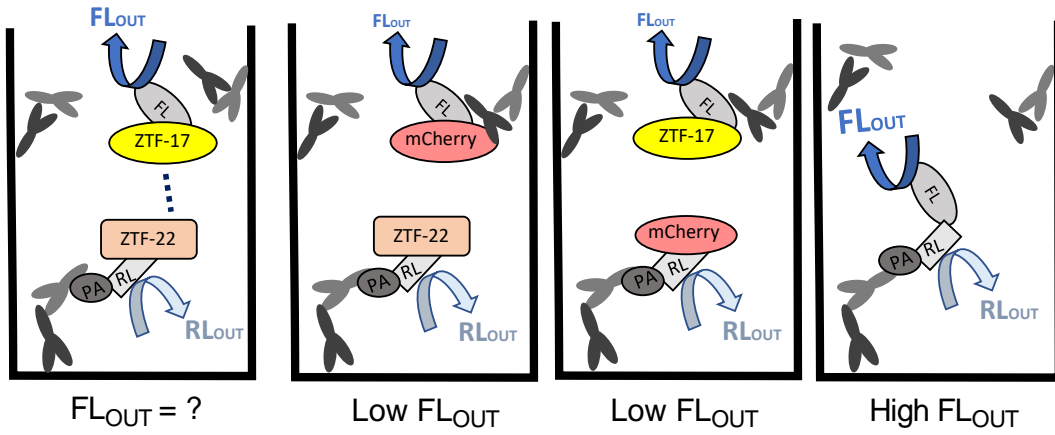
A**B**

Figure legends can be found on the next page.

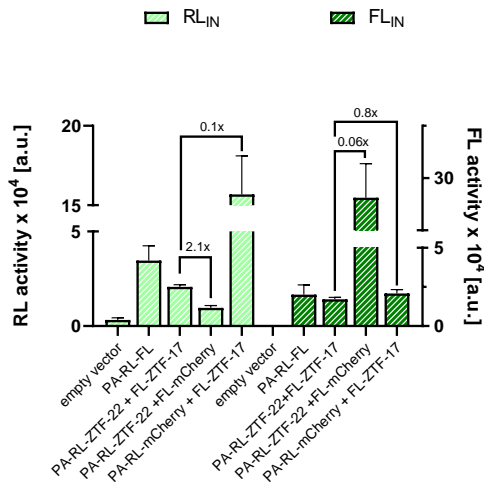
Figure 2.8 Loss of both *ztf-17* and *ztf-22* resulted in a further increase of *gst-4p::GFP* when deletion mutants were treated with RNAi.

(A) Whole worm GFP fluorescence was captured using the Zeiss Observer Z1 Spinning Disk Confocal Microscope. *ztf-17(tm963)* and *ztf-22(gk3296)* transgenic worms expressing *gst-4p::GFP* were fed with HT115 *E. coli* cells that expressed either pL4440 (empty vector) or dsRNA that targeted *ztf-17* or *ztf-22* mRNA for 48 hours prior to visualization. (B) In both mutants, when *ztf-17* and *ztf-22* RNAi-mediated knock-down was done, there was a significant increase in the intensity of the GFP fluorescence of *gst-4* when compared to worms that were fed pL4440. *ztf-22(gk3296)* worms had a higher basal level of *gst-4p::GFP* compared to *ztf-17(tm963)* mutants. Results for n=40 worms are shown as individual points as the difference between the intensity readings per worm minus the background fluorescence. The mean fluorescence intensity is displayed as a solid black line for each worm strain. Statistical analyses were performed using Two-tailed Unpaired Student's *t*-test; **** P < 0.0001 and * P < 0.05.

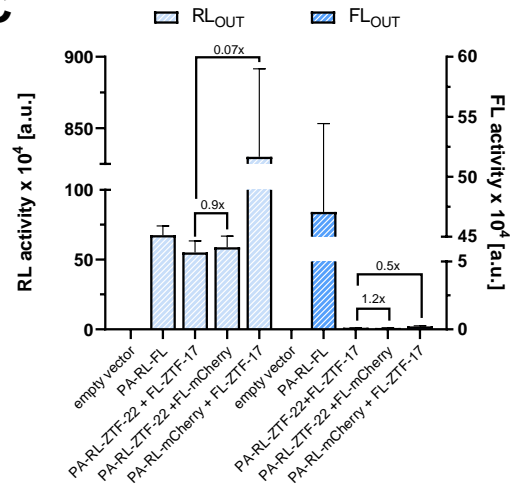
A



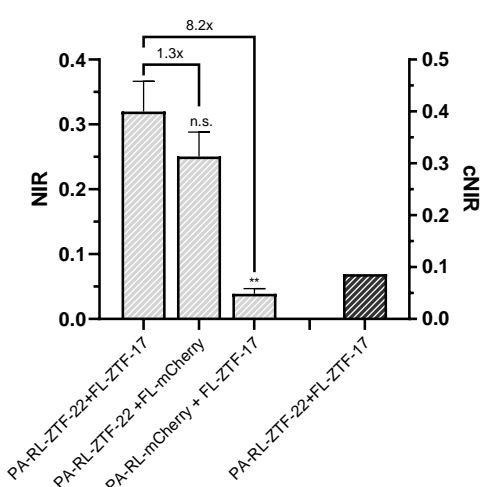
B



C



D



E

Protein-Protein Interaction (PPI):



Control 1:



Control 2:



Control 3:



Figure legend can be found on the next page.

Figure 2.9 The NIR for ZTF-22 and ZTF-17 suggest no detectable interaction between the two proteins.

(A) Schematic of the predicted interaction between PA-RL-ZTF-22 (bait)/FL-ZTF-17 (prey) and the controls, PA-RL-ZTF-22/FL-mCherry, PA-RL-mCherry/FL-ZTF-17 and PA-RL-FL. (B) Analysis of protein expression through quantification of RL and FL luminescence activities in cell lysates were done 48 hr post transfection. (C) Analysis of co-immunoprecipitates through quantification of RL and FL luminescence activities. PA-tagged bait ZTF-22 was immunoprecipitated with Rabbit IgG. (D) Calculation of Normalized Interaction Ratios (NIR) for tested PPIs. The NIR for the interaction between PA-RL-ZTF-22/FL-ZTF-17 was slightly higher than the NIRs for the control PPIs of PA-RL-ZTF-22/FL-mCherry and PA-RL-mCherry/FL-ZTF-17. For PA-RL-ZTF-22/FL-ZTF-17, a background corrected normalized interaction ratio (cNIR) was calculated to be ~0.07. A cNIR of ≥ 3 was determined to be optimal for separating positive and negative PPIs. Data represented are the means of 3 independent experiments \pm SEM and statistical analysis was carried out using Two-tailed Unpaired *t*-test; ** $P < 0.01$. (D) Schematic of the different Co-IPs including the PPI of interest, the PPIs with the mCherry controls and the PPI between RL-FL.

2.3.3 Transcription factor ZTF-17 is a repressor of the *skn-1c* and *sod-3* promoters and negatively regulates SKN-1 and DAF-16 target genes.

After revealing how loss of ZTF-17 had modulated the expression of PI and PII detoxification genes, I was interested in seeing if the opposite effect was true and to determine what exactly were the repressor like functions of ZTF-17. This led me to conduct my luciferase assay and ZTF-17 overexpression experiments. Based on the current research in the literature, ChIP data revealed that there were putative DAF-16 binding sites located on the *skn-1* locus indicating that *skn-1* expression can be activated by the DAF-16 transcription factor [8]. Likewise, many oxidative stress resistance genes have predicted upstream transcription factor binding sites that matched the SKN-1 consensus sequence, *sod-3* promoter being one of them [31]. Knowing that targets of SKN-1 appeared to be shared with DAF-16 and vice versa, I first established that the *skn-1c* promoter (*skn-1cp*) and *sod-3* promoter (*sod-3p*) could be activated by both DAF-16 and SKN-1.

I designed the 3xFLAG:DAF-16A construct and wanted to test to which degree did DAF-16 affect the *skn-1c* promoter and if it would drive the promoter activity. I transfected HEK293T cells with the luciferase reporter construct fused to *skn-1c* along with SKN-1 and/or DAF-16A (Figure 2.10A). pGL4.70 was used as the *Renilla* Luciferase control. When I analyzed the relative Firefly luciferase levels, I found that SKN-1 alone could transactivate its own promoter and the result was an increase in the *skn-1cp* activity by ~3.3-fold when compared to cells that were transfected with EGFP (Figure 2.10A). EGFP acted as my control since it had no affinity for the promoter. DAF-16A alone was unable to activate the *skn-1cp*, however, when SKN-1 and DAF-16A were present together, transcription of the *luc* gene was robustly enhanced to ~5.3x that of the EGFP control (Figure 2.10A). The results suggest the presence of DAF-16A

may enhance SKN-1's ability to drive promoter activity and the two may have a synergistic effect in activating PII detoxification enzymes. Figure 2.10B is a schematic representation showing the reporter gene luciferase expression cassettes and the interactions at the *skn-1cp*.

I performed another luciferase assay with the same SKN-1 and DAF-16A constructs but tested the effects on the *sod-3p* instead. SKN-1 alone was unable to activate *sod-3p* and had very similar luciferase activity as my EGFP control (Figure 2.11A). As expected, DAF-16A was able to drive the *sod-3p* which had ~2.7-fold increase in luciferase activity. Surprisingly, SKN-1 attenuated the *sod-3p* activity that was activated by DAF-16A and I saw ~20% reduction in the *luc* gene transcription (Figure 2.11A). Recent findings in the literature indicate that although SKN-1 plays an essential role in oxidative stress resistance, constitutive activation of SKN-1 or *skn-1* gain of function mutations actually suppresses DAF-16 [8,21,32]. Inversely, SKN-1 inhibition was also found to activate DAF-16 which suggest that SKN-1 has dual roles and acts as an activator of oxidative stress resistance genes and as a negative regulator of DAF-16 in aging regulation [32]. Figure 2.11B is a schematic representation showing the reporter gene luciferase expression cassettes and the promoter activities of *sod-3p*.

Based on my findings related to the interactions observed between DAF-16, SKN-1 and the promoters, I conducted my last sets of luciferase assays adding in the ZTF-17 construct to investigate the effects on their activities. Figure 2.12A-B represent the relative luciferase activity of the *skn1cp* and *sod-3p* promoters normalized to my EGFP control group. ZTF-17 was able to significantly reduce the transcription of the *luc* gene in the presence of SKN-1 when it activated its own *skn-1cp* and was also able to reduce the synergistic effect of SKN-1 and DAF-16 coactivation of the *skn1-cp* by approximately 35% (Figure 2.12A). Similar results were obtained when I tested the *sod-3p* with the same construct combinations with ~36% reduction

that was observed when ZTF-17 was present to impede the activation of *sod-3p* by DAF-16 and/or SKN-1 (Figure 2.12B). Figure 2.12C-D are the schematic representations of the proposed repression seen by ZTF-17. Whether the repression by ZTF-17 is due to a direct interaction with the promoter DNA or if it is through indirect processes that reduce the transcription of the *luc* gene, the mechanism still remains unclear.

To further confirm the repressive qualities of ZTF-17, I cloned ZTF-17 into pSL301 and created two *ztf-17(+)* overexpressing transgenic worm strains (line 1 and line 2) through *C. elegans* microinjection techniques. Figure 2.13A is an image of the *ztf-17(+)* overexpressing transgenic worms captured by confocal microscopy. The red fluorescent marker, *sur-5p::mCherry*, was used for selection and the marker was co-injected with the *ztf-17(+)* overexpressing construct. *ztf-17(+)* overexpressing transgenic worms were harvested for RNA extraction and qRT-PCR experiments. Results are shown in Figure 2.13B and as expected, *gst-4* and all DAF-16 target genes tested (*sod-3*, *ctl-1*, *ctl-2*, *ins-7*, *mtl-1* and *mtl-2*) were all significantly enhanced in the *ztf-17(tm963)* mutants when compared to N2 worms. The *ztf-17(+)* overexpressing worms had no significant differences in the mRNA expression levels of DAF-16 target genes when compared to wildtype, however, I saw a drastic reduction of ~50% in the *gst-4* expression levels (Figure 2.13B). This suggest that overexpressing ZTF-17 could lead to targeted repression of specific genes, in this case, *gst-4*. In this experiment, only a fraction of the progenies carrying the *ztf-17(+)* overexpression construct express the array at ~30-60% frequency from parental worms. When *ztf-17(+)* worms were collected for qRT-PCR, the sample consisted of a mixed population of *ztf-17(+)* overexpressing worms at varying degrees, thus the effect of the ZTF-17 overexpression might not be as robust. I also used the *ztf-22(gk3296)* deletion mutants to see if loss of *ztf-22* would influence DAF-16 target genes like

ztf-17. *ztf-22(gk3296)* were unable to enhance any of the DAF-16 target genes tested, and interestingly there was even a significant reduction in the mRNA levels of *ctl-1*, *ctl-2*, *ins-7* and *mtl-1* (Figure 2.13B). Only *gst-4* expression levels were enhanced in the *ztf-22(gk3296)* mutants which were consistent with the observations I saw when *ztf-22* RNAi was used against *gst-4p::gfp* worms (Figure 2.7E-F and Figure 2.13B).

Since I have shown that ZTF-17 can regulate SKN-1 and DAF-16 target genes, I thought it would be important to begin investigating the mechanism by which ZTF-17 functioned by. Since DAF-16 activation is the most probable explanation for the upregulation of the DAF-16 target genes seen in my *ztf-17(tm963)* mutants, I wanted to see if DAF-16 localization was also affected. Under normal conditions, DAF-16 is negatively regulated and sequestered in the cytosol. But under stress conditions, the IIS pathway is turned off enabling DAF-16 to translocate into the nucleus to promote or repress genes that trigger resistance [10]. I was successful in creating a cross between *ztf-17(tm963)* and TJ356 [*(daf-16p::gfp* expressing)] worms. Using confocal microscopy, I visualized the differences in DAF-16::GFP between *ztf-17(tm963)* and the *daf-16p::gfp* expressing worms (Figure 2.14A). Animals were grouped as either cytosolic, intermediate – which refers to a mix of cytosolic and nuclear, or solely nuclear depending on their GFP signal. *ztf-17(tm963)* worms had nuclear DAF-16::GFP in ~40% of the worms visualized whereas TJ356 worms had mostly DAF-16::GFP expression, ~68%, in the cytosol (Figure 2.14B). Both groups had worms in the intermediate stage but more worms that were *ztf-17(tm963);daf-16p::gfp* mutants showed increased DAF-16::GFP nuclear localization which was indicative of increased DAF-16 activation. In the enlarged images of Figure 2.14A, white arrows point to the nuclei which are located in the *C. elegans* intestines.

To determine if ZTF-17 played a direct role in DAF-16 activation, I performed a DULIP to screen for any potential PPIs between the two transcription factors. After creating the appropriate constructs, HEK293T cells were transfected and analysis of Co-IPs were done. Figure 2.15A-B show the *Renilla* luciferase and Firefly luciferase activity in the cell lysates and in the Co-IPs. Figure 2.15C presents the PPI between ZTF-17 and DAF-16A as a Normalized Interaction Ratio (NIR). Although the interaction between ZTF-17 and DAF-16A was significantly higher than the interactions with the mCherry controls, when I corrected the NIR (cNIR=0.06), the difference became negligible which suggest that the interaction between DAF-16A and ZTF-17 is unlikely. These results indicate that functional ZTF-17 can repress SKN-1 and DAF-16 target genes and is able to reduce the transcriptional activity at said promoters. Whilst ZTF-17 may not directly regulate DAF-16 through physical interaction, it may require other unknown factors to promote the interaction between these proteins. The enhancement of DAF-16 target genes observed in *ztf-17(tm963)* mutants may still be regulated by ZTF-17 through indirect mechanisms affecting DAF-16 and/or in a DAF-16 independent manner.

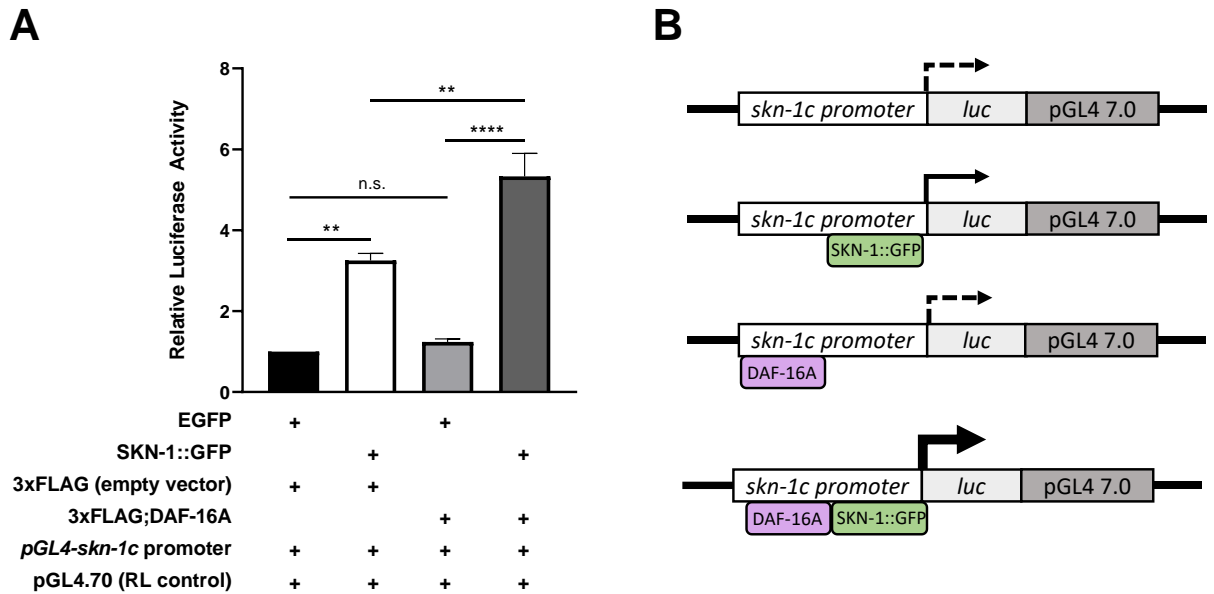


Figure 2.10 The activity of the *skn-1c* promoter was robustly enhanced in the presence of SKN-1 and DAF-16A suggesting that there is a synergistic activating effect.

(A) Results for the Firefly/*Renilla* Dual Luciferase detection assay of the *skn-1c* promoter represented as Relative Luciferase Activity. HEK293T cells were co-transfected with the *skn-1c*-*luc* plasmid, either the expression plasmid for SKN-1, DAF-16A, both, or the empty vectors and the internal *Renilla* control pGL4 7.0. EGFP was used as the experimental control. The Firefly luciferase activity was measured 48 hr post-transfection. SKN-1 enhanced the promoter activity ~3.3x compared to the EGFP control while SKN-1 and DAF-16A together had ~5.3x increase. The data was derived from 3 independent experiments and normalized to EGFP. Statistical analysis was done using One-way ANOVA with Tukey's multiple comparisons test; **** P < 0.0001, *** P < 0.001, ** P < 0.01, * P < 0.05. (B) Schematics of the reporter gene luciferase expression cassettes. Expression of the *luc* gene driven by the *skn-1c* promoter was very low in the absence of the SKN-1 protein but robustly increased in the presence of both SKN-1 and DAF-16 proteins. Dash lines represent weak expression while solid lines represent strong expression with thickness being an indicator of robustness at the promoter.

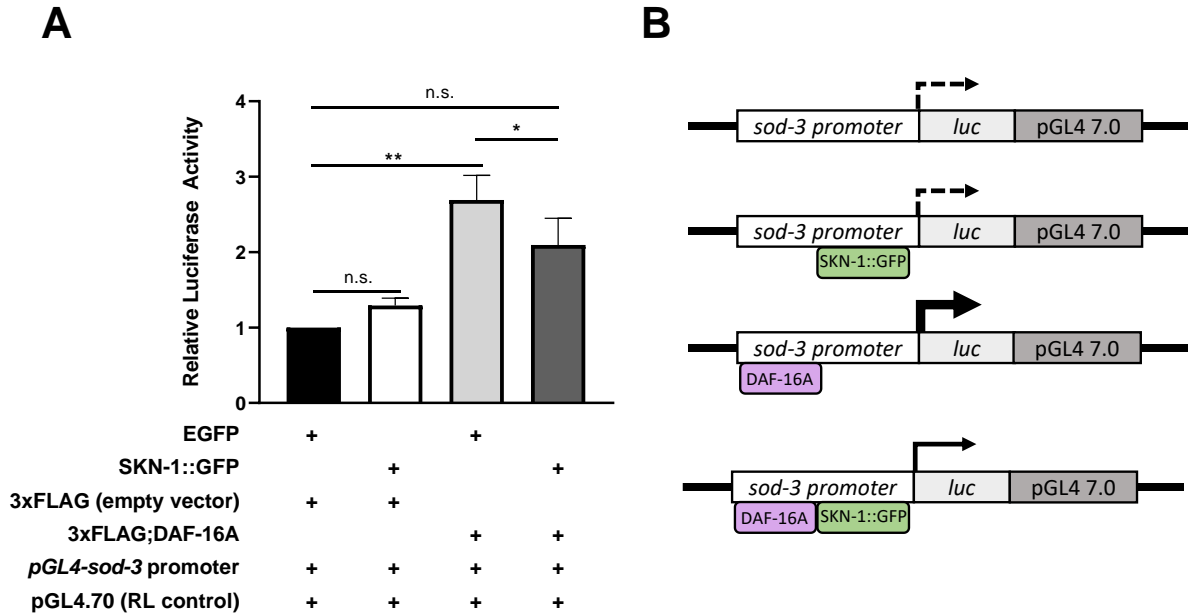


Figure 2.11 DAF-16A alone enhanced the *sod-3* promoter activity but activity was attenuated by the presence of SKN-1.

(A) Results for the Firefly/*Renilla* Dual Luciferase detection assay of the *sod-3* promoter represented as Relative Luciferase Activity. HEK293T cells were co-transfected with the *sod-3p-luc* plasmid, either the expression plasmid for SKN-1, DAF-16A, both, or the empty vectors and the internal *Renilla* control pGL4 7.0. EGFP was used as the experimental control. The Firefly luciferase activity was measured 48 hr post-transfection. DAF-16A alone enhanced the promoter activity ~2.7-fold while the presence of both DAF-16A and SKN-1 reduced the promoter activity. The data was derived from 3 independent experiments and normalized to EGFP. Statistical analysis was done using One-way ANOVA with Tukey's multiple comparisons test; ** P < 0.01, * P < 0.05. (B) Schematic representation of the reporter gene luciferase expression cassettes. Expression of the *luc* gene driven by the *sod-3* promoter was very low in the absence and presence of SKN-1 but was enhanced by DAF-16A. The activity of the *sod-3* promoter by DAF-16A was dampened when both DAF-16A and SKN-1 proteins were present. Dash lines represent weak expression while solid lines represent strong expression with thickness being an indicator of robustness at the promoter.

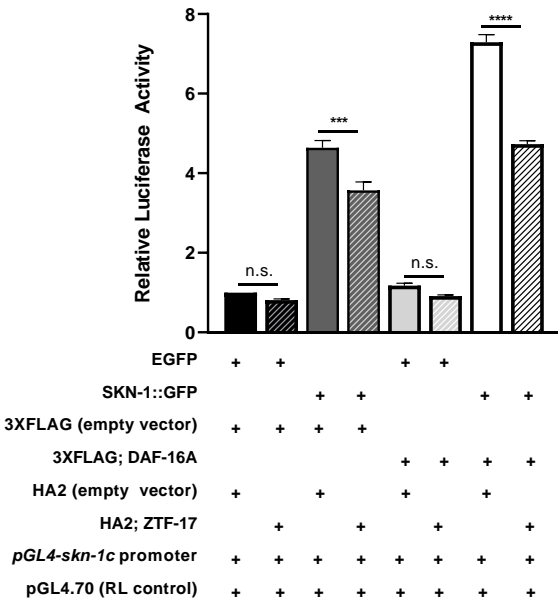
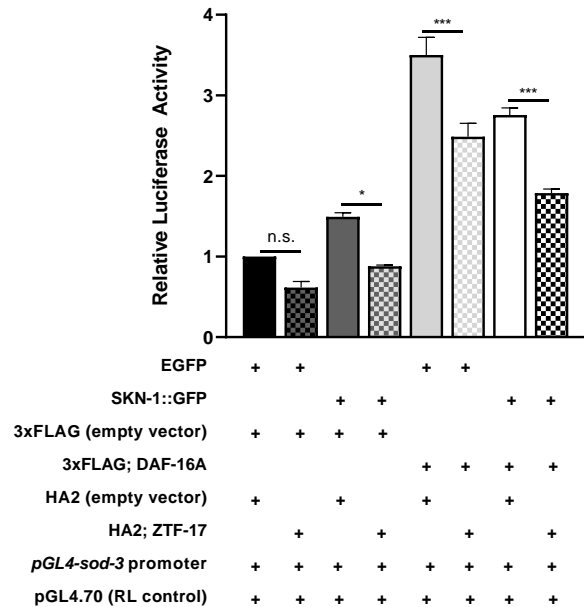
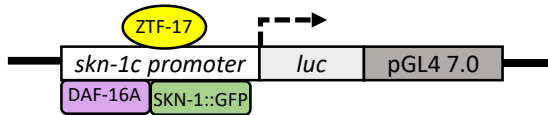
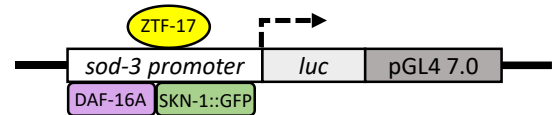
A**B****C****D**

Figure 2.12 ZTF-17 significantly reduced the promoter activity of both *skn-1cp* and *sod-3p* that was enhanced by DAF-16A and SKN-1.

(A-B) Results for the Firefly/*Renilla* Dual Luciferase detection assay of the *skn-1c* and *sod-3* promoter represented as Relative Luciferase Activity. HEK293T cells were co-transfected with specific combinations of the following expression plasmids, SKN-1, DAF-16A, ZTF-17, empty vectors and the internal *Renilla* control pGL4 7.0. EGFP was used as the experimental control. The Firefly luciferase activity was measured 48 hr post-transfection. ZTF-17 repressed the *skn-1cp* and *sod-3p* activity in the presence of SKN-1 and DAF-16A. In both promoters, there was ~35-36% reduction when ZTF-17 was present. The data was derived from 3 independent experiments and normalized to EGFP. Statistical analysis was done using One-way ANOVA with Tukey's multiple comparisons test; **** P < 0.0001, *** P < 0.001, ** P < 0.01, * P < 0.05. (C-D) Schematic representation of the interactions between DAF-16A, SKN-1 and ZTF-17 with the *skn1cp* and *sod-3p* and the repression of the *luc* gene observed. Dash lines represent weak expression at the promoter.

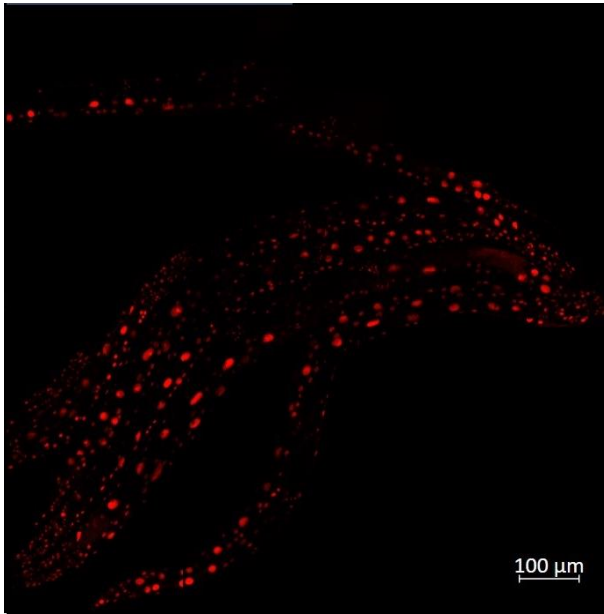
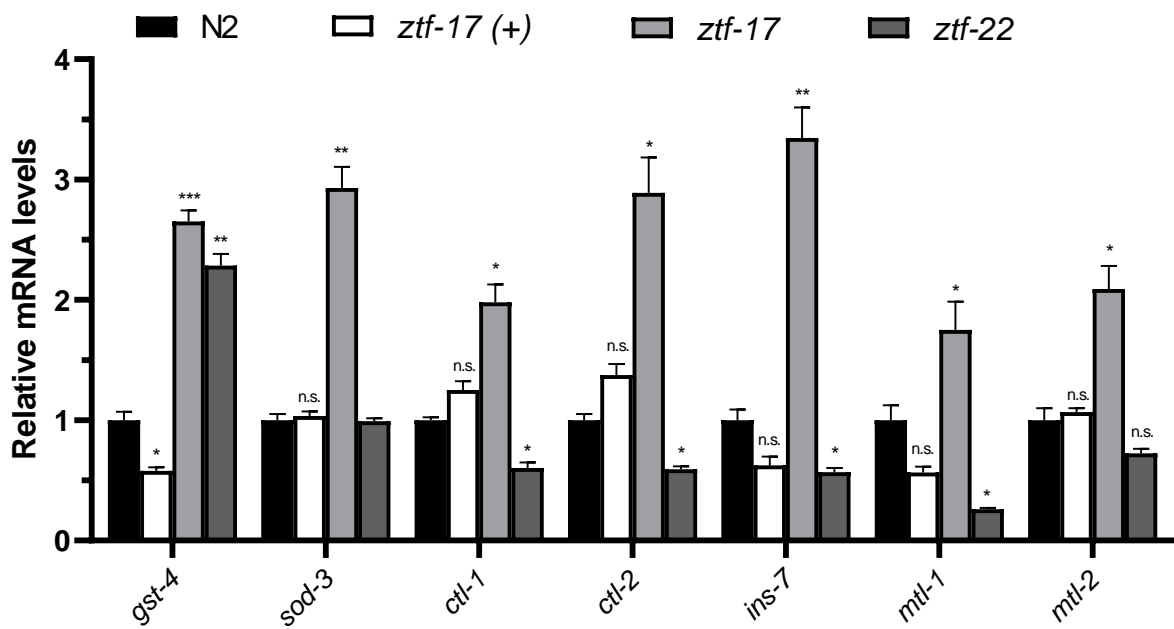
A**B**

Figure legend can be found on the next page.

Figure 2.13 Overexpression of *ztf-17* in transgenic worms resulted in a significant reduction in the mRNA expression levels *gst-4* but no significant changes to DAF-16 target genes.

(A) Transgenic worms were generated by microinjecting an overexpressing *ztf-17* DNA construct containing solution into the gonad. Worms were co-injected with a red fluorescent marker to allow for selection of transgenic animals. The *ztf-17* overexpressing plasmid DNA is extrachromosomal and are stably inherited over generations. (B) qRT-PCR monitoring amplification of *gst-4* and DAF-16 target genes. N2 wildtype worms, transgenic *ztf-17(+)* overexpressing worms, *ztf-17(tm963)* mutants, and *ztf-22(gk3296)* mutants were synchronized to L4 stage prior to RNA isolation. Results show the relative mRNA expression levels for *gst-4*, *sod-3*, *ctl-1*, *ctl-2*, *ins-7*, *mtl-1* and *mtl-2* genes. Data was derived from 4 independent trials and normalized to *cdc-42* reference gene. *ztf-17(tm963)* mutants showed a significant increase in *gst-4* and all the DAF-16 target genes tested. *ztf-22(gk3296)* deletion mutants also showed an increase in *gst-4* but no significant changes in the mRNA levels for *sod-3* and *mtl-2* and a decrease in *ctl-1*, *ctl-2*, *ins-7* and *mtl-1* mRNA expression was observed instead. Statistical analysis was carried out using Multiple *t*-tests with the Holm-Sidak multiple comparisons test. Error bars represent \pm SEM; *** $P < 0.001$, ** $P < 0.01$, * $P < 0.05$.

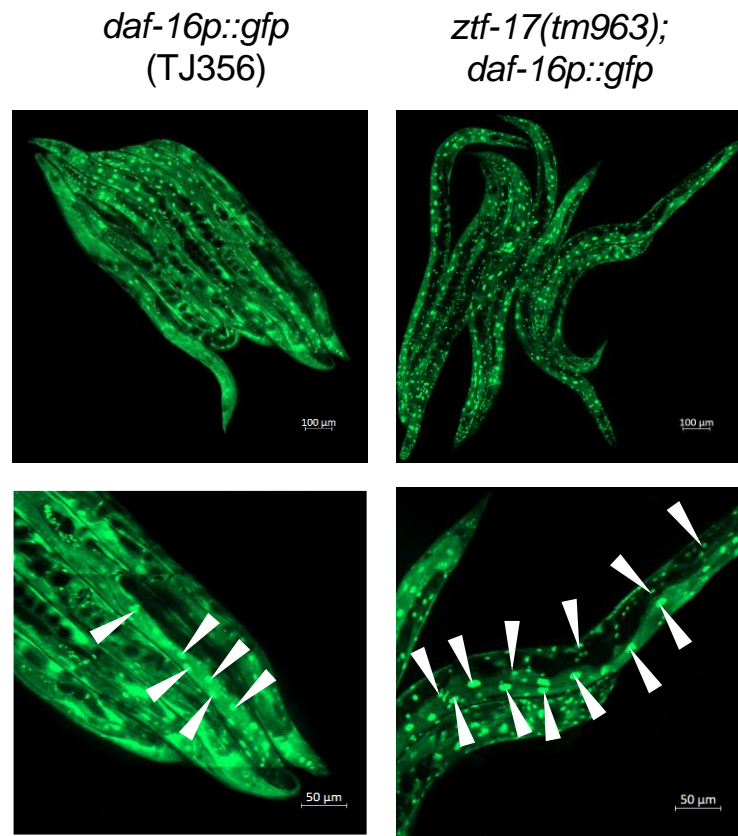
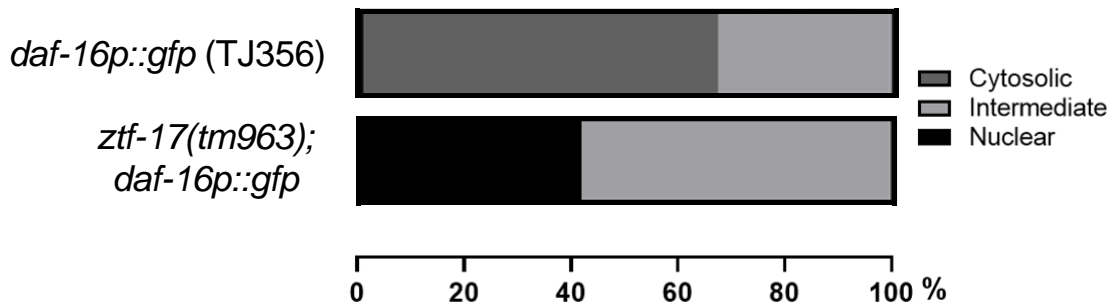
A**B**

Figure 2.14 *ztf-17(tm963)* mutants displayed an increase in DAF-16::GFP nuclear localization under normal, non-stress inducing conditions.

(A) L4 or early adult transgenic worms were picked and GFP fluorescence was visualized using the Zeiss Observer Z1 Spinning Disk Confocal Microscope. *ztf-17(tm963)* mutants displayed an increase in DAF-16::GFP nuclear localization compared to TJ356 worms. White arrows indicate where the nuclei are located in the *C. elegans* intestinal cells. (B) GFP quantification of DAF-16::GFP localization from n=39 animals. Cytosolic refers to animals without nuclear localized GFP signal, intermediate refers to animals with both nuclear and cytosolic GFP and nuclear refers to animals with solely nuclear GFP signal.

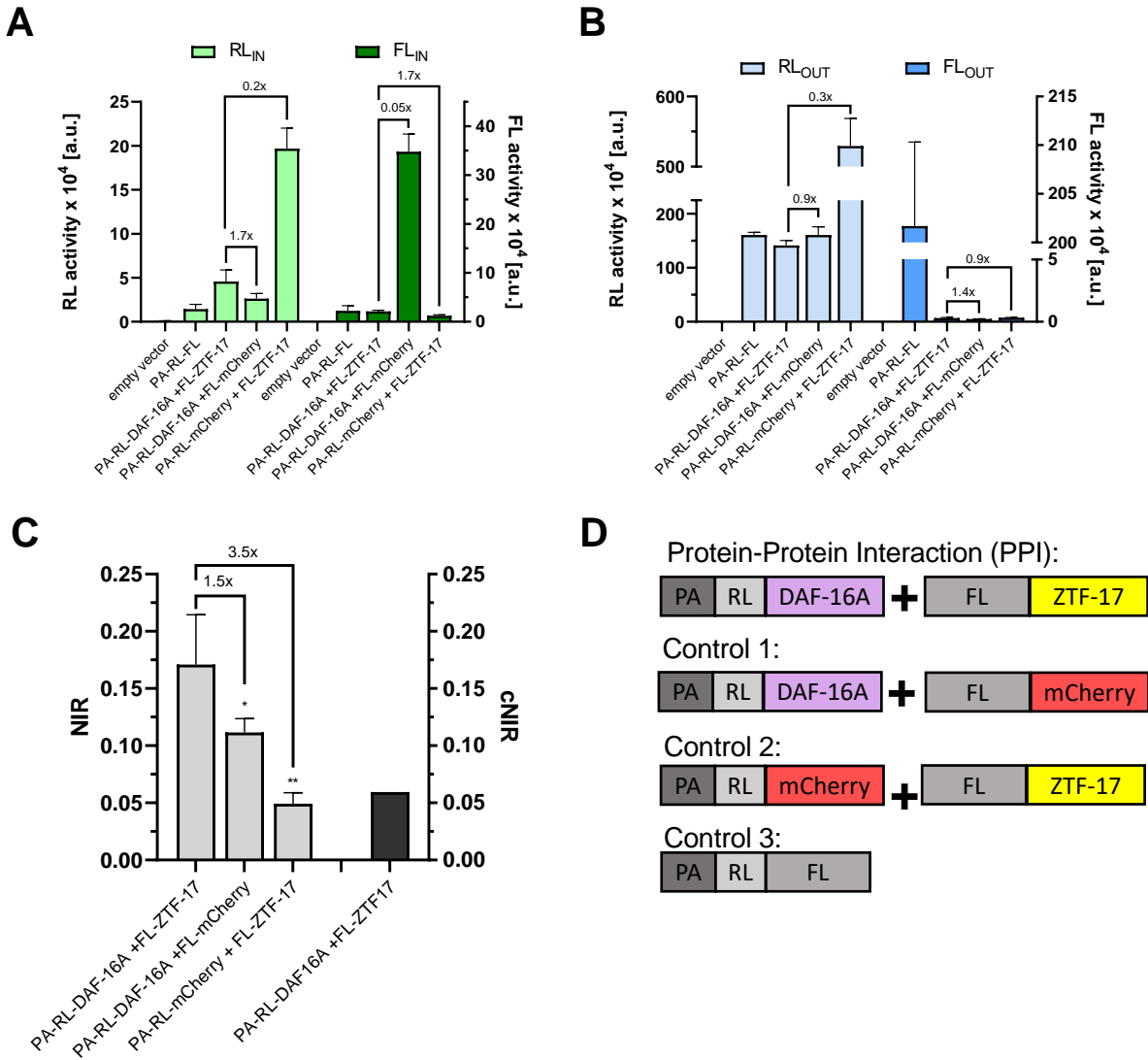


Figure 2.15 DAF-16A and ZTF-17 NIRs suggest that the interaction between both proteins is unlikely.

Investigation of the interaction between DAF-16A and ZTF-17 via DULIP. (A) Analysis of protein expression through quantification of RL and FL luminescence activities in cell lysates were done 48 hr post transfection. (B) Analysis of co-immunoprecipitates through quantification of RL and FL luciferase activities. PA-tagged bait DAF-16A was immunoprecipitated with Rabbit IgG. (C) Calculation of Normalized Interaction Ratios (NIR) for tested PPIs. The NIR for the interaction between PA-RL-DAF-16A/FL-ZTF-17 was slightly higher than the NIRs for the control PPIs of PA-RL-DAF-16A/FL-mCherry and PA-RL-mCherry/FL-ZTF-17. For the PPI of interest, PA-RL-DAF-16A/FL-ZTF-17, a background corrected cNIR was calculated to be ~0.06. A cNIR of ≥ 3 was determined to be optimal for separating positive and negative PPIs. Data represented are the means of 3 independent experiments \pm SEM and statistical analysis was carried out using Two-tailed Unpaired *t*-test; ** $P < 0.01$, * $P < 0.05$. (D) Schematic of Co-IPs.

2.3.4 *ztf-17(tm963)* mutants appear to have better resistance during the initial exposure to oxidative stress inducing compounds but no enhanced survivability.

Since PI and PII detoxification genes were enhanced in the absence of *ztf-17*, I sought to determine if there was a phenotypic difference between *ztf-17(tm963)* deletion mutants and wildtype animals when exposed to oxidative stress. I conducted two different oxidative stress assays using a sodium arsenite (As) solution and *tert*-Butyl hydroperoxide (tBHP) infused agar plates as both compounds are known to activate SKN-1 [13,33]. A 5mM solution of As was prepared in 24-well plates. The assay was performed with triplicates and L4 stage N2 and *ztf-17(tm963)* animals were placed in separate wells. At time 0, worms were counted as alive if actively swimming in solution and worms that were non-moving were excluded then scored hourly for survival. M9 buffer was used as a control. Figure 2.16A is a Kaplan-Meier survival plot showing the fraction of worms alive against time in hours for one trial. *ztf-17(tm963)* and N2 worms (solid blue and black curves respectively) showed no significant differences in survivability and both worm populations reached 100% mortality at around the 10th hour while worms in M9 buffer were still alive (Figure 2.16A). I also poured agar plates containing 15.mM tBHP and exposed L4 stage N2 and *ztf-17(tm963)* animals to the stressor, scoring hourly for survival. Worms on normal NGM plates were used as a control and remained alive throughout the duration of the tBHP-assay. In the first 6 hours of treatment, *ztf-17(tm963)* worms, shown in the green curve, were significantly less sensitive to the oxidative stress induced by tBHP when compared to wildtype, shown in the black curve (Figure 2.16B). However, N2 worms and *ztf-17(tm963)* mutants reached the same endpoint with both groups reaching 100% mortality at approximately the 9th hour of treatment (Figure 2.16B). Statistical calculations for the As-assay and tBHP-assay can be found on Table 3 and Table 4 respectively.

The findings from these two functional assays indicated that although loss of *ztf-17* lead to elevated levels of genes involved in oxidative stress responses, enhanced mRNA levels of genes such as *gst-4* and *sod-3* only promoted short term worm survival during the initial exposure to certain stressors. Whether ZTF-17 influenced lifespan, aging and longevity still remains unclear. Therefore, I conducted qRT-PCR experiments testing genes that were involved in the DAF-2/IIS. First, I produced a double mutant worm strain consisting of *ztf-17(tm963)* and *daf-2(e1370)* mutations. *daf-2(e1370)* has a single substitution mutation that changes an amino acid in the coding sequence rendering the DAF-2 receptor defective and unable to bind its ligand [34]. This results in the constitutive activation of the IIS pathway and *daf-2(e1370)* mutants are long-lived, temperature sensitive dauer constitutive [34,35]. I chose to look at the mRNA levels *gst-4* and *sod-3*, since those were my principle study genes, along with *ins-7*, *hsp-16.2*, *cey-1*, *mtl-1* and *dod-3*. I measured mRNA expression in N2, *ztf-17(tm963)*, *daf-2(e1370)* and my double mutant strains. *ztf-17(tm963)* deletion mutants had increased expression levels of *gst-4*, *sod-3*, *ins-7*, *mtl-1*, and *dod-3* (Figure 2.17). Interestingly, *hsp-16.2* had reduced expression in *ztf-17(tm963)* mutants which was unexpected since other DAF-2/DAF-16 genes were found to be enhanced. *cey-1* is normally downregulated in *daf-2* mutants [34]. I was expecting *cey-1* to be further downregulated in my *ztf-17(tm963);daf-2(e1370)* worms but that was not the case. *hsp-16.2* (heat shock protein) and *cey-1* (cold shock domain family of proteins) encode proteins for stress responses that are implicated in thermotolerance [34]. Since the *ztf-17(tm963)* deletion mutation further enhanced genes that were already upregulated in *daf-2(e1370)* mutants, this suggested that ZTF-17 may also regulate genes involved in the IIS pathway related to lifespan and longevity.

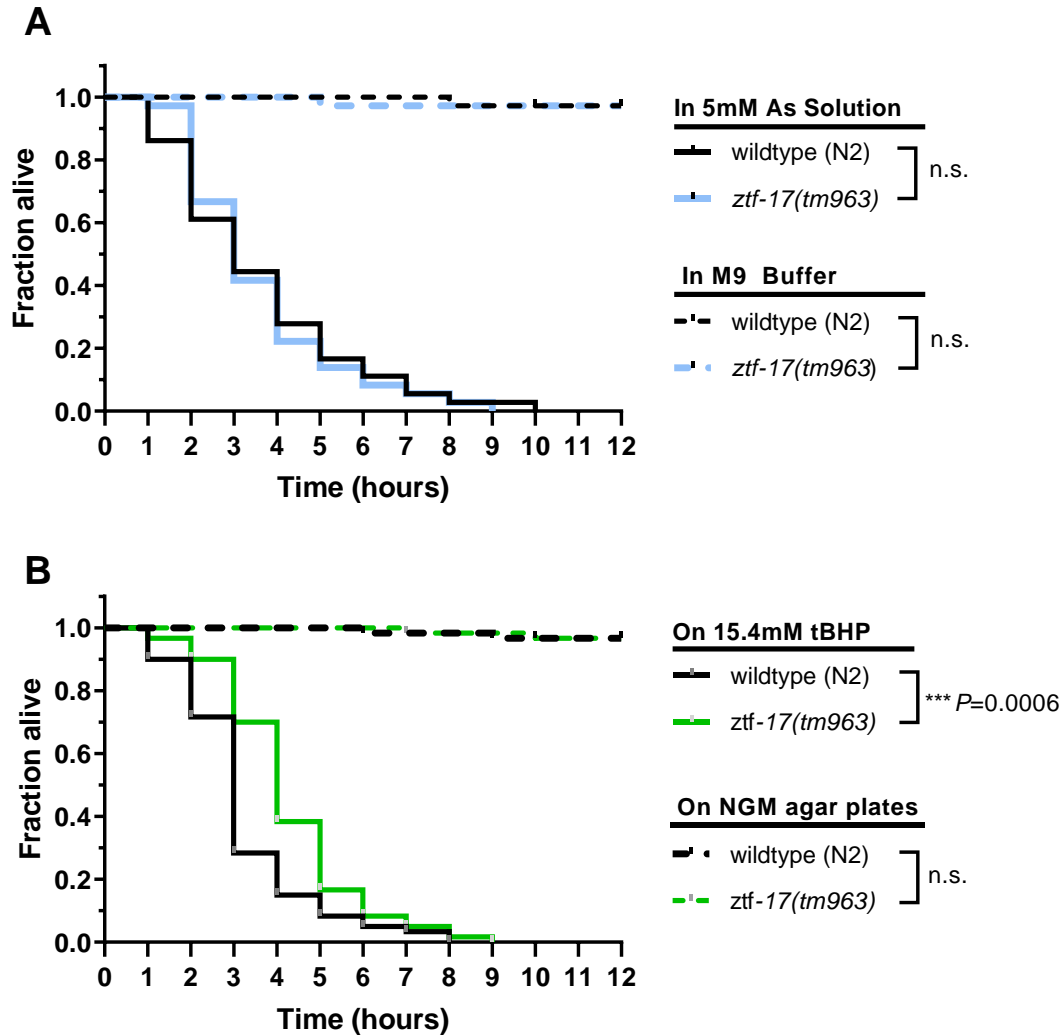


Figure 2.16 *ztf-17(tm963)* mutants showed no significant differences in oxidative stress resistance when treated with As but are more resistant when exposed to tBHP.

(A) Survival plot of the As-assay comparing *ztf-17(tm963)* mutants (blue curves) to N2 wildtype worms (black curves) in 5mM As solution. M9 worm buffer served as the control condition. Three independent experiments were performed with triplicates where $n=36$. For statistical details, please refer to Table 3. (B) Survival plot of the tBHP-assay comparing *ztf-17(tm963)* mutants (green curves) to N2 wildtype worms (black curves) when exposed to 15.4mM tBHP containing agar plates. Regular NGM plates were used as the control condition. Three independent experiments were performed with triplicates where $n=60$. For statistical details, please refer to Table 4. For both the As and tBHP assays, the estimates of the survival functions are calculated using the Kaplan-Meier method and the Log-rank (Mantel-Cox) test was used to calculate significance and P-values; *** $P < 0.001$. Data represents one trial and were analyzed using the online survival analysis program OASIS®.

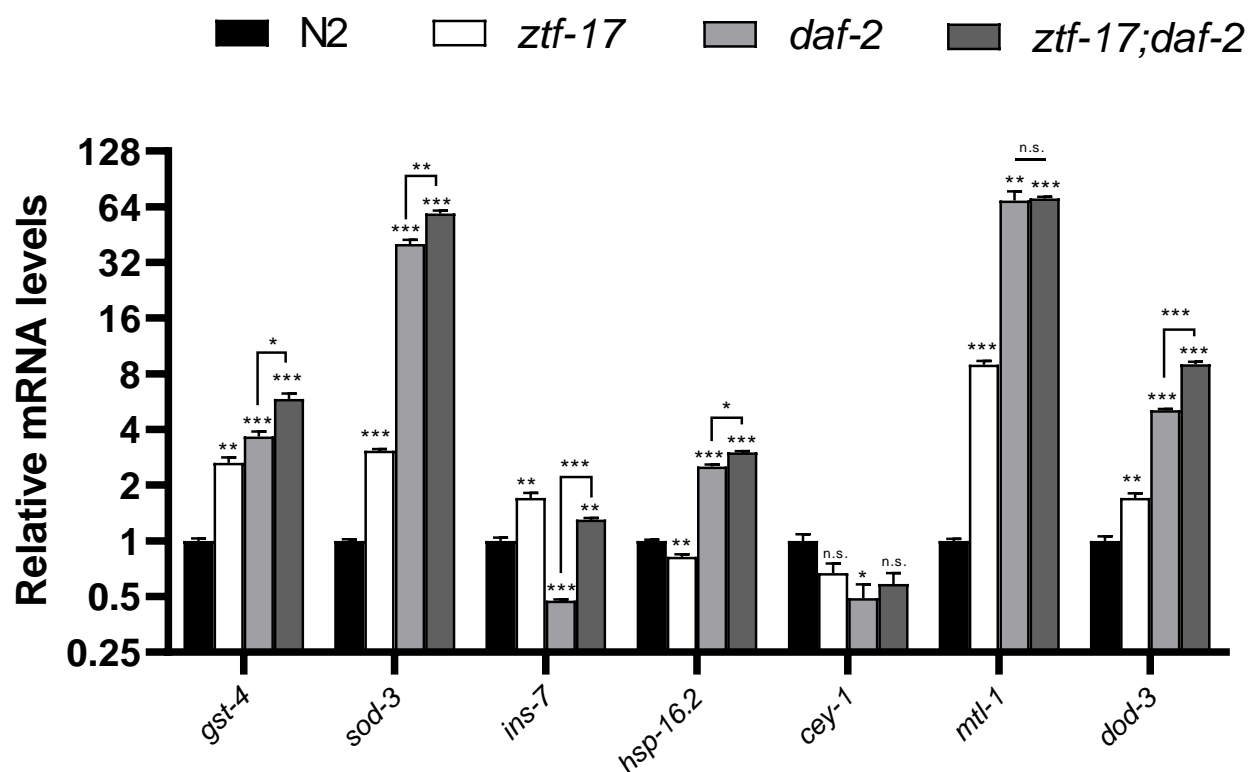


Figure 2.17 *ztf-17(tm963)* mutants had increased mRNA expression for genes related to the DAF-2/insulin signalling pathway but had a reduction in *hsp-16.2* and *cey-1*.

qRT-PCR monitoring amplification of target genes in the DAF-2/insulin signalling pathway. N2 wildtype worms, *ztf-17(tm963)* mutants, *daf-2(e1370)* mutants and transgenic worms carrying both the *ztf-17(tm963)* and *daf-2(e1370)* mutations were synchronized to L4 stage prior to RNA isolation. Results show the relative mRNA expression levels for *gst-4*, *sod-3*, *ins-7*, *hsp-16.2*, *cey-1*, *mtl-1* and *dod-3* genes. Target genes were significantly enhanced in the *ztf-17(tm963);daf-2(e1370)* double mutants when compared to N2 worms. Data was derived from 3 independent trials and normalized to *cdc-42* reference gene. Statistical analysis was carried out using Multiple *t*-tests with the Holm-Sidak multiple comparisons test. Error bars represent \pm SEM; **** P < 0.0001, *** P < 0.001, ** P < 0.01, * P < 0.05.

2.3.5 *ztf-17(tm963)* mutants are more susceptible to heat stress and genes related to thermotolerance are downregulated upon exposure to elevated temperatures.

DAF-16 is a central regulator of many genes involved in longevity and lifespan. DAF-16 activation can be induced by heat stress and leads to the promotion of genes related to heat shock survival [34]. Since *ztf-17(tm963)* mutants have some DAF-16 target genes that were upregulated, but also appear to have downregulation of genes involved in thermotolerance, such as *hsp-16.2* and *cey-1*, I decided to investigate whether *ztf-17* played a regulatory role in heat stress resistance.

Since *sod-3* was a direct target of DAF-16, I subjected *sod-3p::gfp* worms and my transgenic *ztf-17(tm963);sod-3p::gfp* worms to 35°C heat stress for 2 hours then visualized the GFP fluorescence to determine if there were any changes to the *sod-3* expression levels. Whole worm fluorescence comparing untreated *sod-3p::gfp* and *ztf-17(tm963);sod-3p::gfp* heat stressed worms are shown in Figure 2.18A. Wildtype worms carrying the reporter construct *sod-3p::gfp* had increased fluorescence intensity of ~3.1x when exposed to heat stress (Figure 2.18B). Interestingly, there was reduced *sod-3p::GFP* signals in *ztf-17(tm963)* mutants when they were exposed to heat. The average fluorescence intensity for untreated *ztf-17(tm963);sod-3p::gfp* worms was ~1.6 while the heat stressed group had a mean fluorescence of ~1.3. This meant there was a reduction of ~20% in the *sod-3p::GFP* signal in heat stress induced animals.

To further verify the observations seen in whole worm fluorescence, I conducted qRT-PCR experiments measuring the mRNA levels of DAF-16 targets that were induced under heat stress. N2 and *ztf-17(tm963)* mutants were stressed at 35°C for 2 hours then harvested for RNA extraction and qRT-PCR. The relative mRNA expression levels of all target genes tested were significantly enhanced in *ztf-17(tm963)* mutants when compared to N2 wildtype worms during

normal non-stress inducing conditions as expected (Figure 2.19). During heat stress, target genes tested in N2 worms were enhanced, however, mRNA expression levels of *sod-3*, *ctl-1*, *ctl-2*, *mtl-2* and *vit-5* were significantly reduced in *ztf-17(tm963)* mutants. These results indicate that animals with loss of *ztf-17* do have elevated levels of DAF-16 target genes under normal, non-stress inducing conditions but when exposed to heat, the expression drops.

Although heat stress resistance genes were reduced when *ztf-17(tm963)* mutants were exposed to elevated temperatures, the expression of these genes were still significantly higher in my mutant worms than in wildtype worms. To further understand if this reduction had any functional effect on worm thermotolerance, I performed a thermotolerance survival assay by subjecting N2 and *ztf-17(tm963)* deletion mutants to 35°C heat stress and scoring for worm survival hourly. Figure 2.20 is a Kaplan-Meier survival plot showing the fraction of worms alive against time in hours for one trial. Statistical analysis for the other trials conducted can be found in Table 5. N2 and *ztf-17(tm963)* worms that were picked onto normal NGM plates were kept at 20°C throughout the duration of the assay and used as control groups. I found that *ztf-17(tm963)* mutants were more sensitive to elevated temperatures. At the 10th hour, approximately 50% of the *ztf-17(tm963)* worms were dead and the entire population reached 100% mortality at the 15th hour (Figure 2.20). Wildtype had significantly better thermotolerance, and even after being heat stressed for 16 hours, over 60% of worms were still alive (Figure 2.20). These findings suggest that under normal conditions, *ztf-17(tm963)* mutants have upregulated levels of stress resistance genes due to loss of *ztf-17*, but upon exposure to elevated temperatures, these genes are downregulated and impairs the worm's ability to cope with stressful conditions. This makes *ztf-17(tm963)* mutants more susceptible to mortality by heat stress than wildtype worms.

To determine if ZTF-17 affected SKN-1, DAF-16 and its upstream regulators, I measured the mRNA levels by qRT-PCR of *gst-4*, *skn-1a/c*, *skn-1b*, *skn-1a*, *daf-16*, *mpk-1*, *sgk-1*, *akt-1* and *akt-2*. Figure 2.21 showed the qRT-PCR results for the target genes tested in *ztf-17(tm963)* mutants and wildtype worms. The *skn-1a/c*, *daf-16*, *mpk-1*, *akt-1* and *akt-2* mRNA levels remained the same between the N2 and *ztf-17(tm963)* mutants although I did see enhanced expression of *gst-4*, *skn-1a* and *sgk-1* genes and a decrease in *skn-1b* (Figure 2.21). Since there were changes to the mRNA levels of *skn-1a*, *skn-1b* and *sgk-1* with loss of *ztf-17*, the findings together suggests that ZTF-17 may affect the regulation of detoxification pathways through upstream regulators of SKN-1 and DAF-16 or through a mechanism that is independent of IIS and MAPK signaling.

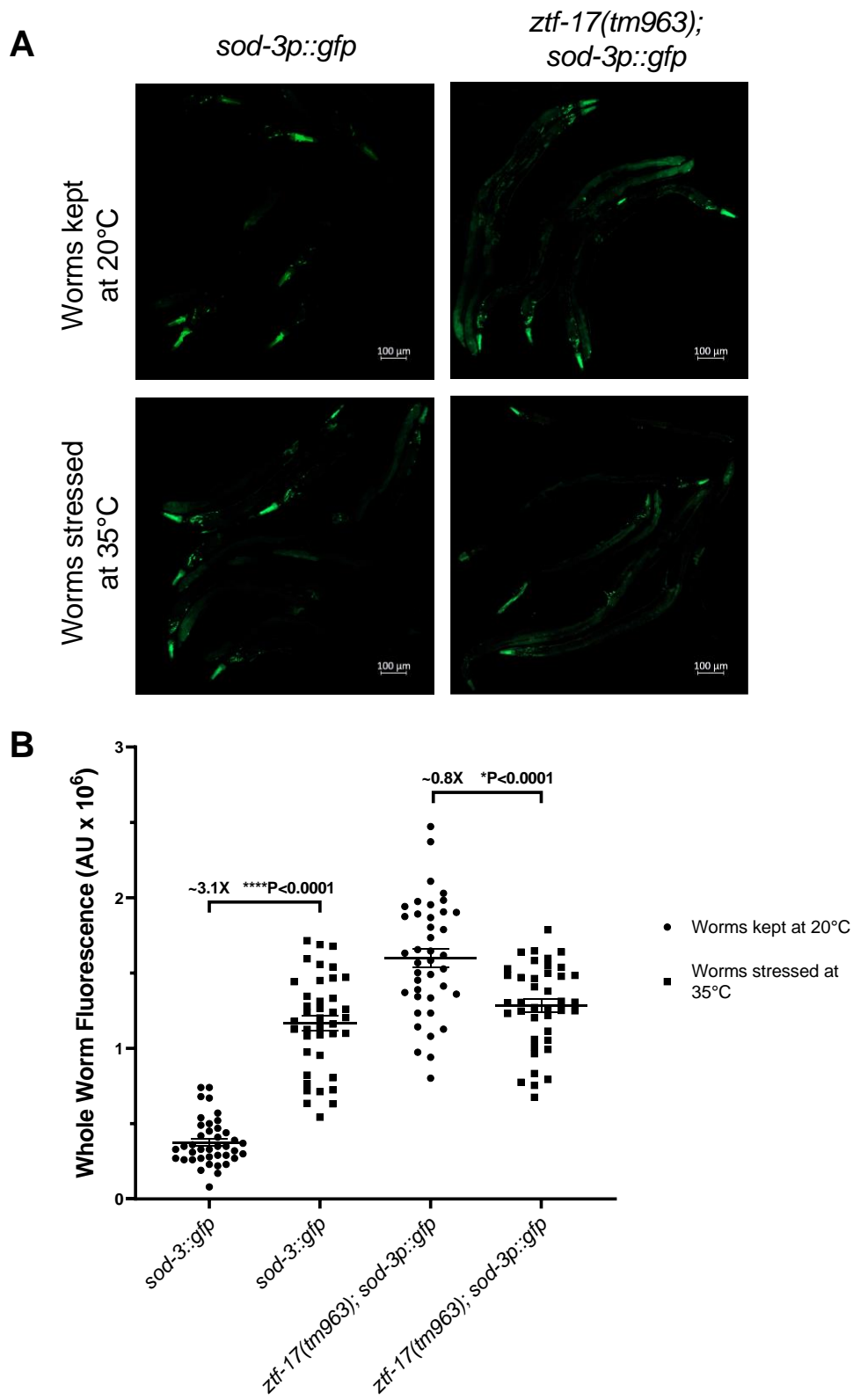


Figure legend can be found on the next page.

Figure 2.18 Exposure to 35°C heat stress resulted in a reduction of *sod-3p::GFP* expression in *ztf-17(tm963)* mutants when compared to worms under non-stress inducing conditions.

(A) Whole worm GFP fluorescence was captured using the Zeiss Observer Z1 Spinning Disk Confocal Microscope. *ztf-17(tm963)* transgenic worms expressing *sod-3p::GFP* and worms expressing *sod-3p::gfp* were incubated at 35°C for 2 hours prior to visualization. (B) *ztf-17(tm963)* mutants had ~20% decrease in the GFP signals when heat stressed compared to when worms were kept at normal conditions (20°C). *sod-3p::gfp* worms displayed enhanced GFP signals when exposed to heat stress. Results for n=40 worms are shown as individual points as the difference between the intensity readings per worm minus the background fluorescence. The mean fluorescence intensity is displayed as a solid black line for each worm strain. Statistical analyses were performed using Two-tailed Unpaired Student's *t*-test; **** P < 0.0001.

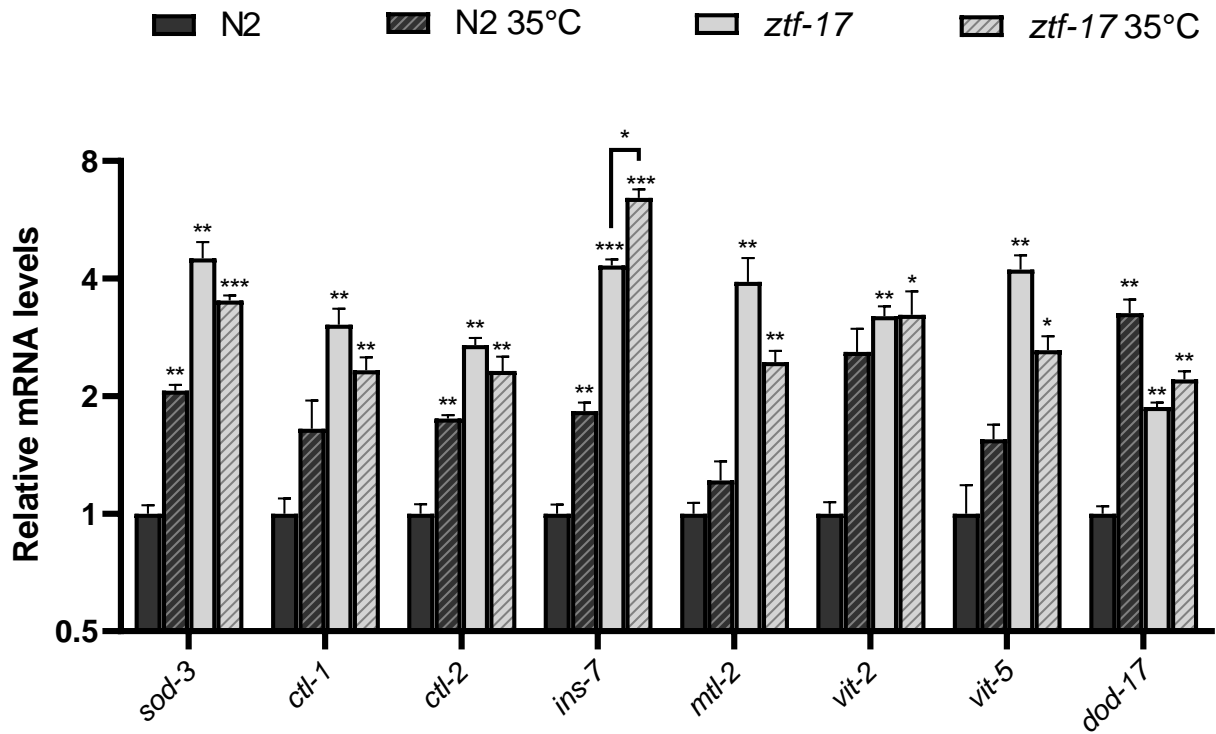


Figure 2.19 mRNA expression levels of DAF-16 target genes that were significantly enhanced in *ztf-17(tm963)* mutants were downregulated under heat stress.

qRT-PCR monitoring amplification of DAF-16 target genes. Worms were synchronized to L4 stage then harvested under normal conditions or exposed to 35°C heat stress for 2 hours followed by RNA isolation. Relative mRNA expression levels of all target genes tested were significantly enhanced in *ztf-17(tm963)* mutants when compared to N2 wildtype worms under normal conditions. During heat stress, all target genes tested in N2 worms were enhanced, however, mRNA expression levels of *sod-3*, *ctl-1*, *ctl-2*, *mtl-2* and *vit-5* were reduced in *ztf-17(tm963)* during heat stress except for *ins-7*, which had ~1.5x increase. Results were derived from 3 independent trials and normalized to *cdc-42* reference gene. Statistical analysis was carried out using Multiple *t*-tests with the Holm-Sidak multiple comparisons test. Error bars represent \pm SEM; *** $P < 0.001$, ** $P < 0.01$, * $P < 0.05$.

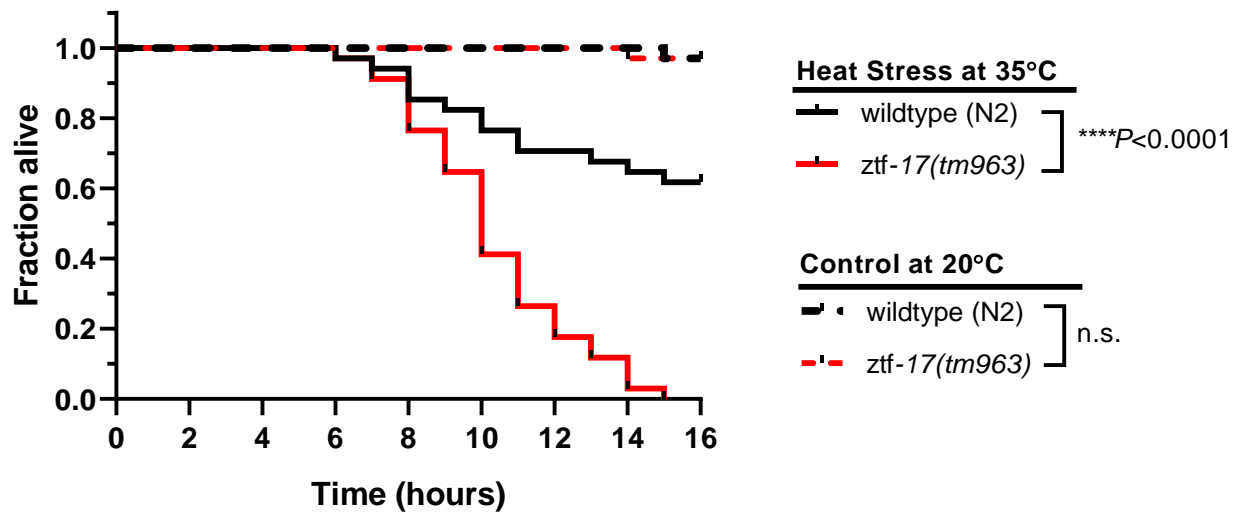


Figure 2.20 *ztf-17(tm963)* animals were significantly more sensitive to heat stress at 35°C with an increased mortality rate compared to wildtype animals.

Survival plot of the thermotolerance assay comparing *ztf-17(tm963)* mutants (red curves) to N2 wildtype worms (black curves) when exposed to 35°C. *ztf-17(tm963)* mutants were highly sensitive to elevated temperatures and at 15 hours, the mortality was at 100% while over 60% of N2 animals were still alive. Worms on regular NGM plates kept at room temperature were used as controls. Three independent experiments were performed with triplicates where n=36. The estimates of survival functions are calculated using the Kaplan-Meier method and the Log-rank (Mantel-Cox) test was used to calculate significance and P-values; **** P < 0.0001. Data represents one trial and was analyzed using the online survival analysis program OASIS®. For statistical details, please refer to Table 5.

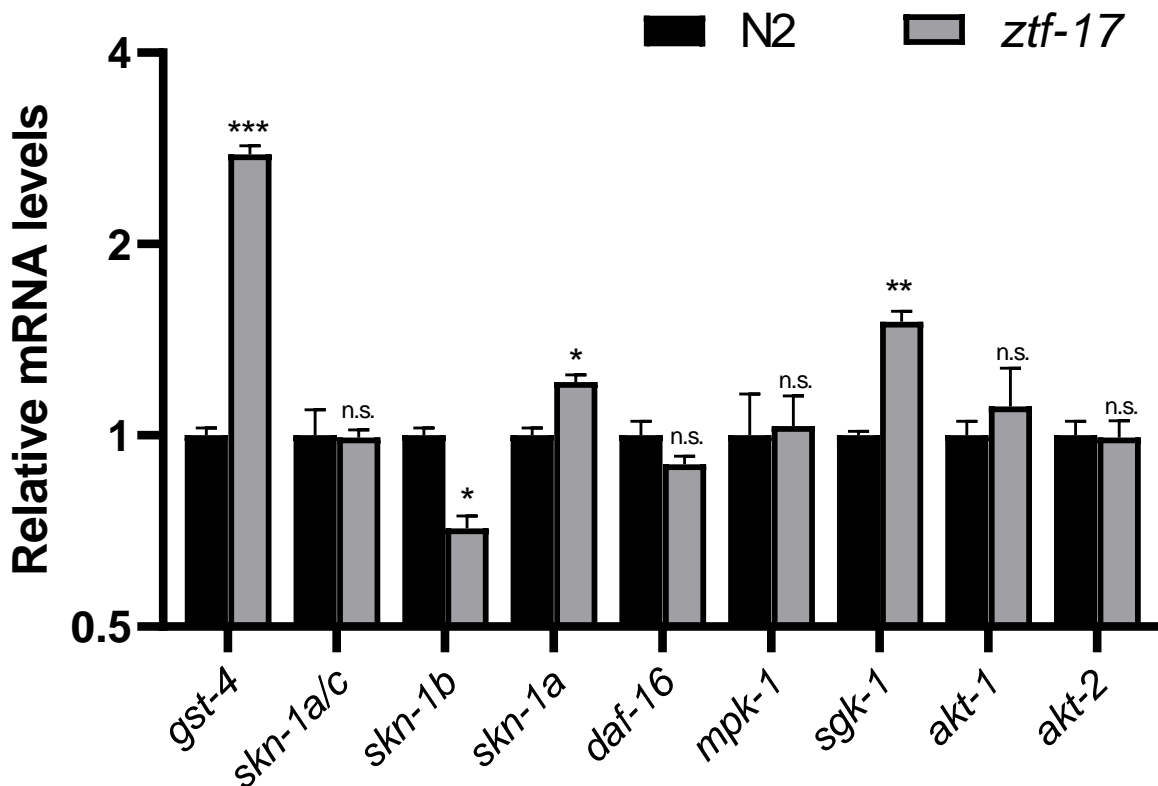


Figure 2.21 mRNA expression levels of *skn-1* isoforms, *daf-16* and upstream regulators were relatively unchanged in *ztf-17(tm963)* mutants but *skn-1a* and *sgk-1* was enhanced.

qRT-PCR measuring the mRNA amplification of the three *skn-1* isoforms, *daf-16* and upstream regulators. Worms were synchronized to L4 stage then harvested for RNA extraction. Relative mRNA expression levels of most of the target genes tested were unchanged when *ztf-17(tm963)* mutants and N2 worms were compared, however, *skn-1a* and *sgk-1* mRNA expression was significantly enhanced in the deletion mutants. *skn-1b* mRNA levels were found to be reduced in the *ztf-17(tm963)* mutants compared to N2. Results were derived from 3 independent trials and normalized to *cdc-42* reference gene. Statistical analysis was carried out using Multiple *t*-tests with the Holm-Sidak multiple comparisons test. Error bars represent \pm SEM; *** $P < 0.001$, ** $P < 0.01$, * $P < 0.05$.

2.4 Discussion

The findings thus far, suggests that the identification of ZTF-17 as a repressor of oxidative stress may lay the foundations for the discovery of a novel regulatory mechanism involving alternative kinetics for transcription factor SKN-1 and DAF-16 activation. Through the use of *C. elegans*, I have shown that *ztf-17(tm963)* deletion mutants have enhanced expression of PI and PII detoxification genes that are under DAF-16 and SKN-1 regulation respectively. ZTF-17 was originally recognized as a potential negative regulator of transcription of detoxification genes when an RNAi screen was performed to look for candidates affecting *gst-4* expression. After the initial findings, I suspected ZTF-17 to have a regulatory role in modulating gene expression involved in the *C. elegans* oxidative stress response. I have then demonstrated that ZTF-17 negatively regulates SKN-1 and DAF-16 function and mediates their target gene expression through the IIS pathway and possibly the mTOR and MAPK pathways.

The *C. elegans* have been studied extensively for their responses to oxidative stress and how aging, lifespan and longevity processes are regulated. Most of these stress responses and longevity strategies are achieved through the regulation and/or expression of specific genes that govern developmental stages and promote survival. For instance, our lab has previously reported that the *C. elegans* BRAP-2 was involved in MAP kinase activity of PMK-1/p38 which negatively regulates transcription factor SKN-1 for the induction of PII detoxification genes [21,36]. Additionally, our lab recently elucidated the role of transcription factor SEM-4 (SEx Muscle abnormal 4) for having a regulatory role in inducing *skn-1c* expression during the oxidative stress response and that SEM-4 was required for expression of PII detoxification enzymes when there was a loss of BRAP-2 [36]. BRAP-2, SEM-4 and ZTF-17 transcription factors all have in common that they are zinc finger containing proteins that were first discovered

for their roles in *C. elegans* development. Having realized that these transcription factors have secondary or even tertiary roles in regulating biological processes in adult worm stages has opened a new area of study that is focused on elucidating their roles outside of development.

In the case of ZTF-17, I reported that *ztf-17(tm963)* deletion mutants have enhanced expression of PI detoxification genes, *sod-3*, *ctl-1*, *ctl-2*, *ins-7*, *mtl-1*, *mtl-2*, *dod-3* and *dod-17*, PII detoxification genes, *gst-4* and *gcs-1*, and also reduced gene expression of certain heat resistance-related genes, *hsp-16.2* and *cey-1*, measured by qRT-PCR. I also confirmed with RNAi and fluorescence microscopy quantification that *C. elegans* transgenic worms expressing *gst-4::gfp* and *sod-3::gfp* reporter constructs had enhanced transcriptional activity of antioxidant genes *in vivo* when there was loss of *ztf-17*. I validated that ZTF-17 was a repressor when I overexpressed *ztf-17* and found that mRNA level of *gst-4* was significantly reduced confirming the repressive effects of ZTF-17 on the SKN-1 target gene. When DAF-16 target genes were examined, I found that the overexpression of *ztf-17* did not have a robust effect on gene reduction. Following these findings, I determined that *ztf-17(tm963)* mutants had enhanced resistance to oxidative stress from initial tBHP exposure, suggesting that loss of *ztf-17* may confer temporary, short-term resistance to oxidative stress. As such, changes in the gene expression patterns in *ztf-17(tm963)* mutants suggests that ZTF-17 may be involved in regulating various processes during oxidative and heat stress and integrates signalling from multiple pathways to confer an appropriate response to said stressors.

Both SKN-1 and DAF-16 are regarded as master regulators, although they may function in different signalling pathways, both regulate expression of genes which affect longevity and oxidative stress responses. Thus, investigating the mechanisms of SKN-1 and DAF-16 activation would be vital to further the understanding of their function. I presented evidence from my

luciferase assays that detected the promoter activity of *skn-1c* was dependent on the transcription factor SKN-1 for expression and was further enhanced with the addition of DAF-16 suggesting that both proteins have a synergistic effect on the *skn-1c* promoter. When I tested the effects of SKN-1 and DAF-16 on *sod-3*'s promoter activity, the luciferase assay results indicated that DAF-16 was required for promoter activity, but SKN-1 had no effect on activating the *sod-3* promoter. Interestingly, I found that the presence of SKN-1 along with DAF-16 reduced the *sod-3* promoter activity that was enhanced by DAF-16 alone. The findings suggest that although DAF-16 and SKN-1 can work together to enhance promoter activity, the effects are specific for certain promoters and SKN-1 and DAF-16 can also have opposing effects as seen with the *sod-3* promoter. Finally, when ZTF-17 was added, I saw that the enhancing effects of SKN-1 and DAF-16 on both the *skn-1c* promoter and *sod-3* promoter were significantly reduced, suggesting that ZTF-17 was capable of negatively regulating SKN-1 and DAF-16 by preventing the transcription factors from driving the expression of genes at said promoters. Although it is still unclear if ZTF-17 directly interacts with SKN-1 and DAF-16 or if ZTF-17 acts directly on the DNA to repress transcription, it is apparent that ZTF-17 functions as a negative regulator of stress resistance gene expression.

DAF-16 is a downstream effector of the DAF-2/IGFR signalling cascade and is activated when *C. elegans* face stress conditions such as heat stress. I observed that DAF-16 nuclear localization appeared to be enhanced in *ztf-17(tm963)* deletion mutants suggesting that ZTF-17 played a role in regulating DAF-16 activation and/or DAF-16-dependent responses. I confirmed by qRT-PCR that downstream DAF-2 target genes, *sod-3*, *mtl-1* and *dod-3*, were enhanced in *daf-2* mutants and in addition, loss of both *daf-2* and *ztf-17* resulted in further enhancement of said genes. This indicated that ZTF-17 played a role in the DAF-2/IGFR signalling cascade to

regulate DAF-16 target genes. When I investigated DAF-16-heat induced activation, I revealed that although genes related to thermotolerance were enhanced in *ztf-17(tm963)* deletion mutants, upon exposure to heat stress, there was downregulation of stress resistance genes and loss of *ztf-17* resulted in worms that were more susceptible to death by heat shock.

Another interesting find was that *vit-2* and *vit-5* genes were enhanced in *ztf-17(tm963)* mutants. *C. elegans* encode for six vitellogenin proteins, *vit-1* through to *vit-6*, which are abundantly found in adult hermaphrodite worms to transport lipids (within the maternal yolk) from the intestines to developing oocytes during sex maturation [37]. Vitellogenins are a family of yolk proteins that supply animals with nutrients. This suggests that they serve an important purpose to support post-embryonic development and fertility, especially in harsh environments where organisms are faced with life-history decisions, vitellogenins will mobilize somatic lipids to the germline [38]. *Vit* RNAi was found to extend lifespan, and it was suggested by recent studies that preventing lipotoxicity and intestinal degradation resulting from production and accumulation of the yolk, would reduce the contribution to age-related pathologies [37,39].

Oxidative stress (SKN-1 dependent), ageing (IIS-dependent) and nutrient availability (mTORC2-dependent) signalling have been found to regulate vitellogenin expression in *C. elegans* (Figure 2.22). Since mTOR acts downstream of and in parallel to IIS, both pathways often converge onto the same downstream targets, such as *sgk-1* and *skn-1*. IIS pathway has been reported to be a repressor of vitellogenins with *daf-2* mutants exhibiting reduced vitellogenin transcription and accumulation in adult worms [40]. The downstream target of the mTORC2 pathway, SGK-1, was found to promote expression of *vit-2* and *vit-3* that was independent of the IIS pathway [41,42]. SGK-1 was also found to act through another nematode specific zinc finger protein, PQM-1(ParaQuat Methylviologen 1) [43]. PQM-1 has roles in protecting *C. elegans*

against gram-negative bacterium, functions in innate immune responses and acts in a mutually antagonistic manner with DAF-16 to modulate adult lifespan (WormBase). PQM-1 can bind DAF-16 associated elements (DAE) to regulate Class II genes and appears to function as a negative regulator of vitellogenesis [37,43].

SKN-1 is well known for coordinating the detoxification mechanisms in response to acute oxidative stress, but recent studies have shown that SKN-1 also has a role in lipid homeostasis. As *skn-1* is a known downstream target of both the IIS and mTORC pathways, this suggests that the crosstalk between these pathways likely means *skn-1* also has a role in regulating vitellogenins and vice versa. In *skn-1* gain-of-function mutants, a phenomenon called “age-dependent somatic depletion of fat” (ASDF) occurs where animals display a lipid depletion phenotype at the end of their reproductive period and lipid stores are transferred and retained in the germline [44]. *vit* RNAi prevents ASDF, suggesting that *vit* activation by *skn-1* causes intestinal depletion and germline accumulation of lipid stores with *vit-6* expression offering some protection against oxidative stress [37,38]. In turn, vitellogenin accumulation and unconsumed yolk for reproduction will produce signals in *C. elegans* that induces nuclear accumulation of SKN-1 and activation [45]. It was also observed that antioxidant treatment led to an accumulation of excess somatic fat and increased stress resistance, thus these results suggest that *skn-1* regulates vitellogenin mobilization as a part of a response to acute oxidative stress [37].

Forward and reverse genetic screens identified that mutations in *alg-1* (Argonaute protein) promoted vitellogenesis by reducing miRNA biogenesis of *lin-4* and *let-7* [46]. Further studies confirmed that *lin-4* and *let-7* miRNAs are required for vitellogenin production in the intestines and directs hypodermal seam cell divisions at specific developmental stages through negative regulation of their mRNA target, LIN-14 and LIN-41 factors respectively [47]. LIN-41

ultimately regulates LIN-29, a zinc finger transcription factor involved in development, and LIN-29 target genes which are required for *vit* gene regulation [37]. Hypodermal development timing was found to be coupled with mTORC2 and IIS signalling, which affects the downstream target, SGK-1, that modulates *vit* gene expression via PQM-1. This suggests that the miRNA machinery also exists to negatively regulate vitellogenin expression in parallel with other pathways (Figure 2.22). Seeing how *ztf-17(tm963)* deletion mutants had upregulated *vit-2* and *vit-5* gene expression, perhaps ZTF-17 functions similar to the other zinc finger proteins found to act upstream of SKN-1 and DAF-16.

SKN-1 function has been observed in several long-lived mutants and its activation has always been thought to have a positive net effect on worm survival, lifespan and longevity. However, recent work suggest that SKN-1 constitutive activation can have a detrimental effect. As previously mentioned, *skn-1* gain-of-function mutants exhibit ASDF which compromises animal health and results in slightly shortened lifespan as animals shift from a pro-survival to a pro-reproductive state. This implies that constitutive activation SKN-1 may actually have harmful effects as animals age [32]. Deng *et al*, reported that *skn-1* gain-of-function animals did exhibit improved resistance to oxidative stress, which was consistent with our current understanding of SKN-1, however, SKN-1 activation inhibited resistance to other stressors such as heat stress, protein misfolding endoplasmic reticulum stress and mitochondrial stress [32]. As DAF-16 was important to mediate heat stress resistance, upon investigating the effects of SKN-1 on DAF-16, it was found that SKN-1 activation repressed DAF-16 nuclear localization and strongly inhibited DAF-16 target gene expression. The opposite was also true, where SKN-1 inhibition was found to activated DAF-16 and promoted heat stress resistance [32]. Further analysis found that genes that are usually upregulated by SKN-1 activation are downregulated when DAF-16 is activated,

and the collective evidence suggested that activation of SKN-1 can suppress the stress response regulator DAF-16. These observations were in line with what I observed in my luciferase assays when SKN-1 reduced the activation of the *sod-3* promoter by DAF-16 and also explains why *ztf-17(tm963)* deletion mutants were less tolerant to heat stress compared to wild type N2 worms.

Lastly Deng *et al*, found that SKN-1 activation mediated the transcription of *vit-2* and increased VIT-2 protein levels. The overexpression of *vit-2*, and possibly other vitellogenin proteins, was found to be required for SKN-1-mediated suppression of DAF-16 and lead to compromised heat stress responses. This supports the notion of SKN-1 having dual roles in stress resistance and aging with pros and cons. In order for SKN-1 to participate in lifespan extension, its activation must be regulated and turned on only when appropriate as SKN-1 can hamper the functions of other stress resistance factors, such as DAF-16.

All together, these findings have provided tremendous insight on the possible mechanisms that ZTF-17 may function by. It is possible that ZTF-17 negatively regulates signal transduction pathways, such as IIS, mTORC and MAPK, under normal conditions to maintain worm homeostasis. With loss of *ztf-17*, I suspect that the repressive effects of ZTF-17 are abolished resulting in enhanced activation of SKN-1 and DAF-16 master regulators. This may explain why I saw an upregulation of PI and PII detoxification genes. Although there was an upregulation of both SKN-1 and DAF-16 target genes, *ztf-17(tm963)* mutants only displayed short-term resistance to oxidative stress while also having compromised resistance to heat stress. I propose that loss of *ztf-17* results in enhanced activation of SKN-1 which in turn, may prevent DAF-16-dependent expression of stress genes through vitellogenin mediated suppression or by another unknown regulatory mechanism that has yet to be determined. When I examined if the loss of *ztf-17* would affect the upstream regulators of SKN-1 and DAF-16, I found that *skn-1a/c*, *daf-16*,

mpk-1, *akt-1* and *akt-2* mRNA levels remained relatively unchanged while *skn-1a* and *sgk-1* mRNA expression were enhanced and *skn-1b* expression was reduced (Figure 2.21). Thus, it suggests that ZTF-17 may exhibit its repressive effects independently of IIS and MAPK pathways and further investigation should help determine if ZTF-17 interacts with said upstream regulators. My prediction of ZTF-17's function in *C. elegans* could reveal a possible novel regulatory mechanism that functions in parallel with the currently known SKN-1 and DAF-16 stress resistance pathways. By understanding how ZTF-17 influences the activation of detoxification genes, we can continue to characterize transcription factors and provide insight into potential chemoprevention and therapeutic targets that combats not only age-associated diseases but also various cancers and neurogenerative diseases that arise from oxidative stress.

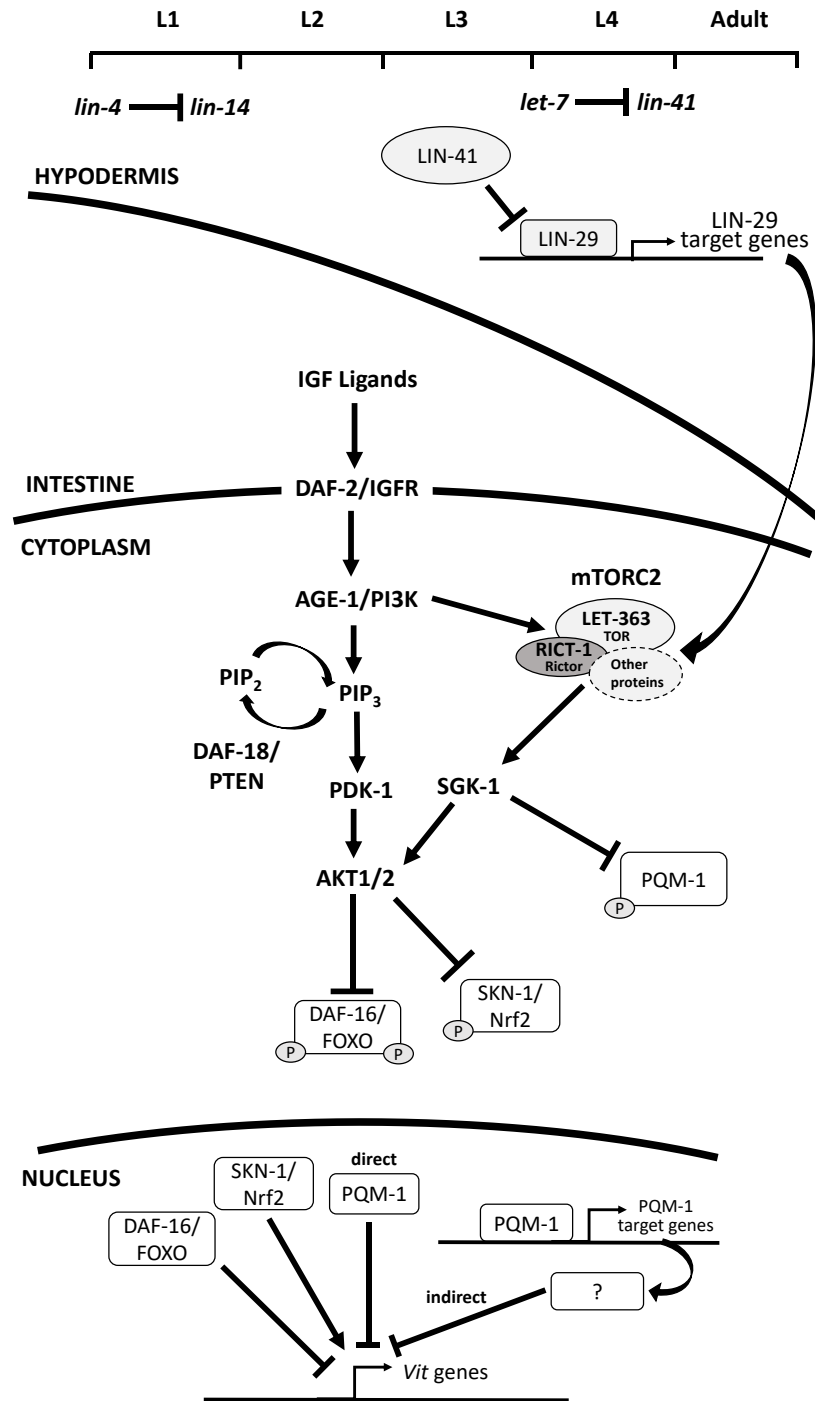


Figure 2.22 mTOR and insulin signaling in *C. elegans* collaborate to modulate vitellogenin expression.

Hypodermal developmental timing genes in the induce mTORC2 signaling to direct the expression of *vit* genes via transcription factor PQM-1 while DAF-16/FOXO represses, and SKN-1 activates *vit* genes. Adapted and modified from Downen *et al.*, 2016 [46].

2.5 References

1. Finkel, T. & Holbrook, N. J. NATURE - Finkel 2000 - Oxidative stress and biology of ageing. *Nature* **408**, 239–247 (2000).
2. Finkel, T. Signal transduction by reactive oxygen species. *J. Cell Biol.* **194**, 7–15 (2011).
3. Benoît D’Autréaux & Toledano, M. B. ROS as signalling molecules: mechanisms that generate specificity in ROS homeostasis. *Nat Rev Mol Cell Biol* **8**, 813–824 (2007).
4. Fleeson, W. *et al.* No {Title}. *J. Pers. Soc. Psychol.* **1**, 1188–1197 (2017).
5. Van Raamsdonk, J. M. & Hekimi, S. Reactive Oxygen Species and Aging in *Caenorhabditis elegans* : Causal or Casual Relationship? *Antioxid. Redox Signal.* **13**, 1911–1953 (2010).
6. Lin, X.-X. *et al.* DAF-16/FOXO and HLH-30/TFEB function as combinatorial transcription factors to promote stress resistance and longevity. *Nat Commun* **9**, (2018).
7. Martins, R., Lithgow, G. J. & Link, W. Long live FOXO: Unraveling the role of FOXO proteins in aging and longevity. *Aging Cell* **15**, 196–207 (2016).
8. Tullet, J. M. A. *et al.* The SKN-1/Nrf2 transcription factor can protect against oxidative stress and increase lifespan in *C. elegans* by distinct mechanisms. *Aging Cell* **16**, 1191–1194 (2017).
9. Blackwell, T. K., Steinbaugh, M. J., Hourihan, J. M., Ewald, C. Y. & Isik, M. SKN-1/Nrf, stress responses, and aging in *Caenorhabditis elegans*. *Free Radic. Biol. Med.* **88**, 290–301 (2015).
10. Sun, X., Chen, W. D. & Wang, Y. D. DAF-16/FOXO transcription factor in aging and longevity. *Front. Pharmacol.* **8**, 1–8 (2017).
11. Brenner, S. The Genetics of CAENORHABDITIS ELEGANS. *Genetics* **77**, 71–94 (1974).
12. Sulston, J. and H. J. The Nematode *Caenorhabditis elegans*. Cold Spring Harbor Laboratory. *Methods.* Wood, W.B. (ed). 587–606 (1988).
13. Ewald, C. Y., Hourihan, J. M. & Blackwell, T. . K. Oxidative Stress Assays (arsenite and tBHP) in *Caenorhabditis elegans*. *Bio-Protocol* **7**, 1–12 (2017).
14. Trepte, P. *et al.* DULIP: A Dual Luminescence-Based Co-Immunoprecipitation Assay for Interactome Mapping in Mammalian Cells. *J. Mol. Biol.* **427**, 3375–3388 (2015).
15. Mello, C. and Fire, A. DNA transformation. *Methods Cell Biol.* **48**, 451–482 (1995).
16. Dickinson, D. Protocols for cloning SEC-based repair templates using SapTrap assembly. (2016) doi:10.1534/genetics.115.184275.For.
17. Schwartz, M. L. & Jorgensen, E. M. SapTrap, a toolkit for high-throughput CRISPR/Cas9 gene modification in *Caenorhabditis elegans*. *Genetics* **202**, 1277–1288 (2016).
18. Dickinson, D. J., Pani, A. M., Heppert, J. K., Higgins, C. D. & Goldstein, B. Streamlined genome engineering with a self-excising drug selection cassette. *Genetics* **200**, 1035–1049 (2015).
19. MacNeil, L. T. *et al.* Transcription Factor Activity Mapping of a Tissue-Specific in vivo Gene Regulatory Network. *Cell Syst.* **1**, 152–162 (2015).
20. Wu, C. W., Deonarine, A., Przybysz, A., Strange, K. & Choe, K. P. The Skp1 Homologs SKR-1/2 Are Required for the *Caenorhabditis elegans* SKN-1 Antioxidant/Detoxification Response Independently of p38 MAPK. *PLoS Genet.* **12**, 1–30 (2016).
21. Hu, Q., D’Amora, D. R., Macneil, L. T., Walhout, A. J. M. & Kubiseski, T. J. The

- Oxidative Stress Response in *Caenorhabditis elegans* Requires the GATA Transcription Factor ELT-3 and SKN-1/Nrf2. *Genetics* **206**, 1909–1922 (2017).
22. Taub, J. *et al.* A cytosolic catalase is needed to extend adult lifespan in *C. elegans* *daf-C* and *clk-1* mutants. *Nature* **399**, 162–166 (2002).
 23. Zheng, S., Liao, S., Zou, Y., Qu, Z. & Liu, F. *ins-7* gene expression is partially regulated by the DAF-16/IIS signaling pathway in *Caenorhabditis elegans* under celecoxib intervention. *PLoS One* **9**, (2014).
 24. Simmer, F. *et al.* Genome-wide RNAi of *C. elegans* using the hypersensitive *rrf-3* strain reveals novel gene functions. *PLoS Biol.* **1**, 77–84 (2003).
 25. Reece-Hoyes, J. S. *et al.* Insight into transcription factor gene duplication from *Caenorhabditis elegans* Promoterome-driven expression patterns. *BMC Genomics* **8**, 1–17 (2007).
 26. Reinke, Valerie, Krause, Michael, Okkema, P. Transcriptional Regulation of Gene Expression in *C. elegans*. *WormBook* 1–34 (2017)
doi:10.1895/wormbook.1.45.2.Transcriptional.
 27. Liu, W. J., Reece-Hoyes, J. S., Walhout, A. J. & Eisenmann, D. M. Multiple transcription factors directly regulate Hox gene *lin-39* expression in ventral hypodermal cells of the *C. Elegans* embryo and larva, including the hypodermal fate regulators LIN-26 and ELT-6. *BMC Dev. Biol.* **14**, 1–21 (2014).
 28. Kroetz, M. B. & Zarkower, D. Cell-Specific mRNA Profiling of the *Caenorhabditis elegans* Somatic Gonadal Precursor Cells Identifies Suites of Sex-Biased and Gonad-Enriched Transcripts. *G3 & #58; Genes/Genomes/Genetics* **5**, 2831–2841 (2015).
 29. Abbott, A. L. Uncovering new functions for MicroRNAs in *caenorhabditis elegans*. *Curr. Biol.* **21**, R668–R671 (2011).
 30. Kato, M., de Lencastre, A., Pincus, Z. & Slack, F. J. Dynamic expression of small non-coding RNAs, including novel microRNAs and piRNAs/21U-RNAs, during *Caenorhabditis elegans* development. *Genome Biol.* **10**, 1–15 (2009).
 31. An, J. H. & Blackwell, T. K. SKN-1 links *C. elegans* mesendodermal specification to a Conserved Oxidative Stress Response. *Genes Dev.* **17**, 1882–1893 (2003).
 32. Deng, J., Dai, Y., Tang, H. & Pang, S. SKN-1 is a negative regulator of DAF-16 and somatic stress resistance in *C. Elegans*. *G3 Genes, Genomes, Genet.* **10**, 1707–1712 (2020).
 33. Oliveira, R. P. *et al.* Condition-adapted stress and longevity gene regulation by *Caenorhabditis elegans* SKN-1/Nrf. *Aging Cell* **8**, 524–541 (2009).
 34. Gami, M. S. & Wolkow, C. A. Studies of *Caenorhabditis elegans* DAF-2/insulin signaling reveal targets for pharmacological manipulation of lifespan. *Aging Cell* **5**, 31–37 (2006).
 35. Senchuk, M. M. *et al.* Activation of DAF-16/FOXO by reactive oxygen species contributes to longevity in long-lived mitochondrial mutants in *Caenorhabditis elegans*. *PLoS Genet.* **14**, 1–27 (2018).
 36. Rafikova, A., Hu, Q. & Kubiseski, T. J. The SEM-4 transcription factor is required for regulation of the oxidative stress response in *caenorhabditis elegans*. *G3 Genes, Genomes, Genet.* **10**, 3379–3385 (2020).
 37. Perez, M. F. & Lehner, B. Vitellogenins - Yolk Gene Function and Regulation in *Caenorhabditis elegans*. *Front. Physiol.* **10**, (2019).
 38. Lynn, D. A. *et al.* Omega-3 and -6 fatty acids allocate somatic and germline lipids to

- ensure fitness during nutrient and oxidative stress in *Caenorhabditis elegans*. *Proc. Natl. Acad. Sci. U. S. A.* **112**, 15378–15383 (2015).
39. Ezcurra, M. *et al.* *C. elegans* Eats Its Own Intestine to Make Yolk Leading to Multiple Senescent Pathologies. *Curr. Biol.* **28**, 2544-2556.e5 (2018).
 40. Depina, A. S. *et al.* Regulation of *Caenorhabditis elegans* vitellogenesis by DAF-2/IIS through separable transcriptional and posttranscriptional mechanisms. *BMC Physiol.* **11**, (2011).
 41. Hertweck, M., Göbel, C. & Baumeister, R. *C. elegans* SGK-1 is the critical component in the Akt/PKB kinase complex to control stress response and life span. *Dev. Cell* **6**, 577–588 (2004).
 42. Wang, H. *et al.* Iron overload coordinately promotes ferritin expression and fat accumulation in *Caenorhabditis Elegans*. *Genetics* **203**, 241–253 (2016).
 43. Tepper, R. G. *et al.* PQM-1 complements DAF-16 as a key transcriptional regulator of DAF-2-mediated development and longevity. *Cell* **154**, 676–690 (2013).
 44. Nhan, J. D. *et al.* Redirection of SKN-1 abates the negative metabolic outcomes of a perceived pathogen infection. *Proc. Natl. Acad. Sci. U. S. A.* **116**, 22322–22330 (2019).
 45. Steinbaugh, M. J. *et al.* Lipid-mediated regulation of SKN-1/Nrf in response to germ cell absence. *Elife* **4**, 1–30 (2015).
 46. Downen, R. H., Breen, P. C., Tullius, T., Conery, A. L. & Ruvkun, G. A microRNA program in the *C. elegans* hypodermis couples to intestinal mTORC2/PQM-1 signaling to modulate fat transport. *Genes Dev.* **30**, 1515–1528 (2016).
 47. Lee, R. C., Feinbaum, R. L. & Ambros, V. The *C. elegans* Heterochronic Gene *lin-4* Encodes Small RNAs with Antisense Complementarity to *lin-14*. *Cell* **75**, 843–854 (1993).

CHAPTER 3: GENERAL DISCUSSION

3.1 Identification of ZTF-17 as a transcription factor that negatively regulates basal expression levels of detoxification genes and target genes of the IIS pathway.

Our lab has demonstrated that zinc finger proteins, such as BRAP-2 and SEM-4, have roles in modulating oxidative stress resistance. Transcription factors are multidimensional, that is, they can regulate an array of biological processes through their interaction with DNA and/or other factors but may also participate in various signalling pathways. By investigating their roles, we can uncover new regulatory mechanisms that will help better our understanding of how transcription factors function. One area of research that our lab had focused on was identifying novel candidate factors that affected stress responses, in particular the underlying genetics of oxidative stress, aging, lifespan and longevity. Through an RNAi screen for potential new regulators of SKN-1, we discovered that *ztf-17* RNAi-mediated knock down in *C. elegans* resulted in enhanced expression of *gst-4*, a major gene target of SKN-1 that confers resistance against ROS. Thus, the focus of this project was to understand the function of the uncharacterized transcription factor, ZTF-17, and to determine if there was a genetic link between *ztf-17*, *skn-1*, *daf-16* and the upstream regulators of the oxidative stress response pathways. My results and significance were already discussed in detail in Chapter 2. The focus for the remainder of this chapter will be to summarize my findings, connect this project to the results of other studies in the literature and to outline the future direction for research on ZTF-17.

With the initial observation that loss of *ztf-17* could induce expression of detoxification genes, I decided to utilize genetic and biochemical approaches to determine which pathways ZTF-17 might function in as well as derive a mechanism for its action. In *ztf-17(tm963)* deletion mutants, I was able to determine that PII detoxification enzymes, *gst-4* and *gcs-1*, were enhanced (Figure 2.3). PII detoxification genes encode for enzymes with major protective roles against

endogenously and exogenously produced toxicants, with GSTs having one of the most prominent effects in neutralizing ROS damage [1]. SKN-1 is a regulator of PII detoxification gene expression and is partially responsible for ROS-induced GST-4 expression [2]. Thus, it was suggested that ZTF-17 was a potential regulator of SKN-1 and was involved in regulating SKN-1 signalling pathways.

Efficient ROS detoxification can be a good indicator for healthy aging and elucidation of these protective mechanisms can further the understanding of how animals achieve long-lived phenotypes. Although SKN-1 activation is instrumental in providing *C. elegans* with protection, ROS originating from different sources can activate SKN-1 in different ways to promote survival. When *C. elegans* are treated with sodium arsenite (As), the BLI-3/NADPH oxidase complex produces localized ROS at the ER or through the mitochondria. Sulfenylation at a cysteine site within the IRE-1 kinase activation loop will induce SKN-1 activation [3]. On the other hand, *tert*-Butyl hydroperoxide (tBHP) attacks proteins and lipids with broader effects than As [4]. Almost all antioxidant genes that are activated by As are SKN-1-dependent whereas genes that are induced by exposure to tBHP appear to be both SKN-1-dependent and SKN-1-independent, with only a minority of the tBHP responses requiring *skn-1* [4,5]. Of the genes that were upregulated with tBHP treatment independent of SKN-1, many were PI genes, which included hormone receptors, transcription regulators and lipid metabolism genes [4]. This suggests that responses triggered from tBHP treatment are more complex than As, and that there is also activation of other oxidative stress response factors in addition to SKN-1. This is perhaps why *ztf-17(tm963)* mutants showed only temporary, short-term oxidative stress resistance when exposed to tBHP because of many factors, that in combination, affect stress responses. *ztf-17(tm963)* worms appeared to have no enhanced survival when treated with As compared to

wildtype worms. Although it is still unclear why this was observed, a possible explanation could be that loss of *ztf-17* has other negative implications that have yet been determined. These negative effects could have overpowered the enhanced SKN-1 activation that was predicted to activate *gst-4* and *gcs-1* expression for increased stress resistance and worm survival against As.

I looked at PI genes since cross talk between SKN-1 and DAF-16 was a possibility. *ztf-17(tm963)* mutants showed significant enhancement of several DAF-16 and DAF-2 target genes, most notably *sod-3*, *ctl-1/2*, *ins-7*, *mtl-1/2*, *dod-3* and *dod-17* (Figure 2.13, Figure 2.17 and Figure 2.19). This observation suggested that ZTF-17 may participate in the regulation of both the IIS and MAPK pathways or facilitated the cross talk between SKN-1 and DAF-16. Interestingly, loss of *ztf-17* resulted in upregulation of genes that both opposed DAF-16 activation whilst also appeared to express genes that were induced from reduced IIS. Mutations in the DAF-2/IGFR, denoted as *daf-2* or *daf-2(-)* mutants, should activate DAF-16. According to microarray analysis from Murphy *et al.*, in *daf-2* mutants, *sod-3*, *ctl-1/2*, *mtl-1* and *dod-3* genes were upregulated as their activation was predicted to confer stress resistance in a DAF-16-dependent manner whilst genes *ins-7*, *mtl-2* and *dod-17* should be downregulated as they were predicted to suppress DAF-16 function [6]. For example, *ins-7* is a prominent inhibitor of the IIS pathway and is a DAF-2 agonist [6]. Under normal conditions, INS-7 binds to the DAF-2 receptor and generates a positive feedback loop, where an increase in transcription of *ins-7* results in amplified DAF-2 signalling and subsequent repression of DAF-16 and SKN-1. RNAi used against *ins-7* have been previously shown to extend lifespan and further increased dauer development in *daf-2* mutants. SKN-1 activation has also been shown to downregulate *ins-7* expression and reduce IIS, suggesting that SKN-1 is also involved in similar feedback loops. Thus, my *ztf-17(tm963)* mutants had some conflicting results where pro-lifespan extension genes

and genes found to inhibit longevity were both upregulated. These findings warrant for further investigation as to why certain DAF-16 and SKN-1 target genes, that are normally downregulated when DAF-16 and SKN-1 are active, are upregulated with loss of *ztf-17*.

3.2 Potential regulation of SKN-1 and DAF-16 target genes highlights new roles for ZTF-17 in *C. elegans*.

Proceeding the qRT-PCR experiments of PI and PII detoxification genes, I investigated other genes related to thermotolerance and genes that were downstream of the DAF-2/IIS pathway. I found *hsp-16.2* to be downregulated while *cey-1* levels remained unchanged between *ztf-17(tm963)* deletion mutants and wild type worms. In *daf-2* mutants, microarray analysis found that heat shock resistance genes, such as *hsp-16.2*, are upregulated while genes related to fertility, such as *vit* genes, are downregulated and *cey-1*, which are cold-shock domain containing proteins, are also downregulated [7]. As *ztf-17(tm963)* mutants appeared to have reduced expression of genes that promoted heat resistance, I tested whether they were also more susceptible to heat shock. I revealed that DAF-16 target genes that were typically enhanced with loss of *ztf-17*, started to downregulate when worms were exposed to elevated temperatures. *hsp-16.2* are among the numerous genes involved in the heat shock response and encodes for a molecular chaperone that prevents protein misfolding and maintenance of proteostasis when there are thermal fluctuations [8]. CEY-1 RNA binding protein is the *C. elegans* Y-Box protein 1 with a conserved cold shock domain [9]. *cey-1* was reported to be a negative regulator of *let-7* and *cey-1* binding sites were also identified in the 3'UTRs of *let-7* targets [10]. This suggested that *cey-1* antagonizes *let-7*-mediated silencing by attenuating *let-7* miRISC activity. Since *let-7* is one of the miRNAs influencing *lin-41* and subsequent mTORC2 activity, loss of *ztf-17* may have a direct affect on *cey-1* expression which in turn modulates SKN-1 and DAF-16 targets –

for example, *vit* genes (Figure 2.22). Perhaps *ztf-17* itself can repress miRNAs similar to *cey-1* as *mir-77* miRNA is a target of ZTF-17 [11]. Although *mir-77* function is not clearly defined, its interaction with ZTF-17 suggests that ZTF-17 could act as a negative regulator of gene expression through miRISC activity.

vit genes, which encode for vitellogenins, regulate lipid metabolism and relocation. *vit* genes are an indirect target of *let-7* miRNA and was found to be upregulated in *ztf-17(tm963)* deletion mutants [12]. It was determined by Deng *et al*, that SKN-1 activation induces the expression of vitellogenin proteins, which are required for SKN-1-mediated suppression of DAF-16 and/or impairment DAF-16-dependent stress responses [13]. Additional findings related to the significance of *vit-2* and *vit-5* upregulation was discussed in detail in Chapter 2. Altogether, I suspect that loss of *ztf-17* promoted defense against certain oxidative stressors at the cost of survivability to other stressors and that the decrease in *hsp-16.2*, upregulation of *cey-1* and increased expression of *vit* genes likely contributed to compromised responses to heat stress. As I investigated the roles of ZTF-17, I have come to find that there are benefits and detrimental consequences associated with SKN-1 activation in *C. elegans* health. These findings emphasize that SKN-1 is a pro-lifespan factor that can also impair anti-aging processes.

Regardless, the interactions between ZTF-17, SKN-1 and DAF-16 are complex. I have already demonstrated that ZTF-17 can regulate PI and PII detoxification genes and that ZTF-17 can attenuate the *skn-1c* and *sod-3* promoters in the presence of SKN-1 and DAF-16 (Figure 2.12). Currently, there is only information about ZTF-17 being a factor involved in the development of larval vulval precursor cells with no reports describing ZTF-17's function outside of *C. elegans* development [14]. The work presented thus far have provided insight into characterising the unknown zinc finger transcription factor and have revealed a connection

between ZTF-17 and the oxidative stress response. Aside from its role in larval development, I believe ZTF-17 has a role to maintain nematode homeostasis. I propose that loss of *ztf-17* allowed the induction of stress resistance genes through activation of SKN-1 and DAF-16 which is consistent with my hypotheses. However, I suspect that *ztf-17(tm963)* mutants may have enhanced, or possibly, constitutive activation of SKN-1 which in turn suppresses DAF-16-dependent stress responses. Thus, *C. elegans* lacking *ztf-17* have gained short-term oxidative stress resistance but are highly sensitive to heat stress. Although luciferase assays indicated that ZTF-17 can prevent expression of SKN-1 and DAF-16 target genes, it is still unclear if this regulation is a direct inhibition or if ZTF-17 interacts with other unidentified regulators to facilitate stress signal transduction. To date, I have defined a potential role of ZTF-17 as a negative regulator of signalling pathways that converge onto SKN-1 and DAF-16 to prevent inappropriate gene expression (Figure 3.1). The study of ZTF-17 has been fruitful in providing valuable information on a possible new regulatory mechanism for oxidative stress response and elucidated aspects involved in IIS, mTOR, MAPK and miRISC pathways affecting how stress resistance can be achieved to promote lifespan and longevity.

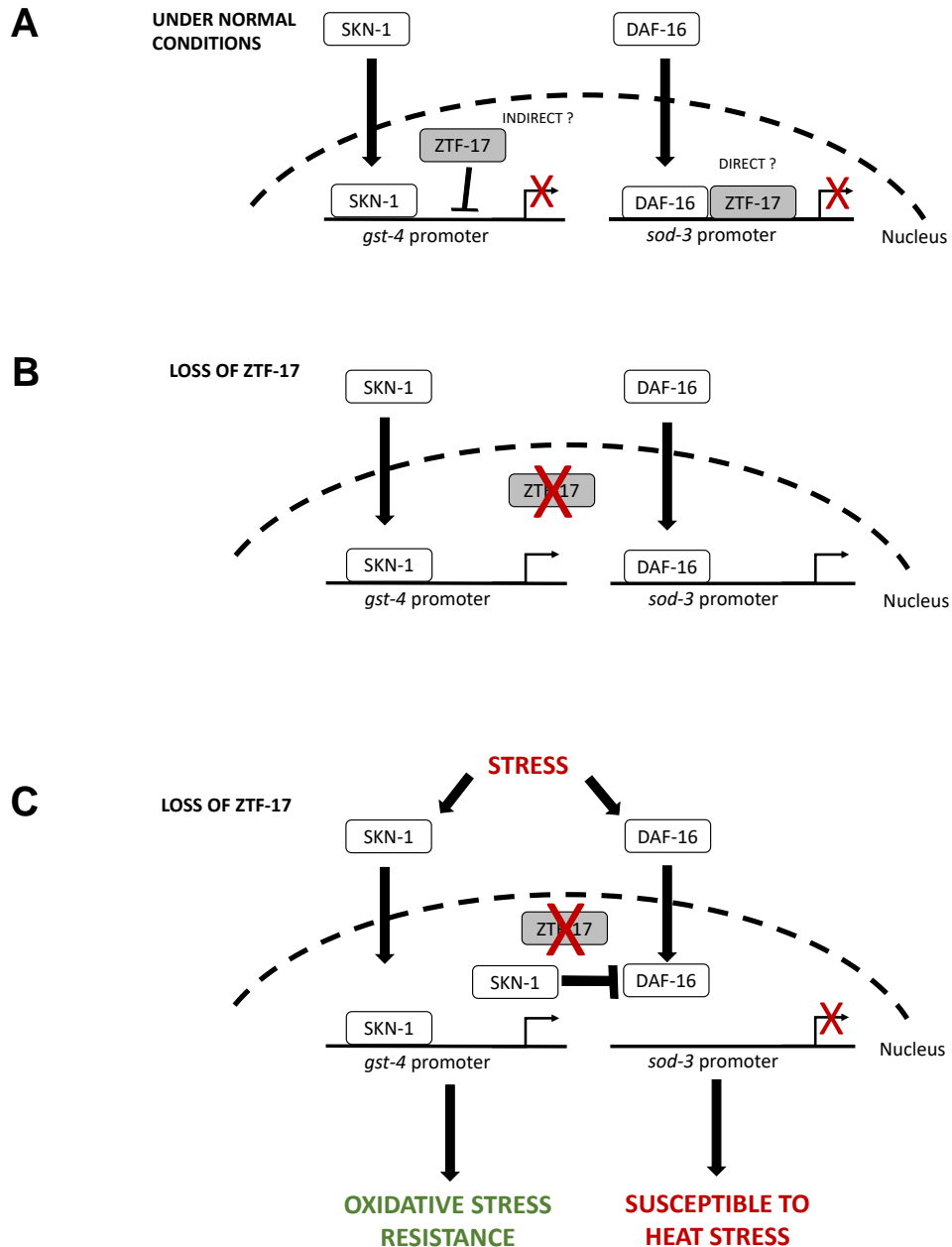


Figure 3.1 The proposed model for the mechanism of ZTF-17 function in the regulation of phase I and phase II detoxification pathways.

(A) Under normal conditions, expression of ZTF-17 negatively regulates detoxification genes, such as *gst-4* and *sod-3*, in the nucleus by binding to and/or indirectly affecting promoters that are normally activated by SKN-1 and DAF-16. (B) Loss of ZTF-17 repression results in the upregulation of genes involved in stress resistance. (C) Stress inducing conditions leads to the upregulation of genes related to the oxidative stress response by SKN-1, but constitutive activation of SKN-1 negatively regulates DAF-16 leading to downregulation of genes that aid in heat stress survival, aging, lifespan and longevity.

3.3 Future directions and studies of ZTF-17 in *C. elegans*.

3.3.1 ZTF-17 localization can be achieved using the SapTrap Assembly approach to generate *ztf-17::mNeonGreen* expressing transgenic worms.

Often, the functionality of a protein is linked to where they are expressed in organisms. By knowing where ZTF-17 is localized, we can determine if it is tissue specific and hopefully, narrow down its function. A method called SapTrap assembly, a high-throughput cloning procedure that was streamlined by Dickinson and Goldstein, was used for the assembly of the ZTF-17 specific repair template and the site-directed mutagenesis Cas9-sgRNA specific plasmid to carry out gene tagging [15]. Currently the ZTF-17 SapTrap assembly has been designed to produce a mNeonGreen (mNG) fluorescent protein knock-in at the *ztf-17* locus using CRISPR/Cas9-triggered homologous recombination [15,16]. Figure 3.2A outlines the components of the ZTF-17 Assembly. Figure 3.2B illustrates the workflow for the ZTF-17::mNG knock-in including the organization at the *ztf-17* locus before the gene edit, the homologous recombination and the SEC removal after with heat shock. Currently, the SapTrap assembly needs to be microinjected into N2 worms, however, our lab has yet to successfully incorporate the assembly and the generation of the ZTF-17::mNG transgenic worms is a future project.

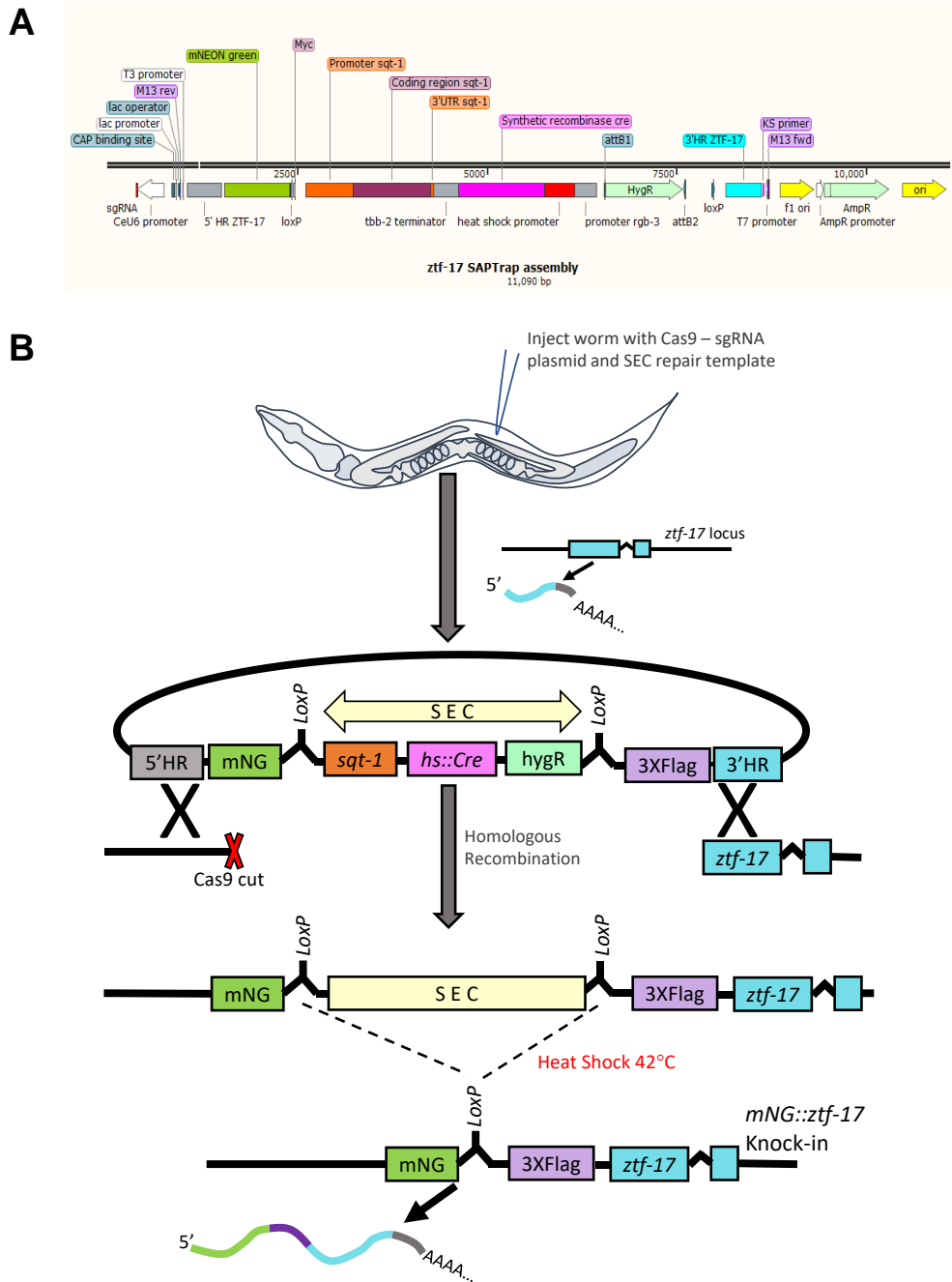


Figure 3.2 CRISPR/Cas-9 mediated *ztf-17::mNG* knock-in using the SapTrap assembly for ZTF-17 localization.

(A) Illustration of the ZTF-17 SAPTrap Assembly Map that makes up the SEC Repair Template. (B) Workflow for tagging of *ztf-17* with mNG^{3XFlag} and the predicted transcript produced from the gene edit. Animals are co-injected with the Cas9-sgRNA and the SEC repair template that consists of a hygR, the *sqt-1* visible marker and the inducible Cre recombinase. Heat shock at 42°C will cause the SEC to excise so that the *LoxP* site that remains is in the intronic region.

3.3.2 Future work to further elucidate the significance of ZTF-17 and the stress genes network.

This project has been successful in providing evidence that ZTF-17 is involved in the stress signalling that regulates SKN-1 and DAF-16. Although I presented evidence that supported a novel regulatory mechanism for SKN-1 and DAF-16 activation, there are still knowledge gaps in defining ZTF-17's precise action in these complex signalling processes. Therefore, my goal for the continuation of this project is to look at upstream regulators of SKN-1 and DAF-16, determine where ZTF-17 may interact and decipher parts of the stress signalling pathway that have yet to be investigated.

First, a relationship was determined between SKN-1, DAF-16 and ZTF-17 in the regulation of oxidative stress responses. However, in the RNAi screen, many other candidates were identified to affect *gst-4* expression, thus it would be important to validate such candidates and look for potential links to ZTF-17. For example, *ztf-22* is a zinc finger protein with very similar structure and appeared to have similar effects on *gst-4* like *ztf-17*. *In vivo* analysis of TRA-1 binding sites revealed four male-biased gonadal transcripts found from genes enriched near the TRA-1 binding sites, one of which included *ztf-22* [17]. TRA-1 is a transcription factor found to determine sex throughout the body in *C. elegans* and TRA-1 may be responsible for regulating a subset of genes within the gonad [17]. Genetic pathways that direct early gonadal development and the regulatory components involved in specific gene expression are currently not well known. Although there is limited information on *ztf-22* in the literature, there is some data suggesting *ztf-22* may mediate sex determination. I believe it would be worthwhile to pursue *ztf-22*, and other candidates from the screen, in future studies of *ztf-17* to determine if these proteins that are involved in development are also linked to oxidative stress, aging and longevity.

The luciferase assays confirmed that ZTF-17 can repress SKN-1 and DAF-16 target genes, although it is not clear whether this interaction is direct or indirect with the promoters. To

address the possibility that ZTF-17 directly interacts with PI and PII detoxification promoters to repress transcription, ChIP (Chromatin Immunoprecipitation sequencing analysis) can be done to capture the protein to DNA interaction and identify ZTF-17 binding sites. Further understanding of where ZTF-17 interacts with the chromatin will help us understand the kinetics occurring at the promoter region and identify other molecular players that may be involved in ZTF-17 transcriptional repression of detoxification genes.

Lastly, to address the possibility that ZTF-17 modifies upstream SKN-1 and DAF-16 regulators, we can generate double mutants containing the *ztf-17* deletion along with each of the following *pmk-1*, *mpk-1*, *mek-1*, *sek-1*, *nsy-1*, *age-1* and *akt-1/2* genes. The aim is to determine precisely where ZTF-17 plays a role in the p38 MAPK/IIS oxidative stress pathways that activates SKN-1 and DAF-16 or if ZTF-17 works through a kinase like BRAP-2 in the ERK/MAPK-Ras pathway. In addition, RNA-sequencing analysis or microarray analysis can be done to determine other genes that are upregulated and/or downregulated with loss of *ztf-17*. This will help identify potential candidates that may be involved in the increased oxidative stress response when *ztf-17* is knocked down. It is known that ZPF42/REX1 regulates the expression of a miRNA that affects the *Xist* gene during X-chromosome inactivation [18]. To explore the possibility that *ztf-17* may also express miRNAs, other than the known *mir-77* target, the transcriptome analysis will help determine if there is some homology with mammalian ZPF42/REX1, in that ZTF-17's negative regulation of SKN-1 and DAF-16 may be achieved through miRISC activity. These future experiments will be important to discovering which pathways ZTF-17 is active in and will be central to fine tuning the holistic mechanism of ZTF-17 function.

3.4 Conclusion

Our lab is interested in studying the oxidative stress response as many human diseases are linked to metabolic regulation, aging and damage that arise from ROS production. Although there are decades of research on how organisms manage oxidative stress and activate resistance, there is still a huge absence of knowledge for understanding how these signalling pathways are modulated and what mechanisms are involved at the molecular level. As previously mentioned, the *C. elegans* represents a relevant model to study oxidative stress *in vivo* and provides invaluable insight into the complex networks that regulate aging, lifespan and longevity. The work presented in this thesis, represents only a small portion of what the roles of transcription factors are in stress pathway regulation. While more work is required to determine how ZTF-17 regulates SKN-1 and DAF-16, the current research supports its role as a negative regulator of detoxification enzymes with emerging new roles outside of *C. elegans* development. As such, an understanding of oxidative stress responses will be important for determining the status of an organism's health and their age-dependent outcomes, including homeostatic distribution of lipids, restoration of stress resistance, and increased lifespan.

3.5 References

1. Hayes, J. D., Flanagan, J. U. & Jowsey, I. R. Glutathione transferases. *Annu. Rev. Pharmacol. Toxicol.* **45**, 51–88 (2005).
2. Hasegawa, K. & Miwa, J. Genetic and cellular characterization of *Caenorhabditis elegans* mutants abnormal in the regulation of many phase II enzymes. *PLoS One* **5**, (2010).
3. Hourihan, J. M., Moronetti Mazzeo, L. E., Fernández-Cárdenas, L. P. & Blackwell, T. K. Cysteine Sulfenylation Directs IRE-1 to Activate the SKN-1/Nrf2 Antioxidant Response. *Mol. Cell* **63**, 553–566 (2016).
4. Oliveira, R. P. *et al.* Condition-adapted stress and longevity gene regulation by *Caenorhabditis elegans* SKN-1/Nrf. *Aging Cell* **8**, 524–541 (2009).
5. Ewald, C. Y., Hourihan, J. M. & Blackwell, T. K. Oxidative Stress Assays (arsenite and tBHP) in *Caenorhabditis elegans*. *Bio-Protocol* **7**, 1–12 (2017).
6. Murphy, C. T. *et al.* Genes that act downstream of DAF-16 to influence the lifespan of *Caenorhabditis elegans*. *Nature* **424**, 277–284 (2003).
7. Gami, M. S. & Wolkow, C. A. Studies of *Caenorhabditis elegans* DAF-2/insulin signaling reveal targets for pharmacological manipulation of lifespan. *Aging Cell* **5**, 31–37 (2006).
8. Dahlstrom, E. & Levine, E. Dynamics of Heat Shock Detection and Response in the Intestine of *Caenorhabditis elegans*. (2019). doi:10.1101/794800.
9. Lindquist, J. A. & Mertens, P. R. Cold shock proteins: From cellular mechanisms to pathophysiology and disease. *Cell Commun. Signal.* **16**, 1–14 (2018).
10. Alessi, A. F. Regulation of the microRNA-Induced Silencing Complex in *C. elegans*. (2015).
11. Reece-Hoyes, J. *et al.* Enhanced yeast one-hybrid (eY1H) assays for high-throughput gene-centered regulatory network mapping. *Nat Methods* **8**, 1059–1064 (2011).
12. Perez, M. F. & Lehner, B. Vitellogenins - Yolk Gene Function and Regulation in *Caenorhabditis elegans*. *Front. Physiol.* **10**, (2019).
13. Deng, J., Dai, Y., Tang, H. & Pang, S. SKN-1 is a negative regulator of DAF-16 and somatic stress resistance in *C. Elegans*. *G3 Genes, Genomes, Genet.* **10**, 1707–1712 (2020).
14. Liu, W. J., Reece-Hoyes, J. S., Walhout, A. J. & Eisenmann, D. M. Multiple transcription factors directly regulate Hox gene *lin-39* expression in ventral hypodermal cells of the *C. Elegans* embryo and larva, including the hypodermal fate regulators LIN-26 and ELT-6. *BMC Dev. Biol.* **14**, 1–21 (2014).
15. Dickinson, D. Protocols for cloning SEC-based repair templates using SapTrap assembly. (2016) doi:10.1534/genetics.115.184275.For.
16. Dickinson, D. J., Pani, A. M., Heppert, J. K., Higgins, C. D. & Goldstein, B. Streamlined Genome Engineering in *Caenorhabditis elegans* with a Self-Excising Drug Selection Cassette. *Genetics* **200**, 1035–1049 (2015).
17. Kroetz, M. B. & Zarkower, D. Cell-Specific mRNA Profiling of the *Caenorhabditis elegans* Somatic Gonadal Precursor Cells Identifies Suites of Sex-Biased and Gonad-Enriched Transcripts. *G3 Genes/Genomes/Genetics* **5**, 2831–2841 (2015).
18. Makhlof, M. *et al.* A prominent and conserved role for YY1 in Xist transcriptional activation. *Nat. Commun.* **5**, 1–12 (2014).

APPENDIX

Table 3. Statistics for the As oxidative stress assay.

	Strain	No. of Samples	Median Survival				Hours at % mortality				
			Hours	SE	95% C.I.	P-value	25 %	50 %	75 %	90 %	100 %
Trial 1	wildtype (N2) in 5mMAs	36	3.58	0.35	2.89~4.28	-	2	3	5	7	10
	<i>zfp-17(tm963)</i> in 5mMAs	36	3.58	0.30	3.00~4.17	0.8727	2	3	4	6	9
Trial 2	wildtype (N2) in 5mMAs	36	3.08	0.30	2.50~3.67	-	2	3	4	6	8
	<i>zfp-17(tm963)</i> in 5mMAs	36	3.17	0.23	2.72~3.61	0.7556	2	3	4	6	8
Trial 3	wildtype (N2) in 5mMAs	36	4.47	0.43	3.64~5.31	-	2	4	6	8	10
	<i>zfp-17(tm963)</i> in 5mMAs	36	4.39	0.35	3.71~5.07	0.5997	3	4	6	8	9

P-values are relative to wild type (N2).

Table 4. Statistics for the tBHP oxidative stress assay.

	Strain	No. of Samples	Median Survival				Hours at % mortality				
			Hours	SE	95% CI	P-value	25 %	50 %	75 %	90 %	100 %
Trial 1	wildtype (N2) on 15.4mM tBHP plates	60	3.22	0.2	2.83~3.60	-	2	3	4	5	8
	<i>zfp-17(tm963)</i> 15.4 mM tBHP plates	60	4.27	0.2	3.87~4.67	0.0006	3	4	5	6	9
Trial 2	wildtype (N2) on 15.4mM tBHP plates	60	3.17	0.19	2.79~3.54	-	2	3	4	5	8
	<i>zfp-17(tm963)</i> 15.4 mM tBHP plates	60	4.30	0.21	3.90~4.70	0.0002	3	4	5	6	9
Trial 3	wildtype (N2) on 15.4mM tBHP plates	60	3.62	0.17	3.28~3.95	-	3	4	5	6	8
	<i>zfp-17(tm963)</i> 15.4 mM tBHP plates	60	4.32	0.22	3.89~4.74	0.0012	3	4	5	7	9

P-values are relative to wild type (N2).

Table 5. Statistics for the thermotolerance assay.

	Strain	No. of Samples	Median Survival				Hours at % mortality				
			Hours	SE	95% C.I.	P-value	25 %	50 %	75 %	90 %	100 %
Trial 1	wildtype (N2) exposed to 35°C	36	-	0.73	-	-	10	-	-	-	-
	<i>zlf-17(tm963)</i> exposed to 35°C	36	10.29	0.38	9.56 ~ 11.03	<0.0001	9	10	12	14	15
Trial 2	wildtype (N2) exposed to 35°C	36	-	0.42	-	-	9	-	-	-	-
	<i>zlf-17(tm963)</i> exposed to 35°C	36	10.57	0.41	9.76 ~ 11.38	<0.0001	8	11	13	14	15
Trial 3	wildtype (N2) exposed to 35°C	36	-	0.51	-	-	11	-	-	-	-
	<i>zlf-17(tm963)</i> exposed to 35°C	36	10.25	0.4	9.46 ~ 10.04	<0.0001	9	10	12	14	15

P-values are relative to wild type (N2).

Table 6. List of Worm Strains. Worm strains were obtained from the *Caenorhabditis* Genetic Center at The University of Minnesota or from the National Bioresource Project (Tokyo, Japan) unless otherwise specified. Double mutants were created according to the standard single-worm PCR protocol.

Strains	Description
N2	Bristol Wildtype
CB1370	<i>daf-2(e1370)III</i>
CF1553	<i>muls84 [(pAD76)sod-3p::GFP+rol-6]</i>
CL2166	<i>dvIs19 [(pAF15)gst-4p::GFP::NLS]</i>
DR466	<i>him-5(e1490)V</i>
NL2099	<i>rrf-3(pk1426)II</i>
TJ356	<i>zIs356 [daf-16p::daf-16a/b::GFP + rol-6(su1006)]</i>
YF15	<i>brap-2(ok1492)II backcrossed 3x</i>
YF208	<i>wdr-23(tm1817) backcrossed 3x</i>
YF209	<i>ztf-17(tm963); dvIs19 [(pAF15)gst-4p::GFP::NLS]</i>
YF210	<i>ztf-17(tm963) backcrossed 2x</i>
YF213	<i>ztf-17(+)</i> overexpression line 2
YF214	<i>ztf-17(+)</i> overexpression line 1
YF215	<i>ztf-22(gk3296)II backcrossed 1x</i>
YF217	<i>ztf-17(tm963); daf-2(e1370)III</i>
YF218	<i>ztf-17(tm963); zIs356 [daf-16p::daf-16a/b::GFP + rol-6(su1006)]</i>
YF219	<i>ztf-17(tm963); muls84 [(pAD76)sod-3p::GFP+rol-6]</i>
YF220	<i>ztf-22(gk3296); dvIs19 [(pAF15)gst-4p::GFP::NLS]</i>

Table 7. List of primers used for genotyping *ztf-17* with SW-PCR and in the SapTrap Assembly.

Name	T_m (°C)	Sequence
CT1	65.0	5' AATTCACATGCTGCGCTACC 3'
CT2	65.2	5' GGCTCTTGTGCTGGGACATA 3'
CT3	69.2	5' GTCGGTTGGCACCCCG 3'
CT4	62.4	5' ACGGCAATAAGTTCGATGAGT 3'
CT5	62.4	5' ACGGCAATAAGTTCGATGAGT 3'
CT6	62.7	5' GAGACGACAAACTCGACTGC 3'
CT7	69.0	5' ATTCGCATATTCCCGCCCTC 3'
CT8	67.2	5' GCTCCTTCTGGAAAACGTGAAA 3'
CT9	66.8	5' TGGAAACCGCAGACTTCCAT 3'
CT10	59.7	5' AGCTAGACTGAAAGAGGAAGAAAT 3'
CT11	64.5	5' CTGTAGTTTTTCGTCAAATTCGC 3'
CT12	65.5	5' TGACAAAGTGCAGAGAGGTGG 3'
Cas9 Rev Primer	58.4	5' CAAGACATCTCGCAATAGG 3'
pDD162 Seq	63.6	5' GGTGTGAAATACCGCACAGA 3'
TK248	55.5	5' TTGGACGTATTCGATGAGCTACT 3'
TK249	54.4	5' AACAGTAGCTCATCGAATACGTC 3'
TK284	62.8	5' GACGTATTCGATGAGCTACTGTTTTAG 3'

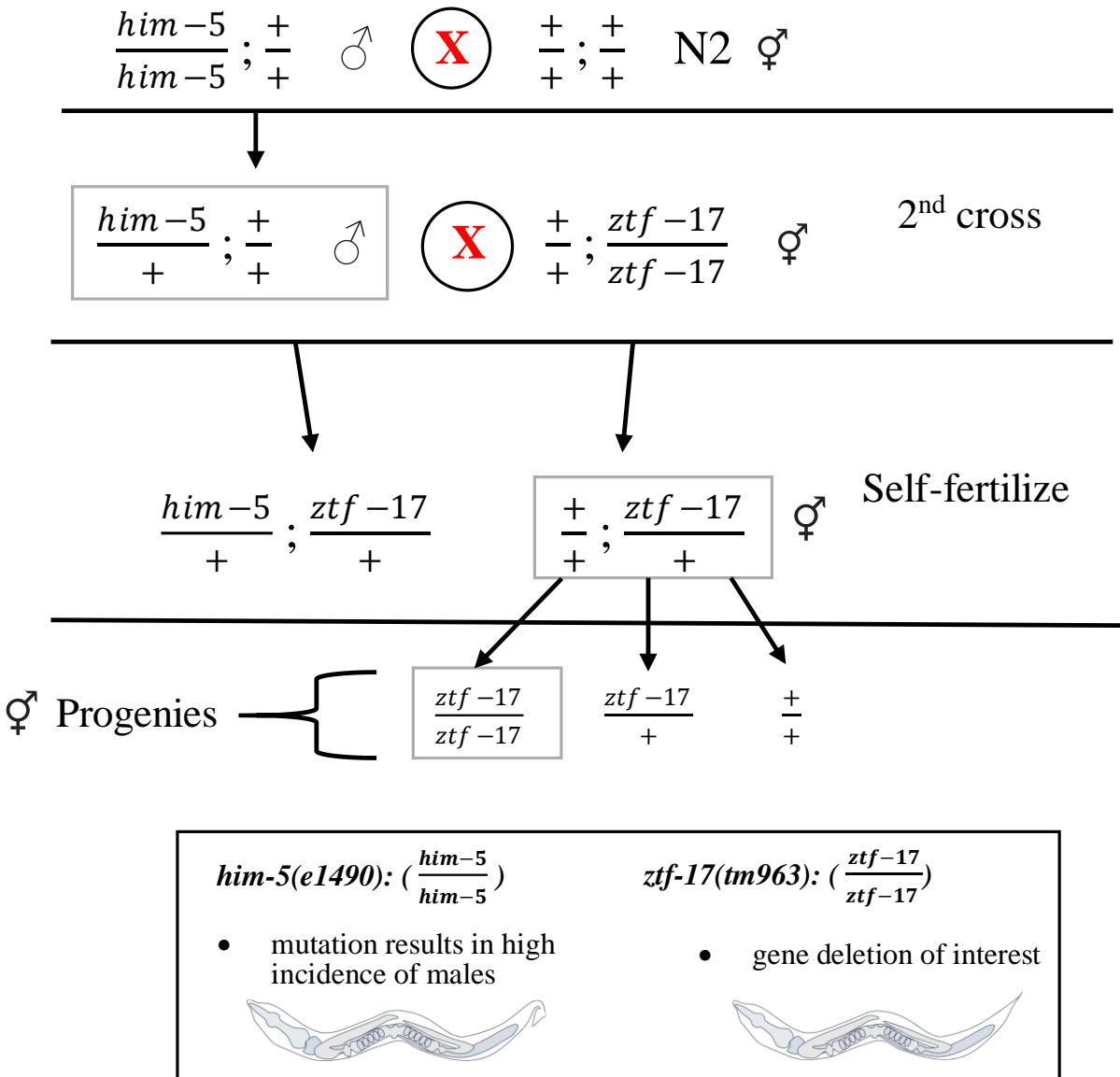
Table 8. List of forward and reverse primers for qRT-PCR.

Name	T _m (°C)	Sequence
<i>act-1</i>	63.9	F: 5' GTCGGTATGGGACAGAAGGA 3'
	64.1	R: 5' GCTTCAGTGAGGAGGACTGG 3'
<i>akt-1</i>	66.1	F: 5' CCCGAAGATGCATTGGAGAT 3'
	62.0	R: 5'GCTTCTACTAGGCGGTGTCA 3'
<i>akt-2</i>	65.6	F: 5' GTGATGTCTGAAACGGACACG 3'
	68.5	R: 5' GATCGTTCCAAGCTTCCCGA 3'
<i>cdc-42</i>	67.6	F: 5' TCGACAATTACGCCGTCACA 3'
	67.7	R: 5' AGGCACCCATTTTTCTCGGA 3'
<i>cey-1</i>	57.0	F: 5' ACGGATTCATCAACCGCACT 3'
	57.3	R: 5' CGAGACCCTTGGATCCTTCG 3'
<i>ctl-1</i>	68.4	F: 5' GTGTCGTTTCATGCCAAGGGA 3'
	65.0	R: 5' CCCAGTTACCCTCCTCGGTA 3'
<i>ctl-2</i>	69.2	F: 5' TCAACCCCGTCAATTCTGGG 3'
	65.7	R: 5' GAGCGAGCCTGTTTCTGGAT 3'
<i>daf-16</i>	69.3	F: 5' TGGAATTCAATCGTGTGGAA 3'
	63.9	R: 5' ATGAATATGCTGCCCTCCAG 3'
<i>dod-3</i>	56.9	F: 5' GTGCATATTGTGGAGCTGCG 3'
	56.6	R: 5' GTACTIONGACGCTGCGAAAA 3'
<i>dod-17</i>	56.9	F: 5' CGAATACAGCACAGGACCGA 3'
	56.9	R: 5' CGTCTGGCAGAGAAGGTTGA 3'
<i>gcs-1</i>	63.8	F: 5'CCAATCGATTCCTTTGGAGA 3'
	63.8	R: 5' GCTACTTCCGGGAATGTGAA 3'
<i>gst-4</i>	64.0	F: 5' TGCTCAATGTGCCTTACGAG 3'
	63.6	R: 5' AGTTTTTCCAGCGAGTCCAA 3'
<i>hsp-16.2</i>	54.9	F: 5' CTCAACGTTCCGTTTTTGGTG 3'
	54.2	R: 5' TGGATTGATAGCGTACGACC 3'
<i>ins-7</i>	63.4	F: 5' AGGTCCAGCAGAACCAGAAG 3'
	64.2	R: 5' GAAGTCGTCGGTGAATTCTT 3'

<i>mpk-1</i>	66.3 69.0	F: 5' CACATAATCGTATCGACATCGAG 3' R: 5' CCATTATTCCTTGCAGCCGCT 3'
<i>mtl-1</i>	56.2 57.5	F: 5' TGCAAGTGCGGAGACAAATG 3' R: 5' GTTCCCTGGTGTGATGGGT 3'
<i>mtl-2</i>	57.9 56.6	F: 5' TGGTCTGCAAGTGTGACTGC 3' R: 5' TAATGAGCAGCCTGAGCACAT 3'
<i>pmp-3</i>	67.1 66.3	F: 5' AGTTCCGGTTGGATTGGTCC 3' R: 5' CCAGCACGATAGAAGGCGAT 3'
<i>sdz-8</i>	64.7 60.4	F: 5' CTGCTGAGGTACGGAACGAA 3' R: 5' TCTGTAFFCGACAACCTGGGA 3'
<i>sgk-1</i>	63.7 63.7	F: 5' ACGCCATGAAAATTCTGTCC 3' R: 5' AAAAATGTTTCTCGCGTTGG 3'
<i>skn-1a/c</i>	57.4 58.1	F: 5' TACTCACCGAGCATCCACCA 3' R: 5' TGATCAGCAGGAGCCACTTG 3'
<i>skn-1b</i>	57.2 56.6	F: 5' CTCCAGCAGCTGTCAACTCTT 3' R: 5' TGCATTCCAATGTAGGCGTAGT 3'
<i>skn-1a</i>	56.5 55.4	F: 5' GCGACGAGACGAGACGATAA 3' R: 5' CCGATCGTATGACGATGATTGG 3'
<i>sod-3</i>	63.9 64.0	F: 5' GGATGGTGGAGAACCTTCAA 3' R: 5' AAGGATCCTGGTTTGCACAG 3'
<i>tba-1</i>	66.4 67.4	F: 5' AGACCAACAAGCCGATGGAG 3' R: 5' TCAGTTCCTTTCCGACGGTG 3'
<i>vit-2</i>	56.8 57.7	F: 5' CAAGGACATGGACTACGCCT 3' R: 5' GAGATGGTGAGTGAAGCCC 3'
<i>vit-5</i>	56.8 57.2	F: 5' CGTCCACGTGTCCAACAAAC 3' R: 5' AAGAGAGCACGGTGAAGCTC 3'

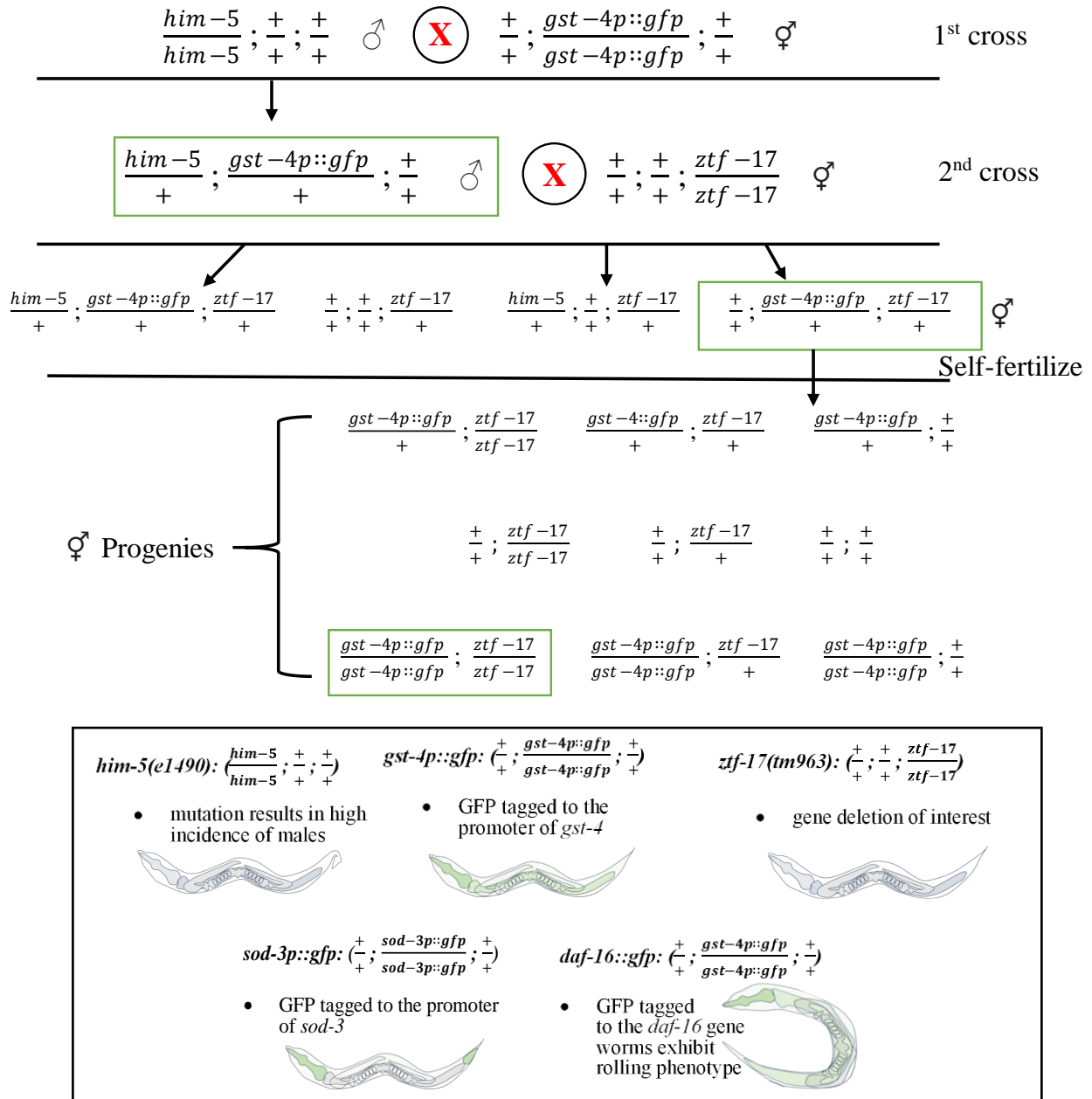
Table 9. List of plasmids used for subcloning constructs.

Name	Description
HA ₂ -pcDNA3.1	Mammalian expression vector with the CMV promoter for expressing N terminally HA-tagged proteins. The Multiple Cloning Site is in the forward (+) orientation.
p3xFLAG-CMV-7.1	Vector for expression of N-terminally 3xFLAG-tagged proteins in mammalian cells.
pDD162	CRISPR/Cas9 and sgRNA plasmid that can be modified to cleave any Cas9 target site in the <i>C. elegans</i> genome.
pDD379	SapTrap destination vector for building combined sgRNA expression and repair template vectors, using the sgRNA scaffold for worm expression.
pDD346	SapTrap mNG-C1 donor for <i>C. elegans</i> codon-optimized mNeonGreen for worm expression.
pDD363	LoxP-flanked SEC donor for the SapTrap cloning system for worm expression.
pDD398	Auxin-inducible degron (AID) N-terminally-tag linker donor in the SapTrap cloning system for worm expression.
pFL-V5-GW	DULIP Prey Destination Vector (Gateway, N-terminal)
pGL4.10	Promoterless vector for measuring the activity of promoter and enhancer sequences with a luciferase assay.
pMLS287	CRISPR vector for the SapTrap flexible linker C-terminal connector donor plasmid.
pPA-RL-GW	DULIP Bait Destination Vector (Gateway, N-terminal)
pSL301	Expression vector with Superlinker Multiple Cloning Site.



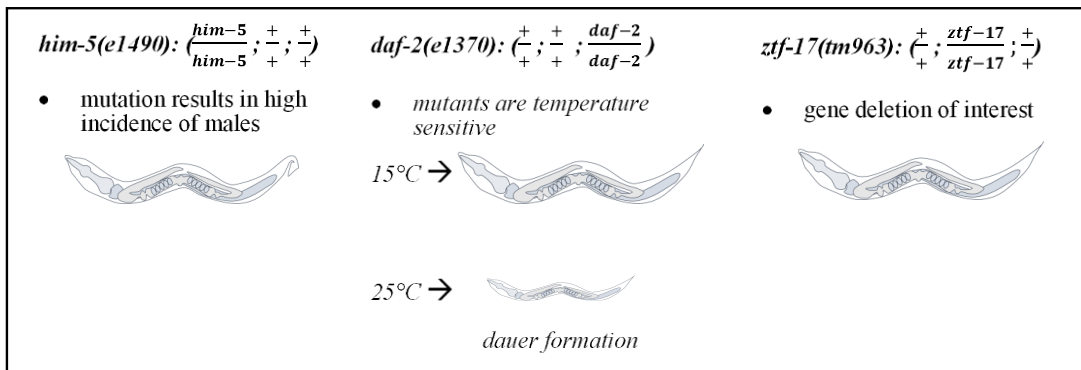
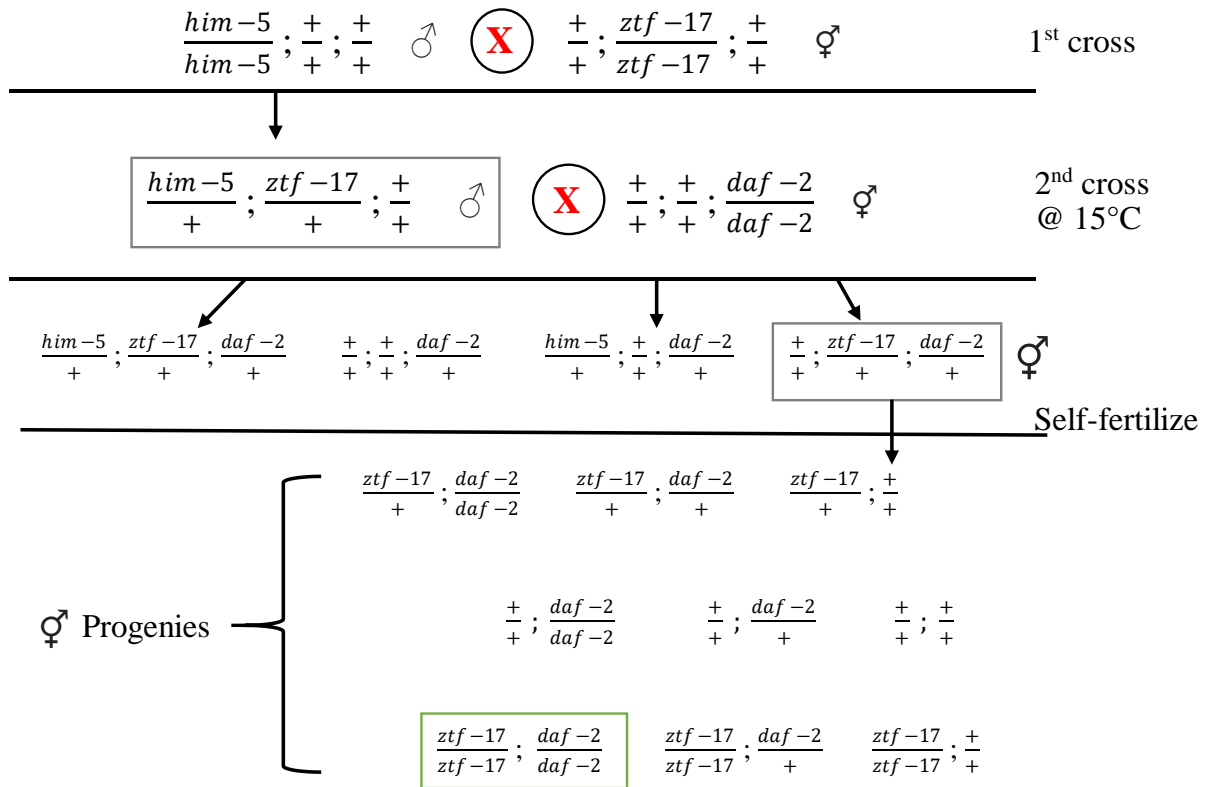
Supplementary Data Figure S1. Schematic of the backcross done to generate the YF210 [*ztf-17(tm963)*].

SW-PCR was performed with specific primers for the *ztf-17(tm963)* gene deletion to genotype.



Supplementary Data Figure S2. Schematic of the approach done to generate the *ztf-17(tm963); dvl1(gst-4p::gfp)* worms and similar transgenic worm strains.

SW-PCR was performed with specific primers for the *ztf-17(tm963)* gene deletion and used to genotype for worms that were homozygous for *ztf-17(tm963)* while fluorescence microscopy was used to detect GFP. Similar approaches were used to generate the *ztf-17(tm963); muls84(sod-3p::gfp)* and *ztf-17(tm963); zIs356(daf-16p::gfp)* worm strains.



Supplementary Data Figure S3. Schematic of the cross done to generate the *ztf-17(tm963); daf-2(e1370)* double mutant worm strain.

SW-PCR was performed with specific primers for the *ztf-17(tm963)* gene deletion and used to genotype for worms that were homozygous for *ztf-17(tm963)*. Worms were sequenced to ensure they also contained the *daf-2(e1370)* mutation.